

Aus dem Bereich Physiologie
Theoretische Medizin und Biowissenschaften
der Medizinischen Fakultät
der Universität des Saarlandes, Homburg/Saar

**GnRH-induced spike activity and calcium signals in GnRHR neuron
during female reproductive cycle**

Dissertation zur Erlangung des Grades eines Doktors der Naturwissenschaften

der Medizinischen Fakultät
der UNIVERSITÄT DES SAARLANDES
2017

vorgelegt von Tong Tong
geboren. am 10. Sept. 1983 in Shaanxi, China

Tag des Prüfungskolloquiums:

Dekan:

Vorsitzender:

Berichterstatter:

Contents

List of figures	I
Abbreviations	III
Abstract	VII
Zusammenfassung	IX

1 Chapter 1: Introduction	1
1.1 Reproductive physiology of female mouse	1
1.1.1 The Hypothalamic-Pituitary-Gonadal (HPG) axis	1
1.1.2 The estrous cycle in female mouse	2
1.2 GnRH	4
1.2.1 Types and structure of GnRH	4
1.2.2 GnRH-secreting neurons	5
1.3 GnRHR	6
1.3.1 Types and structure of GnRHR	6
1.3.2 The distribution of GnRHR neurons in mouse brain	7
1.3.3 The intracellular pathway mediated by GnRHR	8
1.4 The agonist and antagonist of GnRHR in clinical applications	10
1.5 Aims	11
References	12

2	Chapter 2: Materials and methods.....	20
2.1	Materials.....	20
2.1.1	Chemicals and antibodies	20
2.1.2	Solutions and buffers	22
2.1.3	Consumables	23
2.1.4	Equipment	24
2.1.5	Software	27
2.2	Methods.....	28
2.2.1	Animals	28
2.2.2	Assessment of reproductive stages	28
2.2.3	Brain slice preparation	29
2.2.4	Loose-patch recording	29
2.2.5	Analysis of spike data	31
2.2.5.1	Analysis of spike firing patterns	31
2.2.5.2	Short-term and long-term enhancement in spike activity after 1s puff GnRH stimulation	31
2.2.6	Immunohistochemistry	32
2.2.7	Electron microscopy	33
2.2.8	<i>In vivo</i> cetrorelix systemic injection	33
2.2.9	Hematoxylin and Eosin staining	33
2.2.10	Calcium imaging recording on brain slices	34
2.2.11	Simultaneous loose-patch and calcium imaging recording	36
2.2.12	Statistics	36
	References.....	36
3	Chapter 3: Hypothalamic gonadotropin-releasing hormone (GnRH) receptor neurons fire in synchrony with the female reproductive cycle.....	38
	Abstract.....	38
3.1	Introduction.....	39
3.2	Results.....	40
3.2.1	Cyclic transformation of GnRHR neuron firing activity in synchrony with the estrous cycle	40

3.2.2	A switch in action potential burst activity in Pe GnRHR neurons triggered by GnRH	46
3.2.3	The mode of GnRHR neuronal activity is converted by endogenous GnRH	50
3.3	Discussion.....	53
	Reference.....	56
4	Chapter 4: Modulation of GnRHR neuron activity in the periventricular hypothalamus after systemic cetrorelix treatment.....	60
	Abstract.....	60
4.1	Introduction.....	61
4.2	Results.....	62
4.2.1	GnRHR neurons possess close appositions to Pe capillaries	62
4.2.2	Subcutaneous injection of cetrorelix affects reproductive cycle of female mice	66
4.2.3	Cetrorelix inhibits the HPG axis	67
4.2.4	Systemic cetrorelix treatment prevents the switch in burst firing of GnRHR neurons during preovulatory period	69
4.3	Discussion.....	70
	Reference.....	73
5	Chapter 5: GnRH modulates firing activity of GnRHR neurons in arcuate nucleus through calcium-dependent pathway.....	77
	Abstract.....	77
5.1	Introduction.....	78
5.2	Results.....	79
5.2.1	The intrinsic spike activity of GnRHR neurons in the Arc does not depend on the reproductive cycle	79
5.2.2	GnRH is sufficient to increase the firing rate in Arc GnRHR neurons	82
5.2.3	Action potential burst activity is paired with an increase in calcium signal	83
5.2.4	GnRH induce the simultaneous increase of intracellular calcium and firing activity in GnRHR neurons in Arc	85

5.2.5	Action-potential-driven Ca^{2+} influx might involve in GnRH-induced response on GnRHR neuron	85
5.3	Discussion	88
	References.....	92
6	Chapter 6: Summary.....	97
6.1	GnRHR neurons exhibit different firing activity in the different brain area.....	97
6.2	Endogenous GnRH modulates the spike code activity of GnRHR neurons in both Pe and Arc	98
6.3	GnRHR neurons in different brain area receive different source of GnRH.....	99
6.4	Systemic injection of cetrorelix, an antagonist of GnRHR, can influence the firing activity of GnRHR neuron in the brain	100
6.5	GnRH-induced action potential burst activity induces a calcium increase via voltage-dependent ion channels in Arc GnRHR neurons	100
	References.....	101
7	Publications and permission of use	105
8	Acknowledgments.....	106

List of figures

Chapter 1

Figure 1.1 Hypothalamic-Pituitary-Gonadal (HPG) axis in female mice.....	2
Figure 1.2 The reproductive hormone and physiological changes during the female estrous cycle..	3
Figure 1.3 Schematic representation of mammalian GnRH in the folded conformation.....	4
Figure 1.4 Two-dimensional representation of the GnRHR.....	6
Figure 1.5 GnRHR neurons occur in different brain areas.....	7
Figure 1.6 Proposed intracellular signal pathway in hypothalamic GnRHR neurons.....	9

Chapter 2

Figure 2.1 Vaginal cytology representing each stage of estrous from mice.....	28
Figure 2.2 Puff and bath application systems.....	30

Chapter 3

Figure 3.1 Different spontaneous spike activity patterns of GnRHR neuron during the female reproductive cycle.....	41
Figure 3.2 The change of mean frequency and mean burst duration of GnRHR neurons during the female reproductive cycle.....	42
Figure 3.3 Alternation between tonic and bursting spike activity of GnRHR neurons during the reproductive cycle.....	44
Figure 3.4 Increase of firing frequency in the first 10s after 1s GnRH puff stimulation.....	47
Figure 3.5 A long-lasting change in the action potential activity of GnRHR neurons induced by 1s GnRH puff stimulation.....	48
Figure 3.6 A transformation from tonic to bursting firing pattern induced by bath application of GnRH.....	50
Figure 3.7 The transformation in action potential activity of GnRHR neurons is reversed by cetorelix.....	51
Figure 3.8 Cetorelix abolish the endogenous GnRH effect.....	52

Chapter 4

Figure 4.1 The distribution of GnRHR neurons in Pe from rostral to caudal.....	63
Figure 4.2 Multiple close appositions between GnRHR neurons and capillaries.....	64
Figure 4.3 Electron micrographs of different capillary types in the hypothalamus.....	65

Figure 4.4 Influence of subcutaneous injection of cetrorelix on the vaginal cytology of the female mice.....	67
Figure 4.5 Uterus to body mass ratio in SHAM, 10µg, 50µg cetrorelix-treated and proestrous females.....	68
Figure 4.6 Quantification of tertiary/preovulatory follicles and corpora lutea in SHAM, 10µg or 50µg cetrorelix-treated and proestrous females.....	68
Figure 4.7 Influence of systemic cetrorelix injection on GnRHR neuron firing activity.....	70

Chapter 5

Figure 5.1 The spontaneous spike activity of GnRHR neurons in Arc during the female reproductive cycle with and without the synaptic blocker.....	80
Figure 5.2 The increase of firing frequency during late proestrus is abolished in the presence of synaptic blocker.....	81
Figure 5.3 GnRH induces the increase of firing activity in Arc GnRHR neurons.....	82
Figure 5.4 The simultaneous change in spontaneous spike activity and intracellular calcium activity of GnRHR neuron in Arc.....	84
Figure 5.5 GnRH can simultaneously induce an increase of intracellular calcium and firing activity in GnRHR neuron in Arc.....	86
Figure 5.6 In the presence of TTX and synaptic blockers, GnRHR neurons in Arc cannot respond to GnRH stimulation.....	87

Abbreviations

129SvJ	Mouse strain
3V	Third ventricle (<i>ventriculus teritius</i>)
α T3	Human pituitary cell line
AC	Adenylate cyclase
AHP	Anterior hypothalamic area
AM	Acetoxymethyl ester
AOB	Accessory olfactory bulb
Arc	Arcuate nucleus of the hypothalamus
ART	Assisted reproductive technology
ATPase	Adenosinetriphosphatase
BBB	Blood-brain barrier
BES	N, N-Bis (2-hydroxyethyl)-2-aminoethanesulfonic acid
C	Cervix
C57BL/6J	Mouse strain
CAGS	Cytomegalovirus early enhancer chicken beta actin rabbit Beta-globulin gene sequence promoter
CaM	Calmodulin
cAMP	Cyclic adenosine monophosphate
Cav	Voltage-gated calcium channel
COOH terminus	Carboxyl terminus
CRAC	Calcium release-activated channels
CSF	Cerebrospinal fluid
CV _{ISI}	Coefficient of the variation of the interspike interval
D	Diestrus
DAG	Diacyl-glycerol
DM	Dorsal medial hypothalamic nucleus
E	Estrus
EC ₅₀	Half maximal effective concentration

ECLs	Extracellular loops
ER	Endoplasmic reticulum
ER α	Estrogen receptor α
eROSA26	Enhanced Rosa26
F	Fluorescence intensity
F _{n,m}	Degrees of freedom
FSH	Follicle-stimulating hormone
G protein	Guanosine nucleotide-binding protein
G α	Alpha subunit of the guanosine nucleotide-binding protein
G β	Beta subunit of the guanosine nucleotide-binding protein
G γ	Gamma subunit of the guanosine nucleotide-binding protein
G α_i	Inhibiting subtype of alpha subunit of the guanosine nucleotide-binding protein
G $\alpha_{q/11}$	Ca ²⁺ increasing subtype of alpha subunit of the guanosine nucleotide-binding protein
G α_s	Stimulating subtype of alpha subunit of the guanosine nucleotide-binding protein
GFP	Green fluorescent protein
τ GFP	Tau-green fluorescent fusion protein
GnRH	Gonadotropin-releasing hormone
GnRHR	Gonadotropin-releasing hormone receptor
GPCR	G-protein-coupled receptor
GRIC	GnRHR-internal ribosome entry site-Cre
GRIC/eR26- τ GFP	Mouse strain
HPG	Hypothalamus-pituitary-gonadal
ICLs	Intracellular loops
ICSI	Intracytoplasmic sperm injection
IP ₃	Inositol 1, 4, 5-tris-phosphate
IP ₃ R	Inositol trisphosphate receptor
IR-DIC	Infrared-differential interference contrast

ISI	Interspike interval
IVF	<i>In vitro</i> fertilization
LH	Luteinizing hormone
M	Metestrus
mf	Mean frequency
MOB	Main olfactory bulb
MOE	Main olfactory epithelium
mRNA	Messenger ribonucleic acid
MSiB	Mean spikes in burst
NH ₂ -terminus	Amino-terminus
O	Ovary
OV	Oviduct
PCA	Principle component analysis
Pe	Periventricular nucleus of the hypothalamus
P _E	Early proestrus
P _L	Late proestrus
PIP ₂	Phosphatidylinositol 4,5-bisphosphate
PLC	Phospholipase C
PSiB	Percentage of spikes in bursts
ROI	Region of interest
RyR	Ryanodine receptor
SAG	1-stearoyl-2-arachidonoyl-sn-glycerol
SD	Standard deviation
SERCA	Sarco/endoplasmic reticulum Ca ²⁺ -ATPase
TIDA	Tuberoinfundibular dopamine
TMDs	Transmembrane domains
TRP channel	Transient receptor potential channel
TRPC	Transient receptor potential cation channel
U	Uterus
VARiF	Variance of the instantaneous spike frequency

VNO

Vomeronasal organ

Amino acids

Arg

Arginine

Glu

Glutamic acid

Gly

Glycine

Pro

Proline

Ser

Serine

Trp

Tryptophan

Tyr

Tyrosine

Val

Valine

Abstract

Mammalian reproduction is controlled by precise secretion of gonadotropin-releasing hormone (GnRH) through the hypothalamus-pituitary-gonadal (HPG) axis. GnRH-secreting neurons in the preoptic area of hypothalamus release GnRH into the hypophyseal portal vasculature, which subsequently binds to GnRHR on gonadotrope cells in the anterior pituitary gland to regulate the release of gonadotropins. Studies showed that GnRHR neurons not only exist in the anterior pituitary but also are distributed in multiple brain areas involved in regulating the mammalian's reproductive physiology and behavior. However, the physiological character of GnRHR neurons in the specific brain area is still ambiguous. By crossbreeding GnRHR-IRES-Cre (GRIC) mice to eRosa26- τ GFP reporter mice, GnRHR neurons can be visualized in live brain slices with τ GFP. To link the firing activity of GnRHR neurons with female reproductive cyclicity, the spontaneous firing of GnRHR neurons in the periventricular hypothalamus (Pe) is first investigated on brain slices from adult female mice. Using loose-patch recording, I find that GnRHR neurons in Pe alternate their action potential firing patterns in concert with the female reproductive cycle and change firing activity from tonic to burst during the preovulatory period, especially in the presence of network blockers. GnRH stimulation can induce this tonic-to-burst firing conversion of GnRHR neurons. Bath application of an antagonist of GnRHR, cetrorelix, directly on brain slices demonstrates that the endogenous GnRH is the main source for converting the mode of action potential firing during the preovulatory period. Using immunohistochemistry and electron microscope, the source of the endogenous GnRH for GnRHR neurons is explored. We observed that GnRHR neurons possess close appositions to Pe capillaries, and the endothelial cells of capillaries in Pe contain many caveolae-like structures, suggesting a less constrained blood-brain barrier (BBB) there. Therefore, GnRHR neurons in Pe might be susceptible to systemic injection with cetrorelix which is widely used in the clinical treatment. I observed that subcutaneous injection of the cetrorelix can block the HPG axis as manifested by an increase in the number of preovulatory follicles concomitant with a significant inhibition of follicle rupture and more corpora lutea formation. Cetrorelix-treatment can modulate Pe GnRHR neurons to fire more tonically and to mimic spike firing activity as early proestrus, especially with the higher dose treatment. Next to Pe, arcuate nucleus (Arc) is another important brain area in the hypothalamus, which is involved in regulating olfactory-encoded behavior in mammals. Using loose-patch recording, I found that

the intrinsic firing activity of Arc GnRHR neurons does not depend on the reproductive cycle, and GnRHR neurons there receive modulation from network. To further investigate the relationship between intracellular Ca^{2+} and firing activity of GnRHR neuron, a new protocol combined loose-patch and calcium imaging recording is developed. A correlation between the action potential burst activity of GnRHR neuron with an increase in calcium signal is identified. Furthermore, GnRH can simultaneously induce the increase of firing activity and the intracellular Ca^{2+} of GnRHR neuron in Arc, which suggests that the change of intracellular Ca^{2+} is involved in GnRH-GnRHR signaling pathway. This GnRH-induced response may depend on the action-potential-driven influx of calcium. All these studies establish a series of methods and provide key information to begin understanding physiological properties of GnRHR neurons.

Zusammenfassung

Die Reproduktion von Säugetieren wird durch die präzise Freisetzung des Gonadotropin-freisetzenden Hormons (engl.: gonadotropin-releasing hormone; GnRH) durch die Hypothalamus-Hypophyse-Gonaden Achse (engl.: hypothalamus-pituitary-gonadal axis; HPG) gesteuert. GnRH-freisetzende Neurone in dem präoptischen Areal des Hypothalamus sekretieren GnRH in die Hypophysenpfortader, welches anschließend an den zugehörigen GnRH-Rezeptor (GnRHR) auf gonadotropen Zellen der anterioren Hypophyse bindet und die Freisetzung der Gonadotropine reguliert. Durch Studien konnte die Lokalisation der GnRHR-Neurone nicht nur in der anterioren Hypophyse, sondern auch in verschiedenen Hirnarealen nachgewiesen werden. Ihre Funktion umfasst die Kontrolle der Reproduktion und das Verhalten in Säugetieren. Allerdings ist die physiologische Rolle von GnRHR-Neuronen in diesen Gehirnarealen noch unklar. Durch Kreuzung von GnRHR-IRES-Cre (GRIC) Mäusen mit eRosa26- τ GFP Reporter-Mäusen wird eine Visualisierung von GnRHR-Neuronen durch τ GFP Expression in lebenden Hirnschnitten möglich. Um Zusammenhänge zwischen dem Aktivitätsverhalten von GnRHR-Neuronen und dem weiblichen Reproduktionszyklus zu untersuchen wurde die Spontanaktivität von GnRHR-Neuronen des periventriculären Hypothalamus (Pe) in akuten Hirnschnitten adulter weiblicher Mäuse analysiert. Unter Einsatz der loose-patch Methode konnte ich zeigen, dass GnRHR-Neurone des Pe ihr Aktionspotential-Muster in Übereinstimmung mit dem weiblichen Reproduktionszyklus modifizieren und ihre Spontanaktivität in der präovulären Phase von tonisch zu gebündelt/bursting ändern. Verdeutlicht wird dies durch Blockierung des synaptischen Netzwerks. Auch eine Stimulation von GnRHR-Neuronen mit GnRH bewirkt diese Umstellung der Aktionspotentialaktivität von tonisch zu bursting. Badperfusionen von akuten Hirnschnitten mit dem GnRHR-Antagonisten Cetrorelix verdeutlichen, dass endogenes GnRH die Hauptursache für die Veränderung der Spontanaktivität in der präovulären Phase darstellt. Die Quelle des endogenen GnRH wurde durch Immunhistochemie und Elektronenmikroskopie näher bestimmt. Wir stellten fest, dass GnRHR-Neurone im Pe über engen Kontakt zu Blutkapillaren verfügen und, dass die Endothelzellen der Kapillaren im Pe viele Caveolae-ähnliche Strukturen zeigen, was eine schwächere Blut-Hirn-Schranke (engl.: blood-brain barrier; BBB) vermuten lässt. Eine Empfänglichkeit der GnRHR-Neurone des Pe für systemische Applikationen von Cetrorelix, wie sie in der klinischen Anwendung weit verbreitet sind, kann somit vermutet werden. Ich konnte

zeigen, dass subkutane Injektionen von Cetrorelix die HPG Achse aushebeln können. Evidenzen hierfür sind eine erhöhte Anzahl präovulären Follikeln, begleitet von einer signifikanten Einschränkung des Follikelsprungs und eine vermehrte Bildung von Gelbkörpern. Eine Behandlung mit Cetrorelix kann die Spontanaktivität von Pe GnRHR-Neuronen in Dosis-abhängiger Weise zu mehr tonischer Aktivität verändern und somit die Aktionspotentialsequenz des frühen Proestrus imitieren. Neben dem Pe ist der nucleus arcuatus (Arc) ein weiterer wichtiger Bereich des Hypothalamus, der an der Regulation von olfaktorisch codierten Verhalten in Säugetieren beteiligt ist. Mit der loose-patch Methode konnte ich zeigen, dass die Spontanaktivität der Arc GnRHR-Neurone nicht vom Reproduktionszyklus abhängt, sondern von ihrem synaptischen Netzwerk moduliert wird. Um den Zusammenhang zwischen intrazellulärem Kalzium und der Spontanaktivität weiter zu untersuchen wurde ein neuer Versuchsaufbau entworfen, indem die loose-patch Methode mit calcium imaging kombiniert wurde. Eine Abhängigkeit der Burst-Aktivität der Aktionspotentiale und einem Anstieg des intrazellulären Kalziums konnte gezeigt werden. Des Weiteren kann GnRH in Arc GnRHR-Neuronen gleichzeitig die Aktionspotentialfrequenz und die intrazelluläre Kalziumkonzentration erhöhen. Dies lässt vermuten, dass die Veränderung des intrazellulären Kalziums in der GnRH-GnRHR-Signalkaskade eine bedeutende Rolle spielt. Diese GnRH-induzierte Reaktion könnte von einem Aktionspotential-bedingten Kalziumeinstrom abhängig sein. All diese Studien etablieren eine Reihe von Methoden und liefern ausschlaggebende Informationen um die physiologischen Eigenschaften von GnRHR-Neuronen besser verstehen zu lernen.

Chapter 1

Introduction

The Gonadotropin-releasing hormone (GnRH) is the primary regulator of the mammalian sexual development and reproductive function in both male and female via hypothalamic-pituitary-gonadal (HPG) axis. In addition to this classical HPG axis, GnRH is also involved in regulating the signal and neurons in the brain through the GnRH receptor (GnRHR), which is not well understood. The reproductive physiology between female and male mouse is different. This thesis will focus on female mice.

1.1 Reproductive physiology of female mouse

1.1.1 The Hypothalamic-Pituitary-Gonadal (HPG) axis

Mammalian reproduction depends on the appropriate secretion of gonadotropin-releasing hormone (GnRH) from the brain. A few thousands of GnRH neurons are observed in the ventral preoptic area of the brain, with a small number scattered throughout the hypothalamus (Silverman et al., 1988; Merchenthaler et al., 1989). GnRH neurons project their axons to the external zone of the median eminence and release GnRH into the hypophyseal portal system (Figure 1.1) (Clarke and Cummins, 1982; Fink and Jamieson, 1976; Sarkar et al., 1976; Gore, 2002). The release of GnRH occurs in pulses, which substantially increases in magnitude and frequency before ovulation (Sisk et al., 2001; Knobil and Neill, 2006). To retain fertility, secreted GnRH binds to its receptor in the anterior pituitary to control the release of gonadotropins, luteinizing hormone (LH) and follicle-stimulating hormone (FSH). Both of these gonadotropins circulate in the bloodstream to act upon the ovaries to stimulate the secretion of sex steroid hormone, which subsequently regulates the oocyte maturation and ovulation during the female estrous cycle (Gore, 2002; Knobil and Neill, 2006). Importantly the precise release of GnRH in the brain is regulated by diverse signals including metabolic status, season, stress state, immune status, olfactory stimuli, etc.. Gonadal steroid hormones perform the most important effects on the GnRH neuronal function, because they provide positive and negative feedback regulations at both levels of the pituitary and the hypothalamus to modulate the synthesis and release of GnRH (Figure 1.1) (Radovick et al., 2012; Knobil and Neill, 2006; Kalra, 1983; Liu and Yen, 1983).

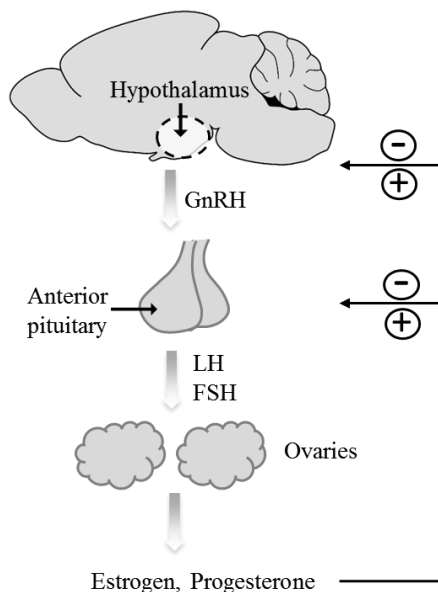


Figure 1.1 Hypothalamic-Pituitary-Gonadal (HPG) axis in female mice. GnRH neurons in the hypothalamus synthesize GnRH and released it into the hypophyseal portal system. The secreted GnRH binds to its receptor in the anterior pituitary to stimulate the release of gonadotropins, luteinizing hormone (LH) and follicle-stimulating hormone (FSH), to the circulatory system. Both gonadotropins act upon the ovaries to stimulate the secretion of sex steroid hormone. Gonadal steroid hormone provide feedback to the pituitary and hypothalamus to modulate the release of GnRH and gonadotropins.

1.1.2 The estrous cycle in female mouse

GnRH regulates the change of reproductive hormones and physiology in the female mouse through HPG axis. The consequence of the change in reproductive hormones occurs through the ovarian cycle, called estrous cycle. The duration of the estrous cycle is approximately 4-5 days. The cycle can be divided into metestrus, diestrus, proestrus, and estrus (Figure 1.2). The first hormone involved in the estrous cycle is follicle-stimulating hormone (FSH), secreted by the anterior pituitary gland. FSH stimulates the follicles in ovaries to develop into the tertiary/preovulatory follicle, especially affecting granulosa cells which produce estradiol. The period, during which the preovulatory follicles develop, is named proestrus. One theory is that the increase of estradiol induces a preovulatory GnRH surge through a positive feedback loop. The preovulatory GnRH surge progresses during the afternoon of proestrus; therefore, the proestrus is divided into the early proestrus (P_E) and late proestrus (P_L) (Figure 1.2) (Sisk et al., 2001). The increase of GnRH stimulates the gonadotrope cells in the anterior pituitary to release more luteinizing hormone (LH). In the following period, a surge of LH secreted from the anterior pituitary triggers the ovulation. This period is called estrus. After ovulation, the follicles transform into the corpus luteum, producing estrogen and progesterone. These hormones change the endometrium lining for

implantation. The early luteal phase is metestrus, during which progesterone is the dominant hormone. The following phase is diestrus. If there is no nidation, the corpus luteum shrinks, leading to the decrease of progesterone. At the end of the luteal phase, FSH is secreted again and the next estrous cycle starts. (Croy et al., 2013; Knobil and Neill, 2006)

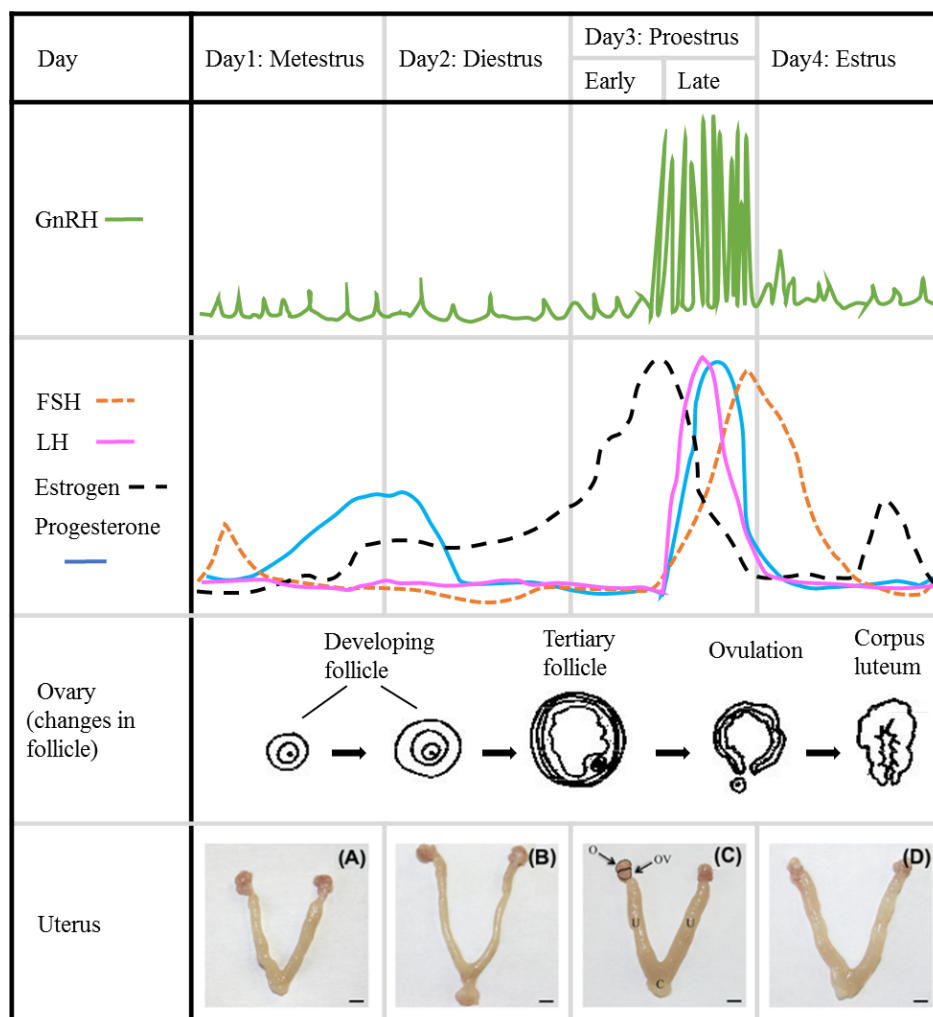


Figure 1.2 The reproductive hormone and physiological changes during the female estrous cycle. The estrous cycle in the female mouse is approximately 4-5 days, which is divided into metestrus, diestrus, proestrus (early, late) and estrus. GnRH is released in small pulses and substantially increases in magnitude and frequency before the ovulation. GnRH surge occurs in the late proestrus. FSH, LH, estrogen, and progesterone fluctuate during the estrous cycle. The follicles in ovaries are stimulated by FSH to develop into the tertiary/preovulatory follicle. A surge of luteinizing hormone (LH) initiate ovulation and the rest part of follicle become corpus luteum secreting progesterone. The weight and lining of the uterus also change during the estrous cycle. FSH, follicle-stimulating hormone; LH, luteinizing hormone; O, ovary; OV, oviduct; U, uterus; C, cervix. Illustration combining data from laboratories hormonal level in the rat blood sample or from microdialysis of the rat median eminence (Butcher et al., 1974; Sisk et al., 2001a). The pictures of uteri are adapted and modified from (Croy et al., 2013).

1.2 GnRH

1.2.1 Types and structure of GnRH

Gonadotropin-releasing hormone (GnRH) is a pivotal hormone, driving sexual maturation and reproductive cyclicality. It was first isolated from pig hypothalamus (Baba et al., 1971; Matsuo et al., 1971; Schally et al., 1971) and subsequently observed in the brain of all vertebrates (Gore, 2002). Nomenclature Committee differentiated GnRH into three types, advocated by the laboratory of Russell Fernald (Fernald and White, 1999). The hypophysiotropic GnRH, mainly found in the preoptic area of the anterior hypothalamus, is named as GnRH-I regulating pituitary gonadotropin (Gore, 2002). Another population of GnRH observed primarily in the midbrain is called GnRH-II. GnRH-II decapeptide molecule differs at several amino acids from the GnRH-I (Millar, 2003). The third type of GnRH referred as GnRH-III, is identified primarily in olfactory and forebrain regions, as found in several organisms including fish, amphibians, and mammals (Kah et al., 2004; Ramakrishnappa et al., 2005). GnRH in this thesis, if not specifically indicated, refers to GnRH-I.

GnRH molecular is a decapeptide (pGlu-His-Trp-Ser-Tyr-Gly-Leu-Arg-Pro-Gly.NH₂), which is highly conserved across species indicating that these features are important for receptor binding and activation (Seeburg and Adelman in 1984) (Figure 1.3). The molecule GnRH is bent around the achiral glycine in position six and bind to the GnRH pituitary receptor in the folded conformation. Both of the NH₂ and COOH termini are involved in the receptor binding, whereas only the NH₂ ending can activate the GnRHR. (Millar, 2005; Millar and Newton, 2013).

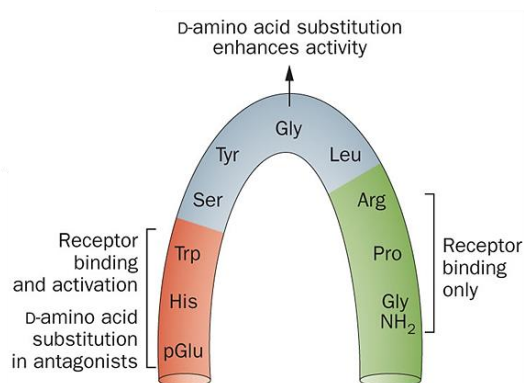


Figure 1.3 Schematic representation of mammalian GnRH in the folded conformation. GnRH is bent around the achiral glycine in position six and bind to the GnRH pituitary receptor in the folded conformation. Substitution with D-amino acids in this position stabilizes the folded conformation, increases binding affinity and decreases metabolic clearance. This feature is incorporated in all agonist and antagonist analogs. The amino (red) and carboxyl (green) termini are involved in receptor binding. The amino terminus alone is involved in receptor activation. The substitutions in this region produce antagonists. Adapted from (Millar and Newton, 2013)

1.2.2 GnRH-secreting neurons

Gonadotropin-releasing hormone (GnRH)-secreting neurons (GnRH neurons) originate from the nasal placode and migrate to the anterior hypothalamus during embryonic development (Schwanzel-Fukuda and Pfaff, 1989; Urbanski, 2012). Interestingly, in sexually mature animals GnRH neurons remain connected with the olfactory system (Boehm et al., 2005; Yoon et al., 2005), which process a variety of sensory signals (Del Punta et al., 2002; Haga et al., 2010; Leinders-Zufall et al., 2000, 2004, 2009) and influence numerous behaviors such as reproduction (Insel and Fernald, 2004; Tirindelli et al., 2009). However, the neural circuits and individual neurons underlying olfactory-induced modulation of the reproductive axis have not been identified. In rodent species, the majority of GnRH neurons (~800 neurons) are found in the ventral preoptic area of the brain, with a smaller number scattered throughout the hypothalamus (Clarke, 1987). With the development of genetic transneuronal tracing technique, GnRH neurons are found to communicate with an extraordinary complex neuronal network. These neurons integrate information from all major hypothalamic subdivisions and also from specific areas of the brain stem, like limbic system, basal ganglia, motor and sensory cortex (Boehm et al., 2005). As a part of HPG axis, GnRH neurons project to the external (secretory) zone of the median eminence, where terminals are shown in proximity to the primary capillary bed of hypophyseal portal system (Page and Dovey-Hartman, 1984). In addition, GnRH neurons send axons to the organum vasculosum of the lamina terminalis (Rothfeld and Gross, 1985). Sarkar et al. measured the level of GnRH in plasma from anesthetized rats and demonstrated a preovulatory surge in GnRH, suggesting that this is the origin of the preovulatory surge in LH secretion (Sarkar et al., in 1976). GnRH neurons have inherent phasic rhythm and release GnRH in discrete pulses (Suter et al., 2000). Studies showed that the frequency and amplitude of GnRH stimulation provide signals for differential regulation of LH and FSH secretion (Haisenleder et al., 1990; Kaiser et al., 1997; Savoy-Moore and Swartz, 1987; Wildt et al., 1981). At higher GnRH pulse frequency (one pulse every 30 minutes) LH secretion increases more than FSH secretion, whereas at lower GnRH pulse frequencies (one pulse every 120 minutes) FSH secretion is favored (Kaiser et al., 1997). During the female reproductive cycle, GnRH is released in small mini-pulses, and its amplitude and frequency are substantially increased during the late proestrus to induce ovulation (Levine et al., 1982; Wildt et al., 1981) (Figure 1.2).

1.3 GnRHR

1.3.1 Types and structure of GnRHR

GnRH is secreted in a pulsatile manner from the hypothalamus and released into median eminence. The GnRH travels down with blood stream to anterior pituitary and binds to its receptors with high affinity on pituitary gonadotropes to stimulate the release of LH and FSH. The amino acid sequence of the GnRHR was first cloned from the pituitary α T3 gonadotrope cell line (Tsutsumi et al., 1992). Three GnRHR types have been reported. Type I and II GnRHRs can be detected in most vertebrates, whereas type III occurs mainly in non-mammalians. In rodents, only GnRHR type I is functionally expressed (Millar, 2005). If not indicated, in this thesis GnRHR refers to GnRHR type I. GnRHR is a member of the rhodopsin-like G-protein-coupled receptor (GPCR) superfamily, containing seven transmembrane domains (TMDs) and an extracellular amino-terminus. However, the GnRHR lacks a typical intracellular C-terminus (Tsutsumi et al., 1992; Sealfon et al., 1997) (Figure 1.4). In general, the intracellular loops (ICLs) and the carboxyl-terminal intracellular tail are thought to engage the G protein. Mammalian GnRHR is unique due to lacking a carboxyl-terminal tail. In this regard, the carboxyl-terminal of ICL3 and a region in ICL2 are supposed to couple to G-protein (Millar and Pawson, 2004).

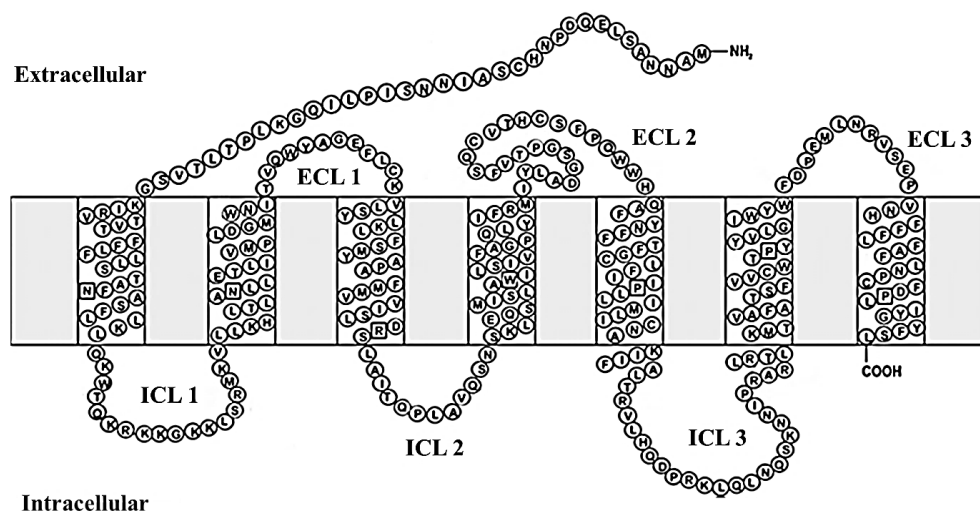


Figure 1.4 Two-dimensional representation of the GnRHR. The GnRHR consists of 328 amino acids and 7-transmembrane (TM) α -helical domains (boxed) which are connected by the three extracellular loops (ECLs) and the three intracellular loops (ICLs). The carboxyl-terminus is completely absent. Adapted from (Millar et al., 2004).

1.3.2 The distribution of GnRHR neurons in mouse brain

GnRHR mRNA and GnRH binding sites have been identified in multiple brain areas (Badr and Pelletier, 1987; Jennes et al., 1997). Wen et al., 2008 developed a new genetic mouse model to identify GnRHR neurons in the brain. By crossbreeding GnRHR-IRES-Cre (GRIC) mice to ROSA26-CAGS-tauGFP (eRosa26- τ GFP) reporter mice, GnRHR neurons can be visualized in live brain slices using the fluorescent τ GFP, a green fluorescent protein (Wen et al., 2011). GnRHR neurons are observed in numerous brain areas implicated in sexual behavior and processing olfactory information to the hypothalamus. As an extremely important brain area involved in the mediation of endocrine, autonomic and behavioral functions, hypothalamus also express abundant of GnRHR neurons for example in the periventricular hypothalamus (Pe), dorsal medial hypothalamus (DM), and arcuate nucleus (Arc) (Figure 1.5). Here we focus on the physiological function of GnRHR neurons in Pe and Arc.

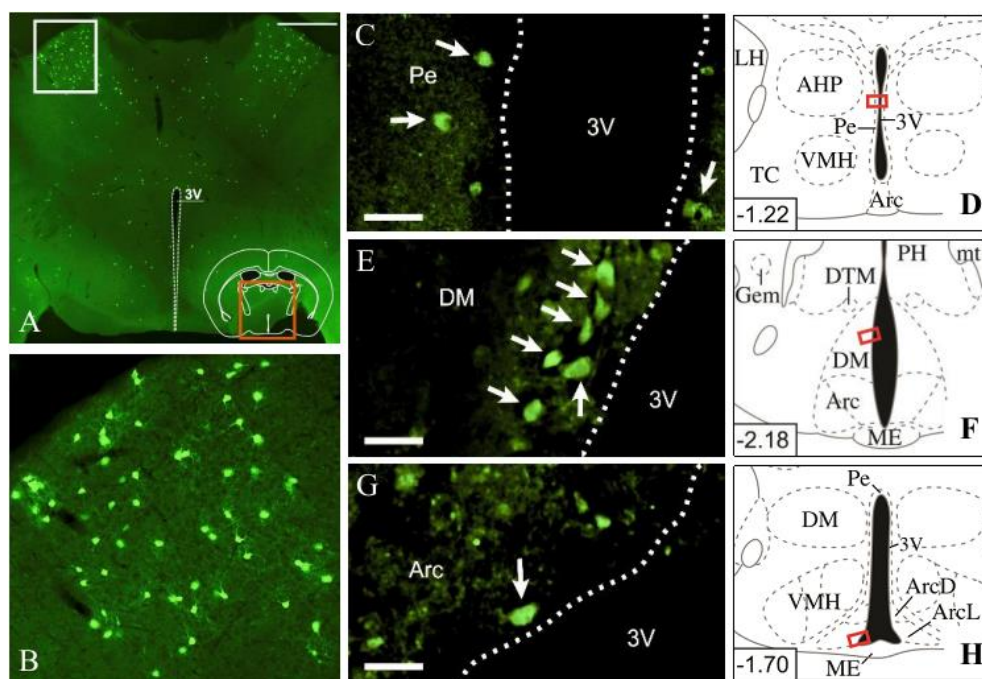


Figure 1.5 GnRHR neurons occur in different brain areas. *A:* Immunostaining of a GRIC/R26-YFP mouse brain slice shows GnRHR expression in different brain areas. *B:* Magnified image (white square) of the thalamus. *C, E, and G,* Individual GnRHR neurons displaying robust τ GFP fluorescence (arrows) are easily visible in 250 μ m thick coronal brain slices from the Pe (*C*), the Arc (*E*), and the DM (*G*). Scale bars is 20 μ m. The schematic diagrams in *D, F, and H* indicate the imaged area (red box) shown in *C, E, and G*, respectively. 3V: third ventricle. The numbers in lower left corner indicate the distance (mm) from bregma. Adapted from (Wen et al., 2011).

Periventricular hypothalamus (Pe) is a thin layer of neurons located in the wall of the third ventricular (3V) in the rostral, intermediate, and caudal hypothalamus (Figure 1.5 C-H). Studies found that Pe does not have an effective blood-brain barrier (Ueno et al., 2000). Due to this special location of Pe, GnRHR neurons are potentially susceptible to various endogenous GnRH sources, such as GnRH-secreting fibers, third ventricular cerebrospinal fluid, or the cerebrovascular system. Therefore, it is interesting to investigate how the endogenous GnRH regulates the GnRHR neurons in this region.

Arcuate nucleus (Arc), next to Pe, is located in the ventral hypothalamus and extends along the base of the 3rd ventricle in close apposition to the median eminence (Figure 1.5 G-H). The neurons in Arc receive afferents from (and send efferents to) numerous brain regions. The Arc plays an important role in the regulation of hormone secretion from the pituitary gland (Bluet-Pajot et al., 1998; Crowley, 2015; Voogt et al., 2001; Yeo, 2013), energy metabolism (Cone et al., 2001; Kim et al., 2014; Sainsbury and Zhang, 2010), cardiovascular regulation (Sapru, 2013) and so on. In arcuate nucleus, there are two important groups of neuroendocrine neurons with nerve endings in the median eminence. One population are dopaminergic neurons, called tuberoinfundibular dopamine (TIDA), which regulate the secretion of prolactin and in turn control the production of milk. TIDA neurons release dopamine into the median eminence and transport it to the anterior pituitary gland to inhibit prolactin secretion (Crowley, 2015; Voogt et al., 2001). Immunohistochemical staining coupled with confocal microscopy studies showed that GnRH neurons communicate directly with TIDA neurons in the adult female (Mitchell et al., 2003). However, the evidence of expression of GnRHR on TIDA neuron is still ambiguous and what functions GnRHR play in Arc are not clear.

1.3.3 The intracellular pathway mediated by GnRHR

G-protein-coupled receptors (GPCRS) are a large class of integral membrane protein receptors, which are divided into class A Rhodopsin-related receptors, class B Secretin and Adhesion-related receptors, and class C Glutamate-related receptors. GnRHR is a member of class A GPCR, Rhodopsin-related receptors (Millar and Pawson, 2004; Reinhart et al., 1992; Tsutsumi et al., 1992). Most studies of the GnRHR-activating intracellular pathway are mainly based on the function of type I GnRHR in pituitary gonadotropes. It is proposed that GnRHR in pituitary gonadotropes interacts mainly with $G\alpha_{q/11}$, which subsequently activates phospholipase C (PLC) (Grosse et al.,

2000; Hsieh and Martin, 1992; Naor et al., 1986) (Figure 1.6). The activation of PLC hydrolyzes phosphatidylinositol 4,5-bisphosphate (PIP₂) into the second messenger inositol 1, 4, 5-trisphosphate (IP₃) and diacylglycerol (DAG) (Neves et al., 2002). DAG could induce external Ca²⁺ influx via Ca²⁺ permeable membrane channels, for example, via transient receptor potential (TRP) channels (Numata et al., 2011). Meanwhile, the increased intracellular IP₃ activates IP₃ receptor (IP₃R), leading to Ca²⁺ release from endoplasmic reticulum (ER) into the cytosol. The increase of Ca²⁺ near ER may also activate ryanodine receptor (RyR) which transport Ca²⁺ from ER to the cytoplasm (Berridge, 1998). To replenish the level of calcium in the ER, the sarco/endoplasmic reticulum Ca²⁺-ATPase (SERCA) pumps the elevated cytosolic Ca²⁺ back to the ER (Periasamy and Kalyanasundaram, 2007). However, some studies reported that GnRHR may interact with other G-proteins like G α_i , G α_s to mediate the various biological actions (Hawes et al., 1993; Liu et al., 2002; Stanislaus et al., 1998).

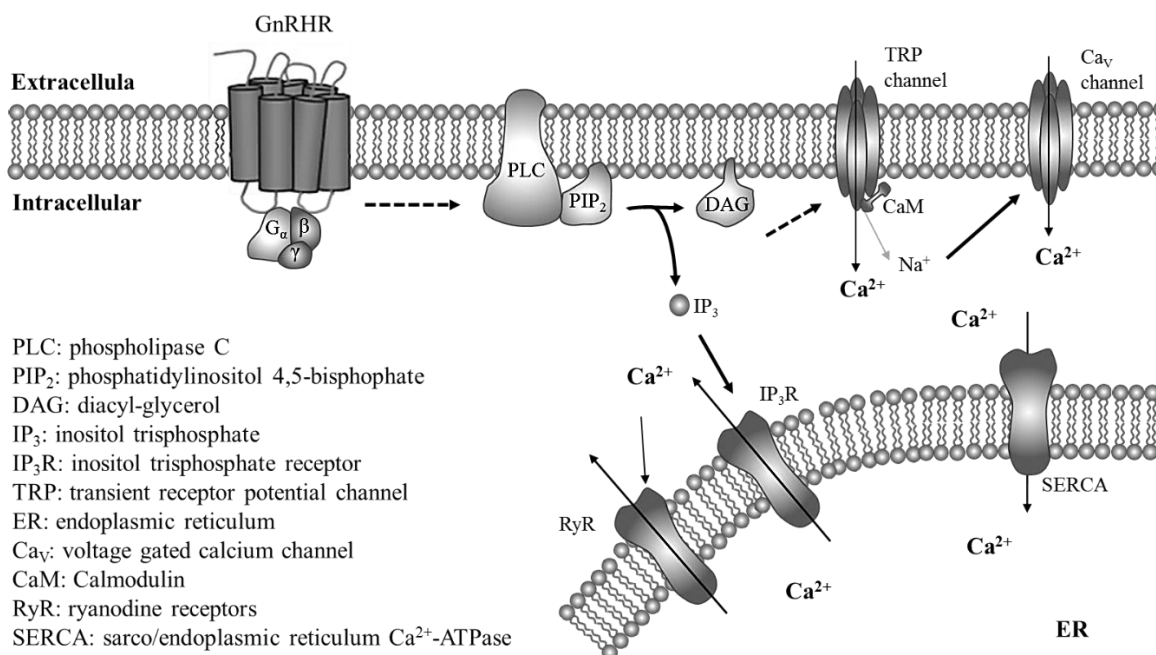


Figure 1.6 Proposed intracellular signal pathway in hypothalamic GnRHR neurons. GnRHR interacts with G $\alpha_{q/11}$, which subsequently activates phospholipase C (PLC). The activation of PLC hydrolyzes the phosphatidylinositol 4,5-bisphosphate (PIP₂) into the second messenger inositol 1, 4, 5-tris-phosphate (IP₃) and diacylglycerol (DAG). DAG could induce external Ca²⁺ influx via Ca²⁺ permeable ion selective membrane channels, for example, transient receptor potential (TRP) channel. The subsequent depolarization could trigger the opening of voltage-gated calcium channel (Ca_v). The increased intracellular IP₃ activates IP₃ receptor (IP₃R), leading to Ca²⁺ release from endoplasmic reticulum (ER) into the cytosol. The increase of Ca²⁺ near ER may activate ryanodine receptor (RyR) which transport Ca²⁺ from ER to the cytoplasm. The sarco/endoplasmic reticulum Ca²⁺-ATPase (SERCA) move the elevated cytosolic Ca²⁺ back and refill the Ca²⁺ in the ER.

The rise in intracellular Ca^{2+} has many important functions for neurons. One main function of the increase of intracellular Ca^{2+} is to trigger the neurotransmitter release (Südhof, 2012). The action potential can open the voltage-dependent Ca^{2+} in the plasma membrane, allowing Ca^{2+} to enter the presynaptic active zone, which subsequently triggers the neurotransmitter release. Another function is that Ca^{2+} can lead to a modulation of neuronal excitability by altering membrane potential (Berridge, 1998). For example, burst firing is a common firing pattern for neuroendocrine neurons (Chu et al., 2012; Grace and Bunney, 1984; Lyons et al., 2010). When the burst firing starts, the neuron is depolarized which could lead the action-potential-driven Ca^{2+} influx. During the burst, the concentration of intracellular Ca^{2+} is building up which depolarizes the neuron to produce more action potential. With the continuous firing, the low voltage-activated calcium channels inactivated and calcium-dependent potassium channels activated which repolarize the neuron to the initial potential (Jahnsen and Llinás, 1984). At this point, the burst terminates, and the intracellular Ca^{2+} concentration begins to decay slowly. The neuron then slowly depolarized and lead to a new burst (Grinnell, 1988). Moreover, the intracellular Ca^{2+} also take part in regulating multiple intracellular signaling pathways. In general, understanding the relationship of intracellular Ca^{2+} and neuronal firing patterns might help further to study the physiological function of the specific neurons.

1.4 The agonist and antagonist of GnRHR in clinical applications

Currently, a substantial number of the agonists and antagonists of GnRHR have been developed for therapeutic use in treating a wide range of hormone-dependent diseases, such as endometriosis, uterine fibroids, benign prostatic hyperplasia, and prostate cancer, as well as *in vitro* fertilization protocols (Cook and Sheridan, 2000; De Falco et al., 2006; Küpker et al., 2002; Sakai et al., 2015a; Shrestha et al., 2015). Mutations of the GnRHR have been observed in hypogonadotropic hypogonadism, a disorder characterized by delayed sexual development and inappropriately low or non-pulsatile release of gonadotropins (Layman, 2007). Therefore, pulsatile injection of GnRH or its analogs has been used in patients with hypogonadotropic hypogonadism to induce puberty (Delemarre et al., 2008). It successfully induces follicular development or sperm production (Fraietta et al., 2013; Han and Bouloux, 2010; Raivio et al., 2007). In addition, the agonists and antagonists of GnRH are also essential components of *in vitro* fertilization (IVF) protocols (Bodri et al., 2006; La Marca and Sunkara, 2014; Lambalk et al., 2006; Lee et al., 2008). For example, cetrorelix is a classic antagonist at the GnRH pituitary receptor and used for the prevention from

the premature luteinizing hormone surge in controlled ovarian stimulation cycles. One protocol for IVF uses the working principle of the HPG axis for regulating oocyte maturation and ovulation by combining a bolus of GnRH agonist during prolonged co-treatment with a GnRH antagonist (Kol and Humaidan, 2013). During the treatment of GnRHR antagonist, follicles develop into mature tertiary follicles and stop just before ovulation. The GnRH agonist displaces the antagonist in the pituitary, and thereby re-activates the GnRHR, resulting in a gonadotropin surge. Subsequently, ovulation is induced and oocytes are collected for the IVF. Depending on the usage of a GnRH agonist versus antagonist analog, GnRH analog IVF protocols are classified as GnRH agonist or GnRH antagonist protocols to facilitate infertility treatments (Reissmann et al., 2000; Duijkers et al., 1998; Shrestha et al., 2015). Furthermore, in hormone-dependent diseases, like endometriosis, uterine fibroids, polycystic ovarian syndrome, the agonists and antagonists of GnRHR are also widely used (De Falco et al., 2006; K pker et al., 2002; Nugent et al., 2000). Several reproductive related cancers are identified expressing GnRHR, including prostate cancer, and breast cancer. Studies revealed that the activation of GnRHR exhibits inhibitory effects on these cancer cells via anti-proliferation, anti-metastasis and anti-angiogenesis (Cheung et al., 2013; Kim et al., 2006; Sakai et al., 2015b). However, due to the physiological function of GnRHR neurons in the brain is still ambiguous, the influence of these treatments on the GnRHR neurons and brain function could induce adverse effects. During my thesis project, I had the opportunity to begin investigating if GnRHR in the brain can be affected by pharmacological treatment used in an IVF protocol.

1.5 Aims

Substantial studies about GnRHR are based on pituitary GnRHR-expressing neurons or cultured GnRHR cell lines. Little information is available regarding the physiological function of GnRHR neurons in the brain. The agonist and antagonist of GnRHR are widely used to treat clinical pathologies without sufficient understanding of their influence on brain function. Thus, it is urgent to investigate the physiological characteristics and the potential role of GnRHR neurons in the brain. The following objectives will be addressed:

- (1) Determine how the spontaneous firing activity of GnRHR neurons in Pe change during the female reproductive cycle as a fundamental step in understanding their physiological characteristics. Examine GnRH itself could be responsible to modulate in the spike activity of GnRHR neurons on brain slices. Identify the mechanism of the mode of GnRHR

neuronal activity regulated by the endogenous GnRH on brain slices during the female estrous cycle, using antagonist of GnRHR, cetrorelix.

- (2) Examine the potential source of GnRH for GnRHR neurons in Pe, such as GnRH-secreting neuronal fibers, third ventricular cerebrospinal fluid or the cerebrovascular system. Assuming Pe has a less constrained blood-brain barrier, identify that the *in vivo* treatment with cetrorelix into female mice can effectively block the HPG axis as in reproductive therapies. Determine whether the *in vivo* treatment with cetrorelix affect the firing activity of GnRHR neurons in Pe.
- (3) Examine the spontaneous firing activity of GnRHR neurons in Arc during the female reproductive estrous cycle and how GnRH and network modulate the GnRHR neurons in Arc. Establish the method to measure calcium signal and neuron firing activity simultaneously and determine the relationship between the calcium signal and GnRHR neurons firing activity. Observe how the calcium signal responds to GnRH stimulation as a first step in understanding the intracellular pathway of GnRHR in Arc.

These studies will reveal detailed information of GnRHR neurons and provide new insights into their physiological function in the brain. This work is highly relevant to clinical treatments and generates important new knowledge for the potential side effects of the clinical application of the agonist and antagonist of GnRHR.

References

1. Baba, Y., Matsuo, H., and Schally, A.V. (1971). Structure of the porcine LH- and FSH-releasing hormone. II. Confirmation of the proposed structure by conventional sequential analyses. *Biochem. Biophys. Res. Commun.* *44*, 459–463.
2. Badr, M., and Pelletier, G. (1987). Characterization and autoradiographic localization of LHRH receptors in the rat brain. *Synap. N. Y. N I*, 567–571.
3. Berridge, M.J. (1998). Neuronal Calcium Signaling. *Neuron* *21*, 13–26.
4. Bluett-Pajot, M.T., Epelbaum, J., Gourdj, D., Hammond, C., and Kordon, C. (1998). Hypothalamic and hypophyseal regulation of growth hormone secretion. *Cell. Mol. Neurobiol.* *18*, 101–123.

5. Bodri, D., Vernaeva, V., Guillén, J.J., Vidal, R., Figueras, F., and Coll, O. (2006). Comparison between a GnRH antagonist and a GnRH agonist flare-up protocol in oocyte donors: a randomized clinical trial. *Hum. Reprod. Oxf. Engl.* *21*, 2246–2251.
6. Boehm, U., Zou, Z., and Buck, L.B. (2005). Feedback loops link odor and pheromone signaling with reproduction. *Cell* *123*, 683–695.
7. Butcher, R.L., Collins, W.E., and Fugo, N.W. (1974). Plasma concentration of LH, FSH, prolactin, progesterone and estradiol-17beta throughout the 4-day estrous cycle of the rat. *Endocrinology* *94*, 1704–1708.
8. Cheung, L.W., Yung, S., Chan, T.-M., Leung, P.C., and Wong, A.S. (2013). Targeting Gonadotropin-releasing Hormone Receptor Inhibits the Early Step of Ovarian Cancer Metastasis by Modulating Tumor-mesothelial Adhesion. *Mol. Ther.* *21*, 78–90.
9. Chu, Z., Tomaiuolo, M., Bertram, R., and Moenter, S.M. (2012). Two types of burst firing in gonadotrophin-releasing hormone neurones. *J. Neuroendocrinol.* *24*, 1065–1077.
10. Clarke, I.J. (1987). GnRH and ovarian hormone feedback. *Oxf. Rev. Reprod. Biol.* *9*, 54–95.
11. Cone, R.D., Cowley, M.A., Butler, A.A., Fan, W., Marks, D.L., and Low, M.J. (2001). The arcuate nucleus as a conduit for diverse signals relevant to energy homeostasis. *Int. J. Obes. Relat. Metab. Disord. J. Int. Assoc. Study Obes.* *25 Suppl 5*, S63–S67.
12. Cook, T., and Sheridan, W.P. (2000). Development of GnRH antagonists for prostate cancer: new approaches to treatment. *The Oncologist* *5*, 162–168.
13. Crowley, W.R. (2015). Neuroendocrine regulation of lactation and milk production. *Compr. Physiol.* *5*, 255–291.
14. Croy, B.A., Yamada, A.T., DeMayo, F.J., and Adamson, S.L. (2013). *The Guide to Investigation of Mouse Pregnancy* (Academic Press).
15. De Falco, M., Pollio, F., Pontillo, M., Ambrosino, E., Busiello, A., Carbone, I.F., Ciociola, F., Di Nardo, M.A., Landi, L., and Di Lieto, A. (2006). GnRH agonists and antagonists in the preoperative therapy of uterine fibroids: literature review. *Minerva Ginecol.* *58*, 553–560.
16. Del Punta, K., Leinders-Zufall, T., Rodriguez, I., Jukam, D., Wysocki, C.J., Ogawa, S., Zufall, F., and Mombaerts, P. (2002). Deficient pheromone responses in mice lacking a cluster of vomeronasal receptor genes. *Nature* *419*, 70–74.
17. Duijkers, I.J., Klipping, C., Willemsen, W.N., Krone, D., Schneider, E., Niebch, G., and Hermann, R. (1998). Single and multiple dose pharmacokinetics and pharmacodynamics of the gonadotrophin-releasing hormone antagonist Cetrorelix in healthy female volunteers. *Hum. Reprod. Oxf. Engl.* *13*, 2392–2398.

18. Fernald, R.D., and White, R.B. (1999). Gonadotropin-releasing hormone genes: phylogeny, structure, and functions. *Front. Neuroendocrinol.* 20, 224–240.
19. Fraietta, R., Zylberstejn, D.S., and Esteves, S.C. (2013). Hypogonadotropic hypogonadism revisited. *Clin. São Paulo Braz.* 68 *Suppl 1*, 81–88.
20. Gore, A.C. (2002). *GnRH: The Master Molecule of Reproduction* (Kluwer Academic Publishers).
21. Grace, A.A., and Bunney, B.S. (1984). The control of firing pattern in nigral dopamine neurons: burst firing. *J. Neurosci. Off. J. Soc. Neurosci.* 4, 2877–2890.
22. Grinnell, A.D. (1988). *Calcium and Ion Channel Modulation* (Springer Science & Business Media).
23. Grosse, R., Schmid, A., Schöneberg, T., Herrlich, A., Muhn, P., Schultz, G., and Gudermann, T. (2000). Gonadotropin-releasing hormone receptor initiates multiple signaling pathways by exclusively coupling to G_(q/11) proteins. *J. Biol. Chem.* 275, 9193–9200.
24. Haga, S., Hattori, T., Sato, T., Sato, K., Matsuda, S., Kobayakawa, R., Sakano, H., Yoshihara, Y., Kikusui, T., and Touhara, K. (2010). The male mouse pheromone ESP1 enhances female sexual receptive behaviour through a specific vomeronasal receptor. *Nature* 466, 118–122.
25. Haisenleder, D.J., Ortolano, G.A., Dalkin, A.C., Ellis, T.R., Paul, S.J., and Marshall, J.C. (1990). Differential Regulation of Gonadotropin Subunit Gene Expression by Gonadotropin-Releasing Hormone Pulse Amplitude in Female Rats. *Endocrinology* 127, 2869–2875.
26. Han, T.S., and Bouloux, P.M.G. (2010). What is the optimal therapy for young males with hypogonadotropic hypogonadism? *Clin. Endocrinol. (Oxf.)* 72, 731–737.
27. Hawes, B.E., Barnes, S., and Conn, P.M. (1993). Cholera toxin and pertussis toxin provoke differential effects on luteinizing hormone release, inositol phosphate production, and gonadotropin-releasing hormone (GnRH) receptor binding in the gonadotrope: evidence for multiple guanyl nucleotide binding proteins in GnRH action. *Endocrinology* 132, 2124–2130.
28. Hsieh, K.P., and Martin, T.F. (1992). Thyrotropin-releasing hormone and gonadotropin-releasing hormone receptors activate phospholipase C by coupling to the guanosine triphosphate-binding proteins G_q and G₁₁. *Mol. Endocrinol. Baltim. Md* 6, 1673–1681.
29. Insel, T.R., and Fernald, R.D. (2004). How the brain processes social information: searching for the social brain. *Annu. Rev. Neurosci.* 27, 697–722.
30. Jahnsen, H., and Llinás, R. (1984). Voltage-dependent burst-to-tonic switching of thalamic cell activity: an in vitro study. *Arch. Ital. Biol.* 122, 73–82.

31. Jennes, L., Eyigor, O., Janovick, J.A., and Conn, P.M. (1997). Brain gonadotropin releasing hormone receptors: localization and regulation. *Recent Prog. Horm. Res.* 52, 475–490; discussion 490–491.
32. Kah, O., Lethimonier, C., and Lareyre, J.-J. (2004). Gonadotrophin-releasing hormone (GnRH) in the animal kingdom. *J. Société Biol.* 198, 53–60.
33. Kaiser, U.B., Jakubowiak, A., Steinberger, A., and Chin, W.W. (1997). Differential effects of gonadotropin-releasing hormone (GnRH) pulse frequency on gonadotropin subunit and GnRH receptor messenger ribonucleic acid levels in vitro. *Endocrinology* 138, 1224–1231.
34. Kalra, S.P., and Kalra, P.S. (1983). Neural regulation of luteinizing hormone secretion in the rat. *Endocr. Rev.* 4, 311–351.
35. Kim, J.D., Leyva, S., and Diano, S. (2014). Hormonal regulation of the hypothalamic melanocortin system. *Front. Physiol.* 5, 480.
36. Kim, K.-Y., Choi, K.-C., Auersperg, N., and Leung, P.C.K. (2006). Mechanism of gonadotropin-releasing hormone (GnRH)-I and -II-induced cell growth inhibition in ovarian cancer cells: role of the GnRH-I receptor and protein kinase C pathway. *Endocr. Relat. Cancer* 13, 211–220.
37. Knobil, E., and Neill, J.D. (2006). *Knobil and Neill’s Physiology of Reproduction* (Gulf Professional Publishing).
38. Kol, S., and Humaidan, P. (2013). GnRH agonist triggering: recent developments. *Reprod. Biomed. Online* 26, 226–230.
39. Küpker, W., Felberbaum, R.E., Krapp, M., Schill, T., Malik, E., and Diedrich, K. (2002). Use of GnRH antagonists in the treatment of endometriosis. *Reprod. Biomed. Online* 5, 12–16.
40. La Marca, A., and Sunkara, S.K. (2014). Individualization of controlled ovarian stimulation in IVF using ovarian reserve markers: from theory to practice. *Hum. Reprod. Update* 20, 124–140.
41. Layman, L.C. (2007). Hypogonadotropic hypogonadism. *Endocrinol. Metab. Clin. North Am.* 36, 283–296.
42. Lee, T.-H., Lin, Y.-H., Seow, K.-M., Hwang, J.-L., Tzeng, C.-R., and Yang, Y.-S. (2008). Effectiveness of cetrorelix for the prevention of premature luteinizing hormone surge during controlled ovarian stimulation using letrozole and gonadotropins: a randomized trial. *Fertil. Steril.* 90, 113–120.
43. Leinders-Zufall, T., Lane, A.P., Puche, A.C., Ma, W., Novotny, M.V., Shipley, M.T., and Zufall, F. (2000). Ultrasensitive pheromone detection by mammalian vomeronasal neurons. *Nature* 405, 792–796.

44. Leinders-Zufall, T., Brennan, P., Widmayer, P., S, P.C., Maul-Pavicic, A., Jäger, M., Li, X.-H., Breer, H., Zufall, F., and Boehm, T. (2004). MHC Class I Peptides as Chemosensory Signals in the Vomeronasal Organ. *Science* *306*, 1033–1037.
45. Leinders-Zufall, T., Ishii, T., Mombaerts, P., Zufall, F., and Boehm, T. (2009). Structural requirements for the activation of vomeronasal sensory neurons by MHC peptides. *Nat. Neurosci.* *12*, 1551–1558.
46. Levine, J.E., Pau, K.Y., Ramirez, V.D., and Jackson, G.L. (1982). Simultaneous measurement of luteinizing hormone-releasing hormone and luteinizing hormone release in unanesthetized, ovariectomized sheep. *Endocrinology* *111*, 1449–1455.
47. Liu, J.H., and Yen, S.S. (1983). Induction of midcycle gonadotropin surge by ovarian steroids in women: a critical evaluation. *J. Clin. Endocrinol. Metab.* *57*, 797–802.
48. Liu, F., Usui, I., Evans, L.G., Austin, D.A., Mellon, P.L., Olefsky, J.M., and Webster, N.J.G. (2002). Involvement of both G_(q/11) and G_(s) proteins in gonadotropin-releasing hormone receptor-mediated signaling in L beta T2 cells. *J. Biol. Chem.* *277*, 32099–32108.
49. Lyons, D.J., Horjales-Araujo, E., and Broberger, C. (2010). Synchronized Network Oscillations in Rat Tuberoinfundibular Dopamine Neurons: Switch to Tonic Discharge by Thyrotropin-Releasing Hormone. *Neuron* *65*, 217–229.
50. Matsuo, H., Baba, Y., Nair, R.M., Arimura, A., and Schally, A.V. (1971). Structure of the porcine LH- and FSH-releasing hormone. I. The proposed amino acid sequence. *Biochem. Biophys. Res. Commun.* *43*, 1334–1339.
51. Merchenthaler, I., Culler, M.D., Petrusz, P., Flerkó, B., and Negro-Vilar, A. (1989). Immunocytochemical localization of the gonadotropin-releasing hormone-associated peptide portion of the LHRH precursor in the hypothalamus and extrahypothalamic regions of the rat central nervous system. *Cell Tissue Res.* *255*, 5–14.
52. Millar, R.P. (2003). GnRH II and type II GnRH receptors. *Trends Endocrinol. Metab. TEM* *14*, 35–43.
53. Millar, R.P., and Pawson, A.J. (2004). Outside-in and inside-out signaling: the new concept that selectivity of ligand binding at the gonadotropin-releasing hormone receptor is modulated by the intracellular environment. *Endocrinology* *145*, 3590–3593.
54. Millar, R.P., Lu, Z.-L., Pawson, A.J., Flanagan, C.A., Morgan, K., and Maudsley, S.R. (2004). Gonadotropin-Releasing Hormone Receptors. *Endocr. Rev.* *25*, 235–275.
55. Millar, R.P. (2005). GnRHs and GnRH receptors. *Anim. Reprod. Sci.* *88*, 5–28.
56. Millar, R.P., and Newton, C.L. (2013). Current and future applications of GnRH, kisspeptin and neurokinin B analogues. *Nat. Rev. Endocrinol.* *9*, 451–466.
57. Mitchell, V., Loyens, A., Spergel, D.J., Flactif, M., Poulain, P., Tramu, G., and Beauvillain, J.-C. (2003). A confocal microscopic study of gonadotropin-releasing hormone (GnRH)

- neuron inputs to dopaminergic neurons containing estrogen receptor alpha in the arcuate nucleus of GnRH-green fluorescent protein transgenic mice. *Neuroendocrinology* 77, 198–207.
58. Naor, Z., Azrad, A., Limor, R., Zakut, H., and Lotan, M. (1986). Gonadotropin-releasing hormone activates a rapid Ca^{2+} -independent phosphodiester hydrolysis of polyphosphoinositides in pituitary gonadotrophs. *J. Biol. Chem.* 261, 12506–12512.
59. Neves, S.R., Ram, P.T., and Iyengar, R. (2002). G Protein Pathways. *Science* 296, 1636–1639.
60. Nugent, D., Vandekerckhove, P., Hughes, E., Arnot, M., and Lilford, R. (2000). Gonadotrophin therapy for ovulation induction in subfertility associated with polycystic ovary syndrome. *Cochrane Database Syst. Rev.* 4, CD000410.
61. Numata, T., Kiyonaka, S., Kato, K., Takahashi, N., and Mori, Y. (2011). Activation of TRP Channels in Mammalian Systems. In *TRP Channels*, M.X. Zhu, ed. (Boca Raton (FL): CRC Press/Taylor & Francis).
62. Page, R.B., and Dovey-Hartman, B.J. (1984). Neurohemal contact in the internal zone of the rabbit median eminence. *J. Comp. Neurol.* 226, 274–288.
63. Periasamy, M., and Kalyanasundaram, A. (2007). SERCA pump isoforms: their role in calcium transport and disease. *Muscle Nerve* 35, 430–442.
64. Radovick, S., Levine, J.E., and Wolfe, A. (2012). Estrogenic regulation of the GnRH neuron. *Front. Endocrinol.* 3, 52.
65. Raivio, T., Falardeau, J., Dwyer, A., Quinton, R., Hayes, F.J., Hughes, V.A., Cole, L.W., Pearce, S.H., Lee, H., Boepple, P., et al. (2007). Reversal of Idiopathic Hypogonadotropic Hypogonadism. *N. Engl. J. Med.* 357, 863–873.
66. Ramakrishnappa, N., Rajamahendran, R., Lin, Y.-M., and Leung, P.C.K. (2005). GnRH in non-hypothalamic reproductive tissues. *Anim. Reprod. Sci.* 88, 95–113.
67. Reinhart, J., Mertz, L.M., and Catt, K.J. (1992). Molecular cloning and expression of cDNA encoding the murine gonadotropin-releasing hormone receptor. *J. Biol. Chem.* 267, 21281–21284.
68. Reissmann, T., Schally, A.V., Bouchard, P., Riethmiiller, H., and Engel, J. (2000). The LHRH antagonist cetrorelix: a review. *Hum. Reprod. Update* 6, 322–331.
69. Rothfeld, J.M., and Gross, D.S. (1985). Gonadotropin-releasing hormone within the organum vasculosum lamina terminalis in the ovariectomized, estrogen/progesterone-treated rat: A quantitative immunocytochemical study using image analysis. *Brain Res.* 338, 309–315.
70. Sainsbury, A., and Zhang, L. (2010). Role of the arcuate nucleus of the hypothalamus in regulation of body weight during energy deficit. *Mol. Cell. Endocrinol.* 316, 109–119.

71. Sakai, M., Elhilali, M., and Papadopoulos, V. (2015a). The GnRH Antagonist Degarelix Directly Inhibits Benign Prostate Hyperplasia Cell Growth. *Horm. Metab. Res. Horm. Stoffwechselforschung Horm. Métabolisme* 47, 925–931.
72. Sakai, M., Martinez-Arguelles, D.B., Patterson, N.H., Chaurand, P., and Papadopoulos, V. (2015b). In Search of the Molecular Mechanisms Mediating the Inhibitory Effect of the GnRH Antagonist Degarelix on Human Prostate Cell Growth. *PLOS ONE* 10, e0120670.
73. Sapru, H.N. (2013). Role of the hypothalamic arcuate nucleus in cardiovascular regulation. *Auton. Neurosci. Basic Clin.* 175, 38–50.
74. Sarkar, D.K., Chiappa, S.A., Fink, G., and Sherwood, N.M. (1976). Gonadotropin-releasing hormone surge in pro-oestrous rats. *Nature* 264, 461–463.
75. Savoy-Moore, R.T., and Swartz, K.H. (1987). Several GnRH stimulation frequencies differentially release FSH and LH from isolated, perfused rat anterior pituitary cells. *Adv. Exp. Med. Biol.* 219, 641–645.
76. Schally, A.V., Arimura, A., Kastin, A.J., Matsuo, H., Baba, Y., Redding, T.W., Nair, R.M.G., Debeljuk, L., and White, W.F. (1971). Gonadotropin-Releasing Hormone: One Polypeptide Regulates Secretion of Luteinizing and Follicle-Stimulating Hormones. *Science* 173, 1036–1038.
77. Schwanzel-Fukuda, M., and Pfaff, D.W. (1989). Origin of luteinizing hormone-releasing hormone neurons. *Nature* 338, 161–164.
78. Sealfon, S.C., Weinstein, H., and Millar, R.P. (1997). Molecular Mechanisms of Ligand Interaction with the Gonadotropin-Releasing Hormone Receptor. *Endocr. Rev.* 18, 180–205.
79. Seeburg, P.H., and Adelman, J.P. (1984). Characterization of cDNA for precursor of human luteinizing hormone releasing hormone. *Nature* 311, 666–668.
80. Shrestha, D., La, X., and Feng, H.L. (2015). Comparison of different stimulation protocols used in in vitro fertilization: a review. *Ann. Transl. Med.* 3, 137.
81. Silverman, A.J., Kokoris, G.J., and Gibson, M.J. (1988). Quantitative analysis of synaptic input to gonadotropin-releasing hormone neurons in normal mice and hpg mice with preoptic area grafts. *Brain Res.* 443, 367–372.
82. Sisk, C.L., Richardson, H.N., Chappell, P.E., and Levine, J.E. (2001a). In vivo gonadotropin-releasing hormone secretion in female rats during peripubertal development and on proestrus. *Endocrinology* 142, 2929–2936.
83. Stanislaus, D., Ponder, S., Ji, T.H., and Conn, P.M. (1998). Gonadotropin-releasing hormone receptor couples to multiple G proteins in rat gonadotrophs and in GGH3 cells: evidence from palmitoylation and overexpression of G proteins. *Biol. Reprod.* 59, 579–586.

84. Südhof, T.C. (2012). Calcium Control of Neurotransmitter Release. Cold Spring Harb. Perspect. Biol. 4, a011353.
85. Suter, K.J., Wuarin, J.P., Smith, B.N., Dudek, F.E., and Moenter, S.M. (2000). Whole-cell recordings from preoptic/hypothalamic slices reveal burst firing in gonadotropin-releasing hormone neurons identified with green fluorescent protein in transgenic mice. *Endocrinology* 141, 3731–3736.
86. Tirindelli, R., Dibattista, M., Pifferi, S., and Menini, A. (2009). From pheromones to behavior. *Physiol. Rev.* 89, 921–956.
87. Tsutsumi, M., Zhou, W., Millar, R.P., Mellon, P.L., Roberts, J.L., Flanagan, C.A., Dong, K., Gillo, B., and Sealfon, S.C. (1992). Cloning and functional expression of a mouse gonadotropin-releasing hormone receptor. *Mol. Endocrinol.* 6, 1163–1169.
88. Ueno, M., Akiguchi, I., Hosokawa, M., Kotani, H., Kanenishi, K., and Sakamoto, H. (2000). Blood-brain barrier permeability in the periventricular areas of the normal mouse brain. *Acta Neuropathol. (Berl.)* 99, 385–392.
89. Urbanski, H. (2012). Differential roles of GnRH-I and GnRH-II neurons in the control of the primate reproductive axis. *Genomic Endocrinol.* 3, 20.
90. Voogt, J.L., Lee, Y., Yang, S., and Arbogast, L. (2001). Regulation of prolactin secretion during pregnancy and lactation. *Prog. Brain Res.* 133, 173–185.
91. Wen, S., Schwarz, J.R., Niculescu, D., Dinu, C., Bauer, C.K., Hirdes, W., and Boehm, U. (2008). Functional characterization of genetically labeled gonadotropes. *Endocrinology* 149, 2701–2711.
92. Wen, S., Götze, I.N., Mai, O., Schauer, C., Leinders-Zufall, T., and Boehm, U. (2011). Genetic identification of GnRH receptor neurons: a new model for studying neural circuits underlying reproductive physiology in the mouse brain. *Endocrinology* 152, 1515–1526.
93. Wildt, L., Häusler, A., Marshall, G., Hutchison, J.S., Plant, T.M., Belchetz, P.E., and Knobil, E. (1981). Frequency and amplitude of gonadotropin-releasing hormone stimulation and gonadotropin secretion in the rhesus monkey. *Endocrinology* 109, 376–385.
94. Yeo, S.-H. (2013). Neuronal circuits in the hypothalamus controlling gonadotrophin-releasing hormone release: the neuroanatomical projections of kisspeptin neurons. *Exp. Physiol.* 98, 1544–1549.
95. Yoon, H., Enquist, L.W., and Dulac, C. (2005). Olfactory Inputs to Hypothalamic Neurons Controlling Reproduction and Fertility. *Cell* 123, 669–682.

Chapter 2

Materials and methods

2.1 Materials

2.1.1 Chemicals and antibodies

Chemicals

Agar-Agar	Carl Roth GmbH Co.KG
2-Aminoethyldiphenylborinate, 2-APB (ab120124)	Abcam
N, N-Bis(2-hydroxyethyl)-2-aminoethanesulfonic acid (BES) BioXtra, for molecular biology, ≥99.5% (T)	Sigma-Aldrich Corp.
Bicuculine methiodid (14343)	Sigma-Aldrich Corp.
Cetrorelix acetate (C5249)	Sigma-Aldrich Corp.
Calcium chloride x2H ₂ O, CaCl ₂ x2H ₂ O	Gruessing GmbH
CGP 52432 (ab120330)	Abcam
2-Chloro-2-(trifluoromethyl)-difluoromethylether, Isoflurane	Baxter International Inc.
CNQX disodium salt (ab120044)	Abcam
D-AP5 (ab120003)	Abcam
D(+)-Glucose monohydrate for microbiology	Merck KGaA
Dimethyl Sulfoxide (DMSO)	Fisher Scientific Inc.
Disodium hydrogen phosphate, Na ₂ HPO ₄	Gruessing GmbH
Eosin G-solution 0,5% aqueous	Carl Roth
Fura-2/AM, cell permanent	Invitrogen AG
Gonadotropin-releasing hormone (GnRH), (Luteinizing Hormone-releasing Hormone, L7134)	Sigma-Aldrich Corp.

25% glutaraldehyde	Sigma-Aldrich Corp.
Hämalaunlösung sauer nach Mayer	Carl Roth
LY341495 sodium salt (ab120400)	Abcam
Magnesium sulfate, ReagentPlus®, ≥99.5%, MgSO ₄	Sigma-Aldrich Corp.
Magnesium chloride, anhydrous, assay ≥98%, MgCl ₂	Merck KGaA
2-Methylbutane, ReagentPlus®, ≥99%	Sigma-Aldrich Corp.
N-(2-hydroxyethyl) piperazine-N'-(2-ethanesulfonic acid) (HEPES)	Sigma-Aldrich Corp.
Normal horse serum, S2000	Vector Labs
Paraformaldehyde reagent grade, crystalline	Sigma-Aldrich Corp.
Pluronic® F-127, BioReagent, suitable for cell culture	Sigma-Aldrich Corp.
Potassium chloride for analysis EMSURE® ACS, Reag. Ph Eur, KCl	Merck KGaA
Potassium dihydrogen phosphate, KH ₂ PO ₄	Gruessing GmbH
Sodium chloride AnalaR NORMAPUR	VWR International
Sodium hydrogen carbonates for analysis EMSURE® ACS, Reag. Ph Eur, NaHCO ₃	Merck KGaA
Sodium hydroxide, assay ≥99%, NaOH	Gruessing GmbH
1-Stearoyl-2-arachidonoyl- <i>sn</i> -glycerol, SAG (S-6389)	Sigma-Aldrich Corp.
D (+)-Sucrose	PanReac Applichem
Tissue-Tek™ CRYO-OCT Compound	Fisher Scientific
Triton X-100	Carl Roth

Antibodies

Primary antibodies:

Chicken monoclonal anti-GFP antibody (ab13970) 1:1000	Abcam
Rat monoclonal anti-CD31 antibody (ab56299) 1:750	Abcam
Rabbit polyclonal anti-GnRH antibody (20075) 1:800	Immunostar
<i>Secondary antibodies:</i>	
Alexa-Fluor 488 goat-anti-chicken (A-11039) 1:1000	Invitrogen
Alexa-Fluor 488 donkey-anti-rat (A-21208) 1:1000	Invitrogen
Alexa-Fluor 633 donkey-anti-rat (20137) 1:1000	Biotium
Alexa-Fluor 633 goat-anti-rabbit (A-21070) 1:1000	Invitrogen

2.1.2 Solutions and buffers

Extracellular solution (S1) (oxygenated with 95% O₂/ 5% CO₂)

NaCl 120 mM, NaHCO₃ 25 mM, KCl 5 mM, BES 5 mM, CaCl₂×2H₂O 1 mM, MgSO₄ 1 mM, Glucose 10 mM, adjust osmolarity to 300 mOs/L.

Extracellular solution (S2)

NaCl 145 mM, KCl 5 mM, CaCl₂×2H₂O 1 mM, MgCl₂ 1 mM, HEPES 10 mM, titrated with NaOH to pH 7.3 and adjust osmolarity to 300 mOs/L.

High potassium solution

NaCl 90 mM, KCl 60 mM, CaCl₂×2H₂O 1 mM, MgCl₂ 1 mM, HEPES 10 mM, titrated with NaOH to pH 7.3 and adjust osmolarity to 300 mOs/L.

Synaptic blocker cocktail solution

LY341495 sodium salt 10 μM, CGP 52432 1 μM, CNQX disodium salt 10 μM, D-AP5 50 μM, Bicuculine methiodid 10 μM, diluted in S1 solution.

Agarose (4%) solution 100 ml

4 g low gelling agarose is dissolved in 100 mL double distilled water, and heat the solution until 100 °C and cooling it to room temperature.

20% Pluronic F127 solution 100 μL

0.02 g Pluronic F127 in 100 μ L DMSO, sonicate 2 min until Pluronic is dissolved

Fura-2/AM loading solution

1 vial of Fura-2/AM 50 μ g, 2 μ L 20% Pluronic F127, 18 μ L DMSO, 3900 μ L synaptic blocking solution, final loading concentration of 12 μ M Fura-2 AM, 0.0001% Pluronic F-127, and 0.4% DMSO

GnRH stimulation solution

25 mL oxygenated extracellular solution (S1), 0.1% BSA, concentration-dependent GnRH (0.1 nM; 0.3 nM; 0.5 nM; 1 nM; 3 nM; 10 nM)

4% PFA 1 L

40 g paraformaldehyde, 1 \times PBS 1 L, heat the solution and add 1 N NaOH drop from a pipette until the solution clears. Cooling the solution and titrated with HCl to pH 7.2 and adjust the volume to 1 L with 1x PBS.

Blocking solution

0.5% Triton X-100, 4% Normal horse serum, diluted in 1 \times PBS

10 \times Phosphate buffered saline solution (10 \times PBS) 1 L

NaCl 1.37 μ M, KCl 27 mM, Na₂HPO₄ 100 mM, KH₂PO₄ 20 mM, titrated with NaOH to pH 7.4 and adjust the volume to 1 L with distilled H₂O.

1 \times Phosphate buffered saline solution (1 \times PBS) 1 L

NaCl 137 mM, Na₂HPO₄ 10 mM, KCl 2.7 mM, KH₂PO₄ 2 mM, titrated with NaOH to pH 7.4 and adjust the volume to 1 L with distilled H₂O.

2.5% glutaraldehyde+2% PFA fixation solution 50mL

25% glutaraldehyde 5 mL, 4% PFA 25 mL, 1 \times PBS 20 mL.

2.1.3 Consumables

6-well Cell Culture Plates

Becton Dickinson AG

Capillary Glass, TW100-F4

World Precision Instruments

Capillary Glass, 8250, Filament, 1.50/0.86, 75 mm	A-M Systems Inc.
Disposable Pasteur Pipettes	Kimble Chase LLC
Filter Holder Swinnex®, 25 mm	EMD Millipore
Glassware, made of Borosilicate 3.3	VWR International
Heat-shrinking tubing, DERAY Set-2000	DSG-Canusa GmbH
Infusion Set with micro adjustment	Becton Dickinson AG
Liquid Blocker Pen, Super PAP	Ted Pella Inc.
Membrane Filter 0.2 µm, Supor®200 PES, 47 mm	Pall Corporation
Membrane Filter 0.2 µm, HT Tuffryn®HPS, 25 mm	Pall Corporation
Microscope slides	VWR International
Pipette Tip 20 µL, 200 µL, 1 mL	Sarstedt AG
Safe-seal micro tube 0.5 mL, 1.5 mL, 2 mL	Sarstedt AG
Single Edge Carbon Steel Razorblade	Electron Microscopy Sciences
Sterile Syringe 1 mL, 10 mL, 50 mL, 60 mL Luer-Lok	Becton Dickinson AG
Super glue, Loctite 406TM	Henkel AG
Transfer pipette 3.5 mL	Sarstedt AG

2.1.4 Equipment

Ca²⁺ Imaging and patch clamp setup

Vibration Isolation Table VH3048W-OPT	Newport Corporation
Upright Microscope Olympus BX-51WI	Olympus GmbH
Imaging Station cell^R	Olympus GmbH
Fluorescence filter 340/26	Olympus GmbH

Fluorescence filter 387/11	Olympus GmbH
Fluorescence filter 470/40 X 266670	Olympus GmbH
Fluorescence filter XF1067 560AF55 91752	Omega Optical
Digital CCD Camera ORCA-R ²	Hamamatsu Photonics
Workstation: Luigs & Neumann Feinmechanik und 2 Micromanipulators Mini 25 Shifting Table 380FM-2P Platform LN Bridge 500 Remote Control Keypad SM-7 Control Box SM-7	Elektrotechnik GmbH
EPC 10 USB Double Patch Clamp Amplifier	HEKA Elektronik GmbH
Low-pass Bessel Filter (LPF-8)	Warner Instruments LLC
Audio Monitor AM10, Grass Technologies	Astro-Med GmbH
Digital Storage Oscilloscope VC-6523	Hitachi Ltd.
Picospritzer®II	Parker Hannifin Corp.
PM-6 platform for Series 20 chambers	Warner Instruments LLC
Large Rectangular Open Bath Chamber RC-27	Warner Instruments LLC
Platinum-iridium harp, 1.5 mm spacing	Own construction
Vibration Vacuum Pump SP302SA-V	Schwarzer Precision GmbH & Co. Kg

General

O ₂ /CO ₂ Incubator, CB210-UL	Binder GmbH
Double spatulas, spoon shape	Bochem Instrumente GmbH
Filter Funnel with Clamp DS0315	Thermo Fisher Scientific Inc.
Gastight Microliter Syringe #1710	Hamilton Bonaduz AG
Gravity flow controller	Becton Dickinson AG

Hazardous material workplace Basic AP 014590	Denios AG
Large Rectangular Open Bath Chamber (RC-27)	Warner Instruments LLC
Light Microscope	Ernst Leitz Wetzlar
LSM 710 confocal microscope	Zeiss
Radiance Confocal Laser Scanning System	Carl Zeiss AG, former Bio-Rad
Medical Forceps, Dumont 7b	Fine Science Tools Inc.
Microforge MF-830	Narishige International
Microgrinder EG-400	Narishige International
Microm™ HM 525 Cryostat	Thermo Scientific
Multi-pipette Puller PMP-107	Microdata Instrument Inc.
Micro spoon spatulas, spoon shape	Bochem Instrumente GmbH
Microwave Midea MWGED 9025 E	Midea Europe GmbH
Modular Syringe Holder 10 mL, Add-on Bracket	Warner Instruments LLC
Modular Syringe Holder 60 mL, Base Mount	Warner Instruments LLC
Osmometer OM-815	Vogel GmbH & Co. KG
Perfusion Mini Manifold, 8 to 1 ports	Warner Instruments LLC
pH Meter PHM240	Radiometer Analytical
Precision Balance 572	Kern & Sohn GmbH
Single Channel Pipettes (0.5-10 µL/20-200 µL/100-1000 µL)	VWR International
Spring Scissors, 7 mm and 3 mm Blades	Fine Science Tools Inc.
Stopcocks with Luer Connections	Cole-Parmer
Ultrapure Water System Direct-Q 5	EMD Millipore
Ultrasonic Bath Aquasonic 50T	VWR International

Vertical Glass Microelectrode Puller PP-830	Narishige International
Vacuum pump Air Admiral@diaphragm	Cole-Parmer
Vibrating-Blade Microtome HM 650V with Cooling Device CU65	Thermo Fisher Scientific Inc.
Vibratome Pelco 101	Technical Products International
Vortex Genie 2	Scientific Industries Inc.
Wagner Scissors	Fine Science Tools Inc.
Water Bath TW 20	JULABO Labortechnik GmbH
2.1.5 Software	
Xcellence rt	Olympus GmbH
Patchmaster	HEKA Elektronik GmbH
NeuroExplorer	Nex Technologies
IGOR Pro	WaveMetrix Inc.
SPSS Statistics	IBM Corp
NCSS Statistical Software	NCSS, LLC
GraphPad PRISM	GraphPad Software Inc
Microsoft office	Microsoft Corp.
ImageJ	Wayne Rasband, NIH
Photoshop CS6	Adobe Systems Inc.
CorelDraw x7	Corel Corp.
Origin 8.6	OriginLab

2.2 Methods

2.2.1 Animals

Animal care and experimental procedures were carried out by the guidelines established by the animal welfare committee of the Saarland University, School of Medicine. All mice were kept under standard light/dark cycle (12:12; lights-on at 0700 hours; lights-off at 1900 hours) with food and water *ad libitum*. GnRHR-IRES-Cre (GRIC) mice (Wen et al., 2008) were bred to ROSA26- τ GFP reporter mice (Wen et al., 2011) to express τ GFP in GnRHR neurons. Mice were kept in a mixed (129/SvJ and C57BL/6J) background. All mice used were 2 to 4 months old females.

2.2.2 Assessment of reproductive stages

Cytological analysis of vaginal smear was used to determine the estrous cycle phases in the mouse as described (Caligioni, 2009). Briefly, vaginal secretion was collected with a fire-polished glass Pasteur pipette filled with 10 μ L 1x phosphate buffer saline (PBS) by placing the tip at the external genital opening and flushing gently three to five times with the PBS solution. Vaginal fluid was placed on glass slides. The unstained material was then taken for analysis under the light microscope with a 10x objective. The estrous cycle stage was determined according to the proportion among the three cell types observed in the vaginal smear: epithelial cells, cornified cells, and leukocytes. Metestrous smear is characterized by a mix of cell types with a predominance of leukocytes and a few nucleated

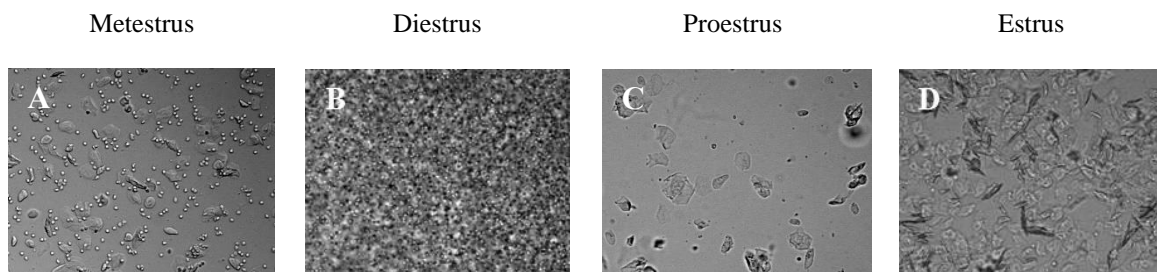


Figure 2.1 Vaginal cytology representing each stage of estrous from mice. (A) metestrus, characterized with leukocytes, nucleated or cornified epithelial cells; (B) diestrus, with a predominance of leukocytes; (C) proestrus, with individually nucleated epithelial cells; (D) estrus, with predominantly of clustered cornified epithelial cells.

epithelial and/or cornified squamous epithelial cells which have no visible nucleus, granular cytoplasm and irregular shape (Figure 2.1A). In diestrus, a predominance of leukocytes can be observed (Figure 2.1B). In proestrus, there is a predominance of nucleated epithelial cells which may appear in clusters or individually (Figure 2.1C). Estrus consists predominantly of clustered cornified squamous epithelial cells (Figure 2.1D).

2.2.3 Brain slice preparation

All acute coronal brain tissue slices were freshly prepared from female GRIC/eR26- τ GFP mice as described (Schauer and Leinders-Zufall, 2012). The animals were anesthetized with isoflurane and decapitated before 1200 hours in the case of metestrus, diestrus, estrus and early proestrus. Late proestrous mice were sacrificed after 1500 hours. The brains were quickly removed and immediately submerged in the ice-cold S1 solution, oxygenated with 95% O₂ and 5% CO₂. For loose-patch recording, coronal brain slices (275 μ m) were cut from the horizontal plane using a vibratome (Microm HM 650 V, Walldorf, Germany). For periventricular hypothalamus (Pe), brain slices were obtained and analyzed between bregma +0.26 and -1.94 mm (Paxinos and Franklin, 2004). However, the most rostral area (four sections between bregma +0.26 and -0.1 mm), as well as the more caudal region (four sections between bregma -1.58 and -1.94 mm), contained between zero and five GnRHR neurons somata per brain slice (~two somata/slice). Most GnRHR neurons were found in the medial region (~16 somata/slice). Their primary location has been documented between -0.22 to -1.46 mm (10-30 somata/slice), and this medial periventricular area was thereby subdivided into nine separate sections according to the method described by Paxinos and Franklin, (2004). For arcuate nucleus (Arc), brain slices between bregma -1.22 and -2.80 mm were obtained and analyzed (Paxinos and Franklin, 2004). Before the start of an experiment, slices were maintained in oxygenated S1 solution at 31.5 °C for 30 min and subsequently at room temperature (20-22 °C) until transferred to the recording chamber. For calcium imaging recording, 100 μ m-thick coronal brain slices were cut.

2.2.4 Loose-patch recording

Loose-patch recordings from individual GnRHR neurons were obtained in acute brain slices (275 μ m). Brain structures were identified using a mouse brain atlas (Paxinos and Franklin, 2004). For the visualization, an Olympus BX51WI fixed stage microscope

equipped with infrared-optimized differential interference contrast (IRDIC) optics was used. Slices were continuously superfused with the oxygenated S1 solution or synaptic blocker solution (~ 3 mL/min; gravity flow) at room temperature (Figure 2.2C). Patch pipettes (1.50 mm OD / 0.86 mm ID; Science Products, Hofheim, Germany) were pulled on a PC-10

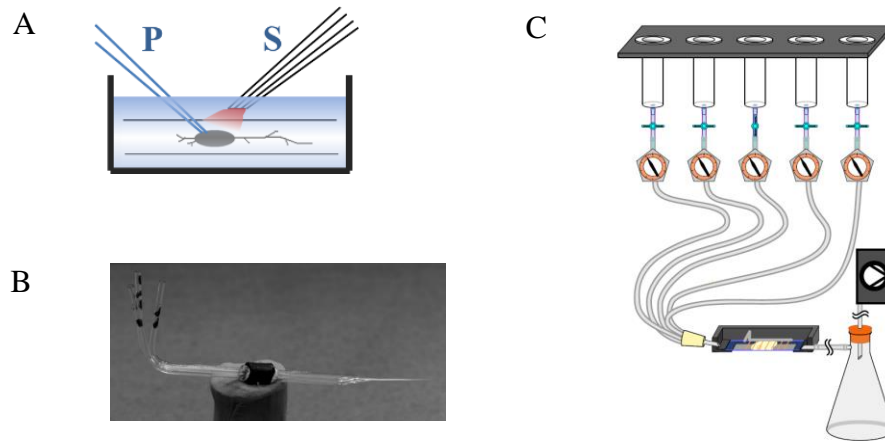


Figure 2.2 Puff and bath application systems. A. The schematic figure is showing the different concentrations of GnRH stimuli. Neuron attached to a patch pipette were stimulated by puff application of GnRH through a multi-barrel pipette. P, patch pipette; S, stimulation multi-barrel pipette. B. An example of a multi-barrel pipette for puff application of GnRH. C. Schematic figure of gravity driven multi-channel perfusion system.

vertical micropipette puller (Narishige Instruments, Tokyo, Japan) and fire-polished using a MF-830 Microforge (Narishige Instruments). Pipettes were filled with the S2 solution and showed resistances ranged from 5–7 M Ω . The τ GFP-tagged GnRHR neurons were visualized using 470 nm wavelength light emitted from a 150W Xenon short arc lamp through fluorescence filter ET470/40 (Olympus GmbH). Action potential-driven capacitive currents from identified GnRHR neurons were recorded extracellularly with seal resistance 20-90 M Ω connected to a computerized EPC-10 patch clamp amplifier (HEKA Elektronik, Lambrecht/Pfalz, Germany). The pipette potential in the loose-patch configuration was kept at 0mV. Consecutive current traces were acquired at a sampling rate of 10 kHz and low-pass filtered (analog 3- and 4-pole Bessel filters in series) with an effective corner frequency (-3 dB) of 3.0 kHz. Different concentrations of GnRH stimuli were applied by puff application for 1 s with an inter-stimulus-interval of 9 min through a

multi-barrel pipette system (Figure 2.2A and B). Bath solution S1 and alternative stimuli were applied using a gravity-driven multichannel perfusion system (Figure 2.2C). The spikes were analyzed off-line using IGOR Pro software with custom-written macros (WaveMetrics) and NeuroExplorer (Nex Technologies).

2.2.5 Analysis of spike data

2.2.5.1 Analysis of spike firing patterns

Four independent parameters were chosen to characterize and classify the different firing patterns of GnRHR neuron. The mean spike frequency (mf) was used as the first parameter. The second parameter, the coefficient of ISI variation (CV_{ISI}), was calculated using the method of Robin et al.(2009), in which the standard deviation (SD) of the interspike interval (ISI) was divided by the mean ISI value. CV_{ISI} can describe the regularity of the firing spikes. To represent the bursting behavior of GnRHR neuron, an interspike interval (ISI) threshold for burst detection was first determined based on the method published by Selinger et al. (2007). A quantitative approach was developed to describe the distribution of ISIs in terms of plotting histograms of the logarithm of the interspike interval. This approach provides a method for automatically classifying spikes into bursts, which does not depend on assumptions about the burst parameters. Using this burst detection method, the third and fourth parameters can be determined by calculating the percentage of spikes in bursts (PSiB) and the mean number of spikes in a burst (MSiB), respectively. With these four parameters, mf, CV_{ISI} , PSiB, and MSiB, a hierarchical cluster analysis was combined with a principal component (PCA) analysis to detect coherent patterns between the spike activities of the GnRHR neurons. All of the four parameters were used for the analysis of the spontaneous activity of GnRHR neuron and for identification of the change in firing pattern after bath application of GnRH or the gonadotropin-releasing hormone antagonist cetrorelix.

2.2.5.2 Short-term and long-term enhancement in spike activity after 1s puff GnRH stimulation

To determine the changes in mean spike frequency of spontaneously active neurons after GnRH stimulation, the mean spike frequency ratio was calculated as the fraction of the mean frequency during the first 10 s after stimulation ($t_0 + 10$ s) and the frequency of action

potentials during the 10 s before stimulation ($t_0 - 10$ s). The parameter t_0 indicates the start of the stimulation. The first-spike latency is defined as the time from the onset of the stimulus (t_0) to the time of the occurrence of the first action potential (Pawlas et al., 2010).

The long-term enhancement of spike activity was calculated by the variance of the instantaneous spike frequency (VARiF) over three periods, one period before stimulation and two periods after GnRH stimulation (total recording time: 180 s).

2.2.6 Immunohistochemistry

Female mice in early proestrus stage were anesthetized using isoflurane and decapitated before 1000 hours. The brains were quickly dissected and immediately submerged in the ice-cold S1 solution. The intact mice brains were then fixed in 1×PBS containing 4% (w/v) paraformaldehyde (PFA) for 2 h at 4 °C. After fixation, the brains were washed three times in PBS and cut into 100 μm coronal slices using a vibratome (Pelco 101, Technical Products International, USA), before blocking and antibody administration. Primary antibodies were: anti-GFP (AB13970, 1:1000, chicken monoclonal; Abcam) (Leinders-Zufall et al., 2014), anti-CD31 (AB56299, 1:750, rat monoclonal; Abcam) (Schmidt and von Hochstetter, 1995), and anti-GnRH (20075, 1:800, rabbit polyclonal; Immunostar) (Ward et al., 2009). Secondary antibodies were: Alexa-Fluor 488 goat-anti-chicken (A-11039, 1:1000, Invitrogen), Alexa-Fluor 633 goat-anti-rabbit (A-21070, 1:1000; Invitrogen), Alexa-Fluor 488 donkey-anti-rat (A-21208, 1:1000; Invitrogen), and Alexa-Fluor 633 donkey-anti-rat (20137, 1:1000; Biotium). Procedures were performed at room temperature (21 °C), except for incubation in primary antibodies (4 °C). Tissue was incubated for 48 h with primary antibodies diluted in blocking solution, washed 3 times with PBS, and subsequently incubated with secondary antibodies in PBS for 90 min. Primary antibody controls indicated the specificity of the primary antibody binding. Confocal fluorescence images were acquired on either a BX51WI attached to a Radiance Confocal Laser Scanning System (Carl Zeiss AG, former Bio-Rad) or a LSM 710 confocal microscope (Zeiss). Image stacks are presented as maximum intensity projections, assembled and minimally adjusted in brightness using Adobe Photoshop CS6 (Adobe Systems, San Jose, CA). Contact points between soma or axon of GnRHR neuron and blood vessel were counted.

2.2.7 Electron microscopy

Two female mice in early proestrus stage were anesthetized with isoflurane and decapitated. The brains were quickly removed and immediately submerged in 2.5% glutaraldehyde + 2% PFA fixation solution for 2 h at room temperature. After fixation, the brain areas containing Pe were cut into 1mm³ cubes and kept in PBS. Tissue was processed for electron microscopy as previously described by Schoch et al. (2006). Ultrathin sections were analyzed using a tecnai Biotwin 12 digital electron microscope by Prof. Franks Schmitz (Department of Anatomy, School of Medicine, Saarland University).

2.2.8 *In vivo* cetrorelix systemic injection

Before the application phase, female mice were monitored using cytological estrous cycle detection over at least two normal estrous cycles. Mice were habituated to handling and injected with 0.9% NaCl daily to reduce the stress caused by the injection. During the application phase, all mice subsequently received daily subcutaneous injections of 0.9 % sodium chloride (SHAM), 10 µg or 50 µg cetrorelix dissolved in 0.9 % sodium chloride in the morning over 9 consecutive days, starting at either diestrus or metestrus. Independent of the treatment group, the females' estrous cycle was determined using vaginal smears. On day 9 of the treatment, all mice were weighted and anesthetized using isoflurane followed by decapitation. The brains were quickly removed for loose-patch recording of GnRHR neurons as described in methods 2.2.3 and 2.2.4. The uteri were dissected and weighted to calculate the ratio of uterus to body mass. Ovaries were extracted for hematoxylin and eosin staining. A control group of female mice did not receive any treatment, to determine their uterus weight and status of their ovaries at early proestrus.

2.2.9 Hematoxylin and Eosin staining

The ovaries from 22 female mice from *in vivo* cetrorelix experiments were carefully dissected and fixed in PBS containing 4% paraformaldehyde overnight at 4°C, before incubation in PBS containing 30% sucrose, also overnight at 4 °C. Fixed ovaries were embedded in O.C.T. (Tissue-Tek), snap-frozen in a 2-methylbutane bath at -80 °C cut into 16 µm slices using a Microm™ HM 525 Cryostat (Thermo Scientific). Cryosections were thaw-mounted onto glass slides and stained with hematoxylin and eosin (H-E) by standard

procedure (Fischer et al., 2008). Briefly, sections were immersed in hematoxylin solution for 1 min, rinsed, immersed in eosin for 1-2 min, rinsed, dehydrated using an ascending alcohol solution, cleared with xylene, and sealed by a coverslip. The number of tertiary/preovulatory follicles and corpora lutea were counted in every section (Myers et al., 2004).

2.2.10 Calcium imaging recording on brain slices

The changing of intracellular calcium on GnRHR neurons was monitored with Fura-2 AM (Molecular Probes, Invitrogen), a membrane-permeant ratiometric fluorescence indicator. To obtain better loading with the Ca^{2+} dye Fura-2 AM, coronal brain slices of 100 μm thickness from female mice were prepared, as described in method 2.2.3 brain slice preparation. After cutting 100 μm -thick brain slices on a vibratome in S1 solution, brain slices were maintained immediately in oxygenated synaptic blocker solution + 10 μM TTX at 31.5 °C for 30 min. 50 μg Fura-2 AM were dissolved in 18 μL DMSO and 2 μL 20% Pluronic F-127 (Molecular Probes). Synaptic blocker solution + 10 μM TTX then was added to obtain a final volume of 1 mL and sonicated briefly. After the incubation of the brain slices at 31.5 °C, all brain slices were transferred into one well of a 6-well cell culture plate with 3 mL synaptic blocker solution + 10 μM TTX at room temperature. 1 mL of fura-2 loading solution was added directly onto the brain slices to give a relatively high initial concentration of 49.9 μM Fura-2 AM, 0.04% Pluronic F-127, and 1% DMSO. The concentration decreased as the Fura-2 AM diffused away from the site of application, resulting a final concentration of 12 μM Fura-2 AM, 0.0001% Pluronic F-127, and 0.4% DMSO. After incubation in the Fura-2 AM loading solution for 60 min at room temperature, all the slices were transferred into the synaptic blocker solution to wash at least 30 min before starting the experiments.

Only the GnRHR neurons, which showed a intact physiologic morphology and were loaded by fura-2, were chosen to record calcium signals. The calcium signals were acquired using Imaging Station cell[^]R attached to an upright Microscope Olympus BX-51WI (Olympus GmbH, Germany). Each GnRHR neuron was imaged individually, with the optical section adjusted to show the cell body. Excitation wavelengths of 340 nm and 380 nm were emitted from a 150W Xenon short arc lamp using fluorescence filters 340/26

and 387/11 (Olympus GmbH, Germany) respectively. Images with 50ms exposure time at 37.5% light intensity using Xcellence rt software (Olympus GmbH, Germany) were captured with a digital CCD camera (Hamamatsu Photonics). High-resolution time series image pairs were acquired by collecting 672×512 pixels fluorescence image pairs at a rate of 4 Hz.

For off-line analysis, all the image series were analyzed using ImageJ (Wayne Rasband, NIH). The somata of fura-2 loaded τ GFP-tagged neurons were marked in the respective image series as regions of interest (ROI), and the mean values of the fluorescence intensity of ROIs were saved for every time point of the image series. Measurements of Ca^{2+} dependent signal changes were determined as the ratio between the baseline fluorescence intensity at 340 nm and 380 nm excitation wavelengths,

$$\text{Ratio} = \frac{F_{340}}{F_{380}} \quad ,$$

Where F_{340} is the measured baseline fluorescence intensity at 340 nm and F_{380} at 380nm. Additional analysis and calculation were performed using Igor Pro software (Wavemetrics). To quantify the change in the complex Ca^{2+} elevations, the area under the Ca^{2+} fluorescence curve (AUC) was calculated (60s before and 60s after the start of the stimulus; total time: 120s). The mean of the baseline before the stimulus start was calculated (F_0). All fluorescence values were normalized by this mean ($\Delta F/F_0$).

$$\text{AUC} = \int_0^t f(t)dt \approx \sum_{i=0}^t \frac{1}{2} (t_{i+1} - t_i) [(f(t_{i+1}) - f(t_0)) + (f(t_i) - f(t_0))] ,$$

$f(t)$ represents the function of the measured intensity of the area of interest. $f(t_0)$ represents the function of the calculated mean of the baseline. A response was defined as a baseline deflection after the onset of stimulation that exceeded twice the s.d. of the mean of the baseline noise.

2.2.11 Simultaneous loose-patch and calcium imaging recording

The simultaneous loose-patch and calcium imaging recording method used in this study was followed protocols in method 2.2.4 loose-patch recording and method 2.2.10 calcium imaging recording on brain slices closely. To record the action potential-driven capacitive

currents from GnRHR neurons, the brain slices were incubated only in synaptic blocker solution without 10 μ M TTX. The GnRHR neurons, which showed an intact physiologic morphology and were loaded by fura-2, were chosen to realize simultaneous loose-patch and calcium imaging recording. First, loose-patch recording was performed as described in 2.2.4 until spontaneous spikes were observed. After 10 min, when the GnRHR neurons reached a stable level of firing, the calcium signals were measured as described in 2.2.10. The recording of loose-patch data on the Patchmaster software (HEKA Elektronik GmbH) was triggered by a start signal from the calcium imaging software Xcellence rt to make sure the simultaneous recording of loose-patch data and calcium imaging data.

2.2.12 Statistics

Student's t-test was used for measuring the significance of the difference between two distributions. One-way or two-way ANOVA were used to compare multiple groups compared. Tukey's multiple comparison tests (Tukey) or Fisher's least significant difference (LSD) were used as *a post hoc* comparison of the ANOVA. The analysis was done using GraphPad PRISM (GraphPad Software Inc., San Diego, USA) or SPSS (IBM Corporation, New York, USA). *P*-values < 0.05 were reported as statistical significance. Data are reported as means \pm SEM.

References

1. Caligioni, C. (2009). Assessing Reproductive Status/Stages in Mice. *Curr. Protoc. Neurosci. APPENDIX 4*, Appendix – 4I.
2. Fischer, A.H., Jacobson, K.A., Rose, J., and Zeller, R. (2008). Hematoxylin and Eosin Staining of Tissue and Cell Sections. *Cold Spring Harb. Protoc. 2008*, pdb.prot4986.
3. Leinders-Zufall, T., Ishii, T., Chamero, P., Hendrix, P., Oboti, L., Schmid, A., Kircher, S., Pyrski, M., Akiyoshi, S., Khan, M., et al. (2014). A Family of Nonclassical Class I MHC Genes Contributes to Ultrasensitive Chemodetection by Mouse Vomeronasal Sensory Neurons. *J. Neurosci. 34*, 5121–5133.

4. Myers, M., Britt, K.L., Wreford, N.G.M., Ebling, F.J.P., and Kerr, J.B. (2004). Methods for quantifying follicular numbers within the mouse ovary. *Reprod. Camb. Engl.* *127*, 569–580.
5. Pawlas, Z., Klebanov, L.B., Benes, V., Prokesová, M., Popelár, J., and Lánský, P. (2010). First-spike latency in the presence of spontaneous activity. *Neural Comput.* *22*, 1675–1697.
6. Paxinos, G., and Franklin, K.B.J. (2004). *The Mouse Brain in Stereotaxic Coordinates* (Gulf Professional Publishing).
7. Robin, K., Maurice, N., Degos, B., Deniau, J.-M., Martinerie, J., and Pezard, L. (2009). Assessment of bursting activity and interspike intervals variability: a case study for methodological comparison. *J. Neurosci. Methods* *179*, 142–149.
8. Schauer, C., and Leinders-Zufall, T. (2012). Imaging Calcium Responses in GFP-tagged Neurons of Hypothalamic Mouse Brain Slices. *J. Vis. Exp.*
9. Schmidt, D., and von Hochstetter, A.R. (1995). The Use of CD31 and Collagen IV as Vascular Markers A Study of 56 Vascular Lesions. *Pathol. - Res. Pract.* *191*, 410–414.
10. Schoch, S., Mittelstaedt, T., Kaeser, P.S., Padgett, D., Feldmann, N., Chevaleyre, V., Castillo, P.E., Hammer, R.E., Han, W., Schmitz, F., et al. (2006). Redundant functions of RIM1 α and RIM2 α in Ca²⁺-triggered neurotransmitter release. *EMBO J.* *25*, 5852–5863.
11. Selinger, J.V., Kulagina, N.V., O’Shaughnessy, T.J., Ma, W., and Pancrazio, J.J. (2007). Methods for characterizing interspike intervals and identifying bursts in neuronal activity. *J. Neurosci. Methods* *162*, 64–71.
12. Ward, D.R., Dear, F.M., Ward, I.A., Anderson, S.I., Spergel, D.J., Smith, P.A., and Ebling, F.J.P. (2009). Innervation of Gonadotropin-Releasing Hormone Neurons by Peptidergic Neurons Conveying Circadian or Energy Balance Information in the Mouse. *PLoS ONE* *4*, e5322.
13. Wen, S., Schwarz, J.R., Niculescu, D., Dinu, C., Bauer, C.K., Hirdes, W., and Boehm, U. (2008). Functional Characterization of Genetically Labeled Gonadotropes. *Endocrinology* *149*, 2701–2711.
14. Wen, S., Götze, I.N., Mai, O., Schauer, C., Leinders-Zufall, T., and Boehm, U. (2011). Genetic Identification of GnRH Receptor Neurons: A New Model for Studying Neural Circuits Underlying Reproductive Physiology in the Mouse Brain. *Endocrinology* *152*, 1515–1526.

Chapter 3

Hypothalamic gonadotropin-releasing hormone (GnRH) receptor neurons fire in synchrony with the female reproductive cycle

Abstract

Gonadotropin-releasing hormone (GnRH) is a master hormone in controlling mammalian reproduction via the hypothalamic-pituitary-gonadal (HPG) axis and regulates gonadotrope cells in the anterior pituitary gland through GnRH receptor (GnRHR). Besides in the pituitary, GnRHR is also identified in many brain areas. It is still unclear how GnRH regulates its potential target cells in the brain. A genetic mouse strain, in which GnRHR neurons express a fluorescent marker τ GFP, allows us to identify and visualize these neurons in the mouse brain. Using loose-patch recording, the firing activity of GnRHR neurons are investigated in the periventricular hypothalamic nucleus (Pe) from adult female mice. Interestingly, GnRHR neurons in Pe alternate their action potential firing pattern in synchrony with the female estrous cycle and show pronounced burst firing during the preovulatory period, especially in the presence of network blocker. Subsequently, I demonstrate that GnRH stimulation is sufficient to trigger GnRHR neurons to convert their firing pattern from tonic to burst firing which can be reversed by a potent GnRHR antagonist, cetrorelix. Furthermore, using bath application of cetrorelix directly on mouse brain slices, it is revealed that endogenous GnRH triggers burst firing activity of GnRHR neurons in Pe during late proestrus and estrus. Taken together, GnRHR neurons appear to switch their action potential activity due to the presence of endogenous GnRH during preovulatory period. The cyclic change in spike pattern behavior may reflect a modification in female reproductive performance.

3.1 Introduction

Gonadotropin-releasing hormone (GnRH) is an essential hormone responsible for mammalian reproductive physiology and behavior via the hypothalamic-pituitary-gonadal (HPG) axis. GnRH-secreting neurons (GnRH neurons) in the preoptic area of the hypothalamus which project axons to the median eminence and release GnRH into the vascular system, ensuring the central control of reproduction via the HPG axis (Gore, 2002). In the female reproductive cycle, GnRH is released in small mini-pulses. Its amplitude and frequency are substantially increased during the late proestrus to induce ovulation (Sisk et al., 2001; Knobil and Neill, 2006). To retain fertility, secreted GnRH binds to its receptor on pituitary gland cells to stimulate the release of luteinizing hormone (LH) and follicle-stimulating hormone (FSH), thus regulating oocyte maturation and ovulation in both rodents and humans. Besides the classical HPG axis, GnRH-target neurons (GnRHR neurons) are documented in multiple brain areas (Badr and Pelletier, 1987; Jenness et al., 1997; Wen et al., 2011). Furthermore, GnRH is suggested to regulate reproductive physiology and behavior independently of gonadotropin release (Dyer and Dyball, 1974; Moss, 1977; Moss and Foreman, 1976; Moss and McCann, 1973; Pfaff, 1973). However, it is not well understood how GnRH modulates the reproductive physiology of the brain through their target neurons because their scattered distribution impedes locating these neurons precisely. In this regard, Wen et al., 2008 developed a new genetic mouse model to identify GnRHR neurons in the brain. By crossbreeding GnRHR-IRES-Cre (GRIC) mice to ROSA26-CAGS-tauGFP (eRosa26- τ GFP) reporter mice, GnRHR neurons can express a fluorescent marker τ GFP, allowing us to identify these neurons independently of the hormonal status of the animal (Wen et al., 2008, 2011). GnRHR neurons were observed in many brain areas. By investigating the calcium signals on these neurons from different brain areas, Wen et al., 2011 found that the duration and shape of the GnRH-induced calcium responses were similar within the same area but different between brain areas. These suggest that GnRH signaling may differentially influence brain functions, which in turn affect reproductive success. GnRHR neurons are found in the periventricular hypothalamic nucleus (Pe), which is a thin region forming a wall around the third ventricle (3V) in the rostral, intermediate, and caudal hypothalamus. Due to this special location,

GnRHR neurons in Pe are potentially susceptible to various endogenous GnRH sources, such as GnRH-secreting fibers, third ventricular cerebrospinal fluid, or the cerebrovascular system. If GnRH level is elevated in the plasma during the preovulatory period (Sisk et al., 2001) and can reach its target neurons in the brain via the vascular or 3V system, the activity of GnRHR neurons in Pe should be linked to female reproductive cycle.

Using loose-patch recording, the firing activity of GnRHR neurons from Pe are investigated in brain slices from adult female mice. Surprisingly, I observed that GnRHR neurons alternate their action potential firing patterns in concert with the female reproductive cycle and change firing patterns from tonic to bursting during the preovulatory period, especially in the presence of network blocker. Puff application of GnRH typically produces a short-lived biphasic response followed by longer-latency and long-lasting changes in action potential activity. All of these responses are concentration dependent. GnRHR neurons are exquisitely sensitive to subnanomolar GnRH concentrations, with $K_{1/2}$ values around 0.5nM. The results from a bath application of cetrorelix, a GnRHR antagonist, directly on mouse brain slices indicate that GnRH stimulation is the main source of converting the mode of action potential firing during the preovulatory period. These properties enable GnRHR neurons to switch their firing modes depending on fluctuations of GnRH level during the estrous cycle and thus play an important functional role in female reproductive performance.

3.2 Results

3.2.1 Cyclic transformation of GnRHR neuron firing activity in synchrony with the estrous cycle

The spontaneous activities of GnRHR neurons in Pe are investigated in female mice brain. By breeding GRIC mice to eRosa26- τ GFP reporter mice resulting a GRIC/eR26- τ GFP mouse, all of the female mice exhibit regular estrous cyclicity (4.5 ± 0.2 days) (Figure 3.1A). GnRHR neurons in the GRIC/eR26- τ GFP mouse brain can be visualized by expressing τ GFP using a combination of fluorescence and infra-red differential interference contrast (IR-DIC) illumination (Wen et al., 2011) (Figure 3.1B). Since endogenous GnRH secretion fluctuates during the female reproductive cycle, the

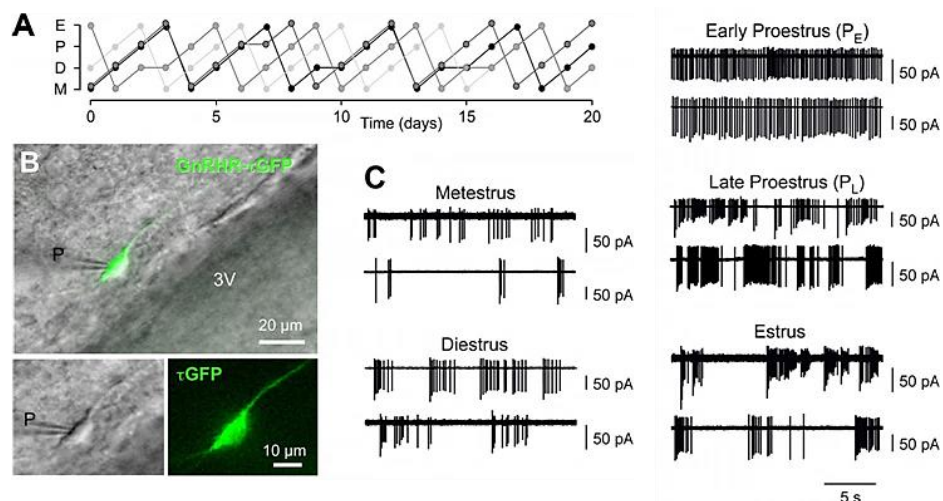


Figure 3.1 Different spontaneous spike activity patterns of GnRHR neuron during the female reproductive cycle. *A*: Representative plot of the estrous cycle from four GRIC/eR26- τ GFP mice (indicated with different line colors). The females display a normal cycle length of 4.5 ± 0.2 days ($n = 6$). M, metestrus; D, diestrus; P, proestrus; E, estrus. *B*: Overlay of a fluorescence image on top of an infrared-differential interference contrast (IR-DIC) micrograph of a brain tissue slice identifying a GnRHR neuron in the Pe, which is located next to the third ventricle (3V). The soma of the GnRHR neuron is clearly visible in the IR-DIC image (*lower left*) and expresses tau green fluorescent protein (τ GFP) (*lower right*) after Cre-mediated excision of a transcriptional stop sequence dependent on the activation of the *GnRHR* promoter. P, patch electrode. *C*: Example recordings of trains of extracellularly recorded, action-potential-driven capacitive currents of 10 different GnRHR neurons (two different neurons per reproductive stage). The pipette potential was 0 mV. Neuronal activity during proestrus was recorded in brain slices obtained either in the morning [early proestrus, P_E (800 – 1200 hours)] or afternoon [late proestrus, P_L: (1500 – 1800 hours)]. (Schauer, Tong et al., 2015)

spontaneous activity of GnRHR neurons in Pe is measured at different stages of estrous cycle (metestrus, diestrus, proestrus, and estrus) using extracellular loose-patch recordings (Leinders-Zufall et al., 2007) (Figure 3.1B). GnRHR neurons ($n = 94$), located in the Pe from 54 gonadally intact GRIC/eR26- τ GFP females, exhibit spontaneous spike activity recorded as action-potential-driven capacitive currents (Figure 3.1C). During metestrus, diestrus, and estrus, GnRHR neurons show burst firing patterns, which refer to the periods of time with a high action potential firing rate separated by periods of lower activity. As the preovulation GnRH surge progresses during the afternoon of proestrus (Sisk et al., 2001), the activities of GnRHR neurons in brain slices are recorded either in the morning (early proestrus, P_E: 800 – 1200 hours) or afternoon (late proestrus, P_L: 1500 – 1800 hours) (see Chapter 1.1.2). Notably, in proestrus, neurons reveal diverse firing patterns. Regular tonic firing occurs mainly during early proestrus; however, in late proestrus primarily bursting neurons occur (Figure 3.1C). In general, GnRHR neurons change their firing

activity in synchrony with the estrous cycle, especially in proestrus with its change in GnRH plasma concentration.

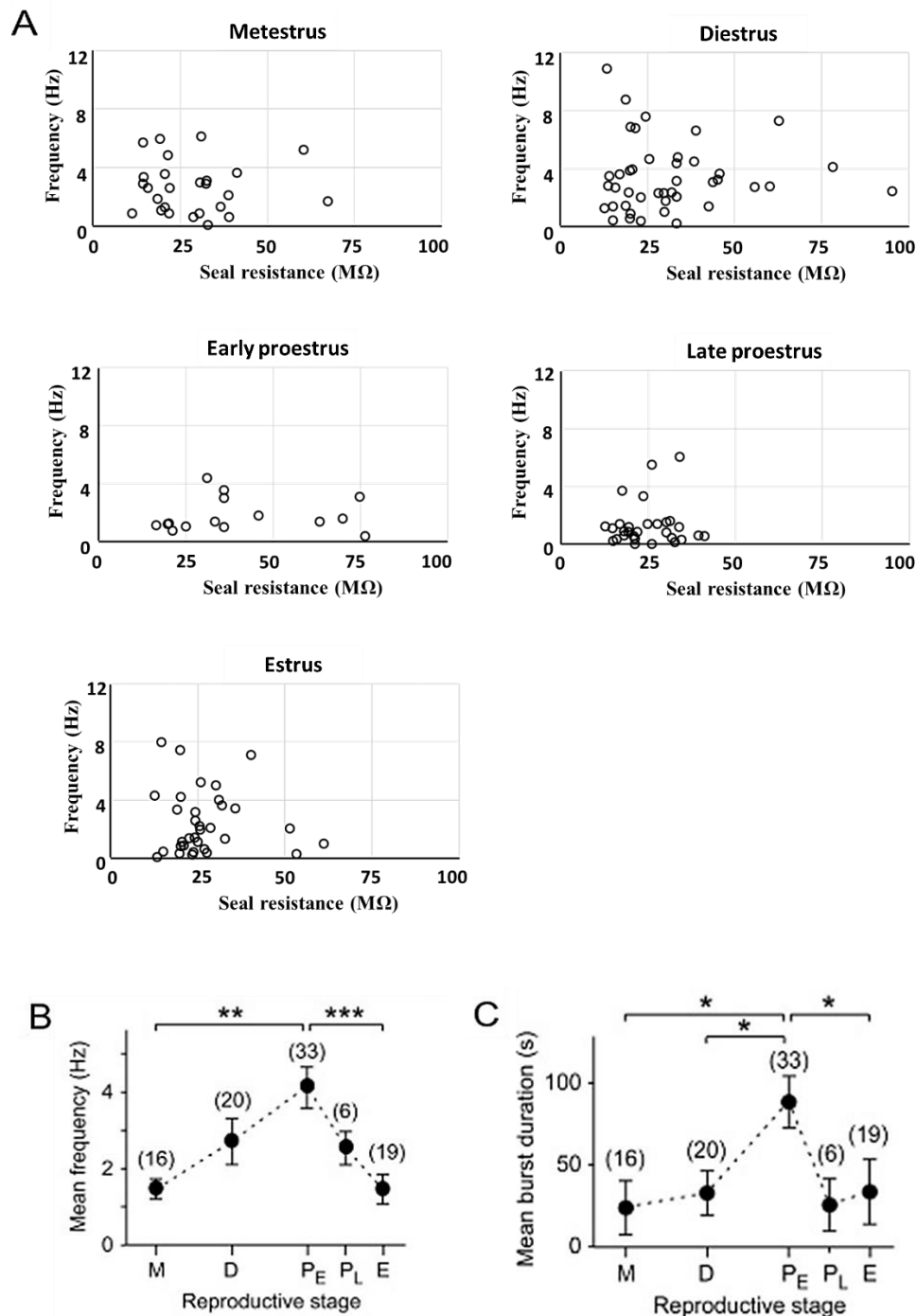


Figure 3.2 The change of mean frequency and mean burst duration of GnRHR neurons during the female reproductive cycle. *A*: The plots show the firing frequency of neurons is not correlated with their seal resistance in each estrous stages. (Pearson's r : M: $r = -0.028$, $P = 0.89$; D: $r = -0.067$, $P = 0.71$; PE: $r = -0.092$, $P = 0.55$; PL: $r = 0.053$, $P = 0.85$; E: $r = 0.072$, $P = 0.71$). *B*: The mean spike frequency of

GnRHR neurons changes during the estrous cycle (ANOVA: $F_{4,89} = 6.137$, $P < 0.001$), peaking at early proestrus. M: 1.3 ± 0.2 Hz; D: 2.5 ± 0.6 Hz; P_E: 4.0 ± 0.5 Hz; P_L: 2.2 ± 0.5 Hz; E: 1.2 ± 0.3 Hz). Tukey: *** $P < 0.001$, ** $P < 0.01$. The number of neurons recorded is shown in brackets above each bar. C: The mean burst duration of GnRHR neurons depends on the reproductive cycle (ANOVA: $F_{4,89} = 3.962$; $p < 0.01$), with a pronounce peak during the early phase of proestrus. M: 19.8 ± 13.4 s; D: 29.8 ± 12.4 s; P_E: 85.9 ± 15.5 s; P_L: 21.4 ± 13.7 s; E: 27.0 ± 15.6 s; Tukey: * $P < 0.05$. The number of neurons recorded is shown in brackets. Figure B and C are from Schauer, Tong et al., 2015.

To characterize the different firing patterns during estrous cycle, several parameters are calculated as described in Chapter 2.2.5. Firing frequency is not correlated with the seal resistance, and there is no indication of a relationship between them during the various stages of the cycle (Pearson's r : M: $r = -0.028$, $P = 0.89$; D: $r = -0.067$, $P = 0.71$; P_E: $r = -0.092$, $P = 0.55$; P_L: $r = 0.053$, $P = 0.85$; E: $r = 0.072$, $P = 0.71$) (Figure 3.2A). The plot of mean spike frequency reveals a cyclicity in action potential firing during the different reproductive stages which increase from 1 Hz during metestrus and estrus up to 4.0 Hz during P_E (Figure 3.2B). Due to the long quiet periods between bursts, the mean spike frequency is relatively low in the burst firing neuron. Therefore, high mean spike frequency values, as seen during P_E, could point to a higher presence of tonically firing neurons in this stage. As the action potential firing patterns differ substantially, a quantitative approach is developed to characterize and sort the firing patterns in an unbiased manner. First, an interspike interval (ISI) threshold for burst detection is calculated basing on the methods published by Selinger et al., 2007. The determined burst detection threshold, 1.3s in Pe neuron is used to calculate another parameter, the mean burst duration. Theoretically, tonically firing neurons should have one long burst that lasts the entire recording time due to their low ISI value and will lack the characteristic quiet periods of burst firing. Hence, a high mean burst duration indicates a more tonically firing neuron, while a low mean burst duration indicates the presence of primary burst firing neuron. Short bursts of action potential activity are detected in all stages of the reproductive cycle, except P_E (Figure 3.2C), suggesting that potential hormonal input such as GnRH influences the firing pattern of these neurons.

The percentage of spikes in bursts (PSiB) together with the coefficient of ISI variation (CV_{ISI}) are used to classify the firing patterns into the tonic, bursting and irregular. The interspike interval (ISI) is computed to establish the coefficient of ISI variation (CV_{ISI} ;

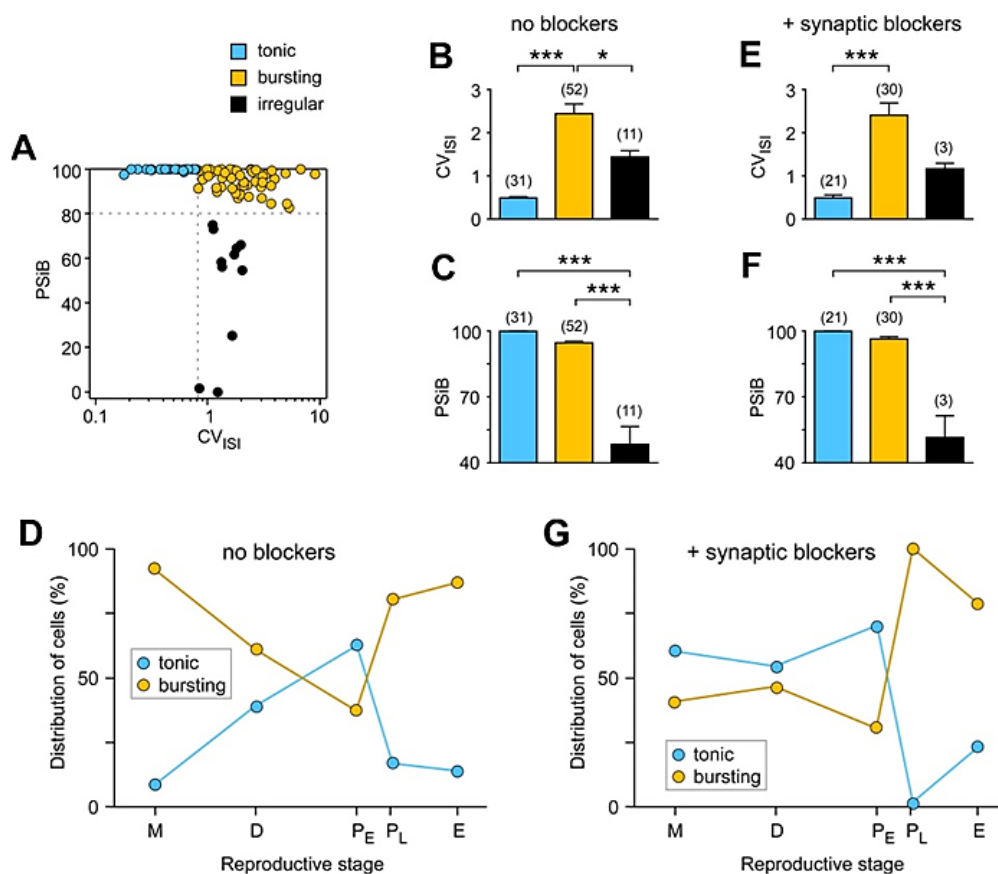


Figure 3.3 Alteration between tonic and bursting spike activity of GnRHR neurons during the reproductive cycle. **A:** Distribution of GnRHR neurons plotted in a two-dimensional space using the PSiB and CV_{ISI} values of each recorded GnRHR neuron ($n = 94$). Depending on the threshold values (dashed lines) determined from the cluster analysis (*see text*), the neurons were categorized as firing tonically (*blue*), in a burst pattern (*yellow*) or irregularly (*black*). **B and C:** The values of the CV_{ISI} (**B**) and the PSiB (**C**) depending on the spike activity classification of the GnRHR neurons (ANOVA: $F_{2,91} = 25.82$; $P < 0.001$ and $F_{2,91} = 120.8$; $P < 0.001$, respectively). **B:** Neurons firing in bursts are distinguishable from both tonic and irregular firing neurons due to their high CV_{ISI} value (tonic: 0.49 ± 0.03 ; bursting: 2.44 ± 0.22 ; irregular: 1.44 ± 0.14). **C:** GnRHR neurons with irregular spike activity can be distinguished based on their significantly different PSiB values (tonic $99.88 \pm 0.08\%$; bursting $95.07 \pm 0.66\%$; irregular $48.72 \pm 8.72\%$). **D:** Plot of the distribution of all GnRHR neurons ($n = 94$) firing either tonically (*blue*) or in a burst (*yellow*) by reproductive stages. **E and F:** Values of the CV_{ISI} (**E**) and the PSiB (**F**), depending on the spike activity classification of the GnRHR neurons in the presence of synaptic blockers (ANOVA: $F_{2,51} = 19.04$; $P < 0.0001$ and $F_{2,51} = 120.2$; $P < 0.0001$, respectively). **E:** Neurons firing in bursts are distinguishable from tonically firing neurons because of their high CV_{ISI} values (tonic: 0.50 ± 0.04 ; bursting: 2.43 ± 0.27 ; irregular: 1.17 ± 0.15). **F:** GnRHR neurons with irregular spike activity can be distinguished based on their significantly different PSiB values (tonic: $99.92 \pm 0.05\%$; bursting $96.59 \pm 0.92\%$; irregular: $51.54 \pm 9.83\%$). **G:** Plot of the distribution of all GnRHR neurons ($n = 54$) firing either tonically (*blue*) or in a burst (*yellow*) by reproductive stage, in the presence of synaptic blockers. M: metestrus, D: diestrus, PE: early proestrus, PL: late proestrus, E: estrus. Tukey: *** $P < 0.0001$, * $P < 0.05$. The number of neurons is plotted in brackets above each bar. (Schauer, Tong et al., 2015)

see Methods chapter 2.2.5) which can describe the regularity of firing pattern. The smaller CV_{ISI} is, the more tonically firing is. Using principle component analysis (PCA) combined with hierarchical cluster analysis, the criteria (CV_{ISI} : 0.8; $PSiB$: 80%) were determined by my collaborators Dr. Hugues Petitjean, Dr. Christian Schauer and myself (Schauer et al., 2015). Tonic firing neurons are recognized by a $CV_{ISI} < 0.8$, and both of bursting and irregularly firing neurons have a $CV_{ISI} > 0.8$. Subsequently, bursting and irregularly firing neurons are distinguished by a $PSiB > 80\%$ and a $PSiB < 80\%$, respectively (Figure 3.3A). Using the classification criteria, 33 % of the GnRHR neurons could be identified as firing tonically, 55 % as firing in a burst pattern and only 12 % as irregularly firing (Figure 3.3A-C). Irregularly firing neurons ($n = 11$) rarely occur at any stage during the reproductive cycle; therefore, I excluded all the irregularly firing neurons from further analysis. Interestingly, the distribution of tonic and bursting GnRHR neurons alternates during the female reproductive cycle (Figure 3.3D). Tonic firing GnRHR neurons are virtually absent during metestrus (1 out of 13 neurons) and increase steadily to a maximal value of 63 % (20 out of 32 neurons) during P_E , but drop dramatically back to an occasional tonic GnRHR neuron measured during P_L (1 out of 5 neurons) or estrus (2 out of 15 neurons). A similar but inverse cyclicity of bursting GnRHR neurons is found, with most being observed during metestrus (12 out of 13 neurons, 92 %) and decline over the following stages to a low of 12 out of 32 cells (37 %) to dramatically increase again on the day of estrus (13 out of 15 cells, 87 %).

To exclude synaptic input onto GnRHR neurons as the cause for the change in the amount of tonic versus bursting firing neurons during the reproductive cycle, I repeated the experiments in the presence of synaptic blockers (Figure 3.3E-G). The percentages of tonic, bursting and irregular firing neurons are similar as that in the absence of synaptic blocker (39% tonic, 55% bursting, 6% irregular) (Figure 3.3E-F). Comparing the parameters (e.g. CV_{ISI} , $PSiB$, and mean spike frequency) in the presence to the absence of synaptic blocker in each firing patterns, no significant difference is observed ($P = 0.16 - 0.87$). The distribution of tonic and bursting GnRHR neurons during the female reproductive cycle is considerably reorganized (Figure 3.3G). During the preovulatory period, the number of bursting GnRHR neurons dramatically increase in P_L and no tonic firing neurons could be detected at this stage. Thus, the network dampens the occurrence of burst firing GnRHR

neurons during the preovulatory period. On the contrary, in metestrus, the percentage of tonic vs. bursting neuron indicates that the network enhances the presence of bursting firing neurons (Figure 3.3G). These results suggest that state- (or hormone)-dependent network pathways influence the neural activity of GnRHR neurons in this hypothalamic regions.

Taken all together, these results demonstrate a cyclic transformation of GnRHR neuron activity in synchrony with the estrous cycle, particular during the proestrous stage, where pronounced changes in GnRH concentration are observed in the median eminence of rodents (Sisk et al., 2001).

3.2.2 A switch in action potential burst activity in Pe GnRHR neurons triggered by GnRH

A transformation from tonic to bursting firing of GnRHR neuron occurs particularly during the proestrous stage when the upsurge of GnRH takes place; therefore, I address the question if GnRH itself could be responsible for this conversion in the spike activity of GnRHR neurons. To test whether GnRH can directly affect the τ GFP-tagged neurons, the GnRH-induced responses are recorded in the presence of synaptic blockers during P_E (Figure 3.4A, B). Without interfering with the composition of the cytoplasm by using the loose-patch recording technique, GnRH increases the spike frequency within the first 10s following GnRH stimulation, from 5.0 ± 1.3 to 6.8 ± 1.3 Hz ($P < 0.05$; Figure 3.4A, B). The presence of synaptic blocker isolates the GnRHR neurons from the neural network to a great extent; therefore, the increase of the firing frequency demonstrates that GnRH can directly affect the τ GFP-labelled neurons and that GnRHR neurons have to express functional GnRHR. This conclusion is further substantiated by the experiments described below. For further experiments, we refrain from using synaptic blockers to avoid inadvertently impairing the fundamental neural mechanisms which influence the activity of GnRHR neurons by disrupting neurotransmission. Without synaptic blockers, we imitate a more natural environment. During P_E, GnRHR neurons fire tonically in the absence of a synaptic blocker cocktail with a mean spike frequency of 0.47 ± 0.04 Hz ($n = 20$) which is the same as in the presence of synaptic blockers (0.53 ± 0.09 Hz, $n = 7$; $t(25) = 0.79$, $P = 0.43$). Through puff application of different concentration of GnRH, GnRHR neurons respond to the stimulation with a rise in spike frequency within a certain concentration

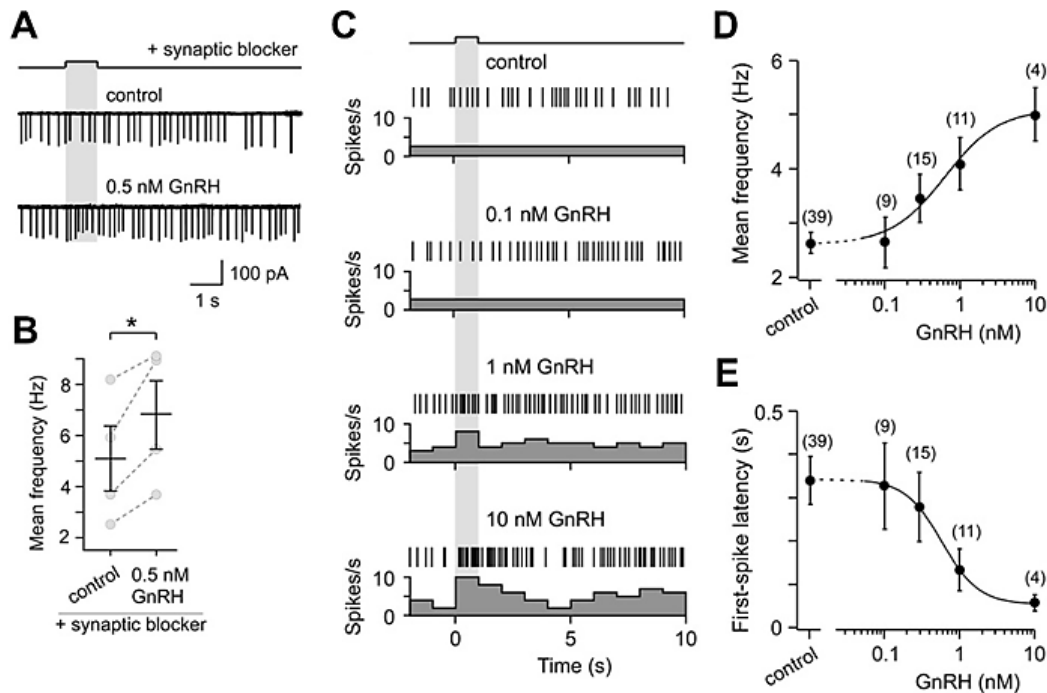


Figure 3.4 Increase of firing frequency in the first 10s after 1s GnRH puff stimulation **A**: Example of an individual GnRHR neuron responding to a 1-s pulse of 0.5nM GnRH with an increase in extracellular recorded action-potential-driven, capacitive currents in the presence of a cocktail of the synaptic blocker (pipette potential: 0mV). **B**: GnRH increased the spike frequency in all GnRHR neurons tested, compared to control stimulation (*gray dots connected by dashed lines*). Control, 5.0 ± 1.3 Hz ($n = 4$); GnRH, 6.8 ± 1.3 Hz ($n = 4$). Paired t -test: $t(3) = 3.59$ * $P < 0.05$. **C**: Raster plot and corresponding perievent histograms (bin size 1 s) of extracellularly recorded, action-potential-driven, capacitive currents to 1-s pulses of either control or GnRH in the absence of synaptic blockers (pipette potential: 0 mV). **D**: The mean spike frequency increased with increasing GnRH concentration, giving a $K_{1/2}$ value of 0.62 ± 0.13 nM and Hill coefficient of 1.2 ± 0.3 . ANOVA: $F_{4,74} = 2.15$, $P < 0.01$. **E**: The first-spike latency decreases with increasing GnRH concentration, having a $K_{1/2}$ value of 0.61 ± 0.43 nM and a Hill coefficient of -1.9 ± 1.7 . ANOVA: $F_{4,47} = 2.64$, $P < 0.05$. The number of recordings is plotted in brackets above each bar. (Schauer, Tong et al., 2015)

range. Dose response curve shows that a higher GnRH concentration elicits a higher increase in mean spike frequency, with a $K_{1/2}$ value of 0.62 ± 0.13 nM (Figure 3.4D; ANOVA: $F_{4,74} = 2.15$, $P < 0.01$). The first spike latency, the timing of the first spike following GnRH stimulation, is examined to determine whether any spatio-temporal pattern for GnRH-induced change occurs in the initial action potential sequence (Chase and Young, 2007; Pawlas et al., 2010). Independent of the noise caused by spontaneous action potential activity, a dose-dependent change of the first-spike latency is observed (Figure 3.4E). With the increase in GnRH concentration, the latency decreases from a value

of 340 ms at 0.1nM to ~60 ms at 10nM GnRH. This indicates that a hormonal modulation of behaviors likely relies on neural firing over extended periods.

In addition to the short-lived responses, 1-s GnRH stimulation could also induce a long-lasting change in spike activity on GnRHR neurons persisting for 1-2 min at saturating 10nM GnRH (Figure 3.5A). To use our analysis tools for distinguishing the tonic and burst firing patterns, at least 3.5 min recordings are required, which go beyond the changes

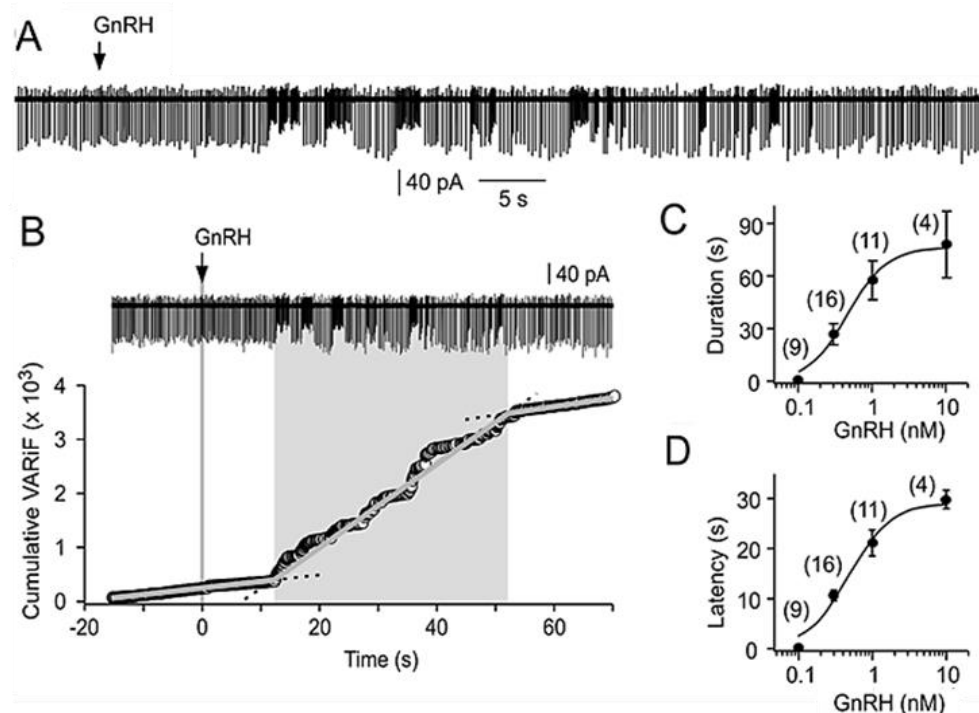


Figure 3.5 A long-lasting change in the action potential activity of GnRHR neurons induced by 1s GnRH puff stimulation. *A*: Example recording of an extracellularly recorded, action-potential-driven capacitive current of a tonic GnRHR neuron from an early proestrous female mouse stimulated with a 1-s pulse of 1 nM GnRH, revealing a dramatic change in the spike firing of the GnRHR neurons occurring ~10 s following stimulation (pipette potential 0 mV). *B*: The cumulative variance in instantaneous spike frequency (VARiF) of the GnRHR neuron shown in *A* is plotted versus time. The GnRH-induced change in VARiF can be visualized by the shift in the cumulative VARiF slope, allowing the determination of the latency and duration of this long-lasting conversion in spike activity. The original recording is positioned above the cumulative VARiF plot. *C* and *D*: Dose dependency of the latency (*C*) and duration (*D*) of the long-lasting conversion in spike activity. Both values rise with increasing GnRH concentration, giving $K_{1/2}$ values and Hill coefficients of 0.48 ± 0.11 nM, 1.5 ± 0.4 (latency, mean \pm SD); and 0.46 ± 0.17 nM, 1.6 ± 0.7 (duration, mean \pm SD), respectively. ANOVA: latency, $F_{3,36} = 36.35$, $P < 0.0001$; duration, $F_{3,36} = 11.24$, $P < 0.0001$. All dose-response curves are fits of the Hill equation in combination with an iterative Levenberg–Marquardt nonlinear, least-squares fitting routine (Chi-square test: $P = 0.99$). The number of recordings is plotted in brackets above each bar. (Schauer, Tong et al., 2015)

induced by a 1-s pulse. As the variance of the interspike interval is another essential feature to describe the spike patterns, the cumulative variance of instantaneous spike frequency (VARiF) is calculated and analyzed by my collaborator Dr. Hugues Petitjean and myself (Figure 3.5B). Except 0.1 nM, GnRH do not alter the firing pattern (VARiF control, 0.23 ± 0.11 , $n = 21$; 0.1nM GnRH, 0.19 ± 0.10 , $n = 9$; t -test $P = 0.27$), from 0.3 nM up to 10 nM GnRH, both the duration and latency in spike activity conversion increase significantly (Figure 3.5C and D) (duration: 0.3 nM: 10.6 ± 1.1 s, $n = 16$; 10 nM: 29.9 ± 1.8 s, $n = 4$; latency: 0.3nM: 27.2 ± 5.9 s, $n = 16$, 10 nM: 77.7 ± 18.5 s, $n = 4$; Tukey: $P < 0.01$). Both dose-dependent properties are subsequently fitted with a Hill equation, giving $K_{1/2}$ values (mean \pm SD) of 0.46 ± 0.17 and 0.48 ± 0.11 nM for the duration and latency of the long-lasting conversion in spike activity, respectively. Remarkably, all $K_{1/2}$ values are in proximity to each other and also to the values published for GnRHR in cultured pituitary and immortalized gonadotrope-like cells (Barran et al., 2005; Hazum and Conn, 1981; Lu et al., 2005). This indicates that the observed modulations in spike activity occur due to activation of the receptor itself. All of these findings suggest that GnRH can act as a strong modulator of the firing activity of GnRHR neurons. The long-lasting change in VARiF following a short pulse of GnRH could be the first indication of the initiation of action potential plasticity, leading to the transformation from a tonic to a burst or irregular firing pattern.

To explore the possibility that GnRHR neurons could alter their firing pattern for a prolonged period due to sustained GnRH stimulation, I assess the change of firing pattern of tonic GnRHR neurons from early proestrous female by bath application with 10 nM GnRH for 10 min up to 1½ h (Figure 3.6A-D). All of these recordings, the mean firing frequency and the two parameters of spike code classification (CV_{ISI} and PSiB) are evaluated every 220 s (Figure 3.6B-D). All tonically firing GnRHR neurons have a basic $CV_{ISI} < 0.8$ and a PSiB of 99.8 ± 0.21 ($n = 6$). After 10 min GnRH perfusion, the mean spike frequency decreases and the characteristic parameter CV_{ISI} increases without significant change of PSiB (77.1 ± 33.2 , $n = 6$; t -test: $P = 0.17$). All of the initially tonic firing GnRHR neurons are thus reclassified as bursters. Therefore, GnRH stimulation is sufficient to trigger GnRHR neurons to switch their mode of activity from tonic to burst firing.

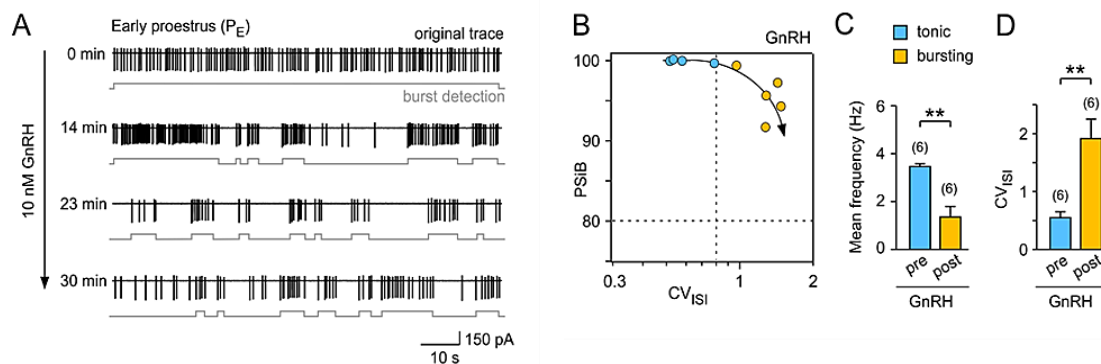


Figure 3.6 A transformation from tonic to bursting firing pattern induced by bath application of GnRH. **A:** Extracellularly recorded, action-potential-driven capacitive current traces of a GnRHR neuron from an early proestrous female taken at various times after starting a bath perfusion of 10 nM GnRH. The burst detection pattern is illustrated below the original recording using an automated unbiased process (see MATERIAL AND METHODS). The pipette potential was 0 mV. **B:** GnRH-induced change in the spike activity from the example shown in (A). Percentage of spikes in burst (PSiB) and the coefficient of variation of the interspike interval (CV_{ISI}) values of the spike activity were determined every 4 min and plotted in a two-dimensional space (see also Figure 3.3 and the main text). Contingent on threshold values for CV_{ISI} and PSiB (dashed lines), the neuron can be categorized as firing tonically (blue), and this changes to a burst pattern (yellow) during GnRH stimulation. **C** and **D:** Bar histogram of the mean spike frequency (C) [pre: 3.5 ± 0.3 Hz; post: 1.4 ± 1.1 Hz; paired *t*-test: *t*(5)=4.69, ** *P* < 0.01] and the CV_{ISI} (D) [pre: 0.55 ± 0.24; post: 1.9 ± 0.8 Hz; paired *t*-test: *t*(5)=4.38, ** *P* < 0.01] 4 min before the start (pre) and during the final 4 min of the GnRH treatment (post) of GnRHR neurons. The number of recordings is plotted in brackets above each bar. (Schauer, Tong et al., 2015)

3.2.3 The mode of GnRHR neuronal activity is converted by endogenous GnRH

If GnRH stimulation can trigger tonically firing GnRHR neurons to fire in bursts, the neuronal activity of bursting GnRHR neurons during the reproductive cycle might be reversed by blocking the GnRHR. To test this, I treated GnRHR neurons with a competitive GnRHR antagonist cetrorelix (Reissmann et al., 2000). First, I tested the effectiveness of cetrorelix to reverse the GnRH-induced burst firing in GnRHR neurons. As expected, cetrorelix treatment could reverse the GnRH-induced burst firing of GnRHR neurons to tonically firing again (Figure 3.7A-D). As previously observed, under GnRH stimulation tonically firing neurons reduce the mean spike frequency and increase the CV_{ISI}, causing the reclassification of the neurons as bursters. A subsequent cetrorelix treatment converts the firing pattern back to its original values labeling the neurons once more as tonically firing. This suggests that the spontaneous burst firing of GnRHR neurons during estrus, metestrus, and diestrus (Figure 3.7) could be triggered by the presence of GnRH.

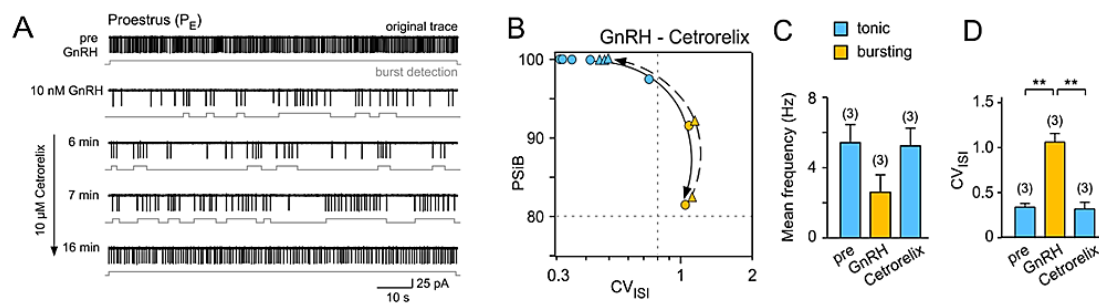


Figure 3.7 The transformation in action potential activity of GnRHR neurons is reversed by cetrorelix. *A:* Extracellularly recorded, action-potential-driven capacitive current traces of a GnRHR neuron from a female mouse in early proestrus taken at various times after starting a bath perfusion of 10nM GnRH, followed by 10 μ M of cetrorelix, a GnRHR antagonist. The burst detection pattern is depicted below the original recording using an automated unbiased process (see MATERIAL AND METHODS). The pipette potential was 0 mV. *B:* The plot of PSiB versus CV_{ISI} (determined every 4 min) illustrates the transformation of spike activity in the GnRHR neuron shown in (*A*). Contingent on threshold values for CV_{ISI} and PSiB (gray dashed lines), the neuron can be categorized as firing tonically (blue) or in burst pattern (yellow). Thus, GnRH stimulation converts the tonically firing neuron into a burster (solid arrow), an effect that is reversed by cetrorelix (dashed arrow). *C* and *D:* Bar histogram of the mean spike frequency (*C*) and the CV_{ISI} (*D*) 4 min before treatment (pre) and during the final 4 min of the GnRH and cetrorelix perfusion of the GnRHR neurons, respectively. Mean spike frequency: pre, 5.4 \pm 1.8 Hz; GnRH, 2.6 \pm 1.7 Hz; cetrorelix, 5.2 \pm 1.7 Hz (ANOVA: $F_{2,8} = 6.82$; $P = 0.051$); CV_{ISI}: pre, 0.34 \pm 0.07 Hz; GnRH, 1.1 \pm 0.16 Hz; cetrorelix, 0.32 \pm 0.13 Hz (ANOVA: $F_{2,8} = 1.186$; $P < 0.01$; Tukey's test ** $P < 0.01$). The number of recordings is plotted in brackets above each bar. (Schauer, Tong et al., 2015)

If spontaneous burst firing depends on endogenous release of GnRH, then by inhibition of GnRHR with cetrorelix, GnRHR neurons should shift from burst to tonic firing. To test this, the spike firing activity of GnRHR neurons during the various stages of the estrous cycle are examined before (control) and after cetrorelix treatment on brain slices (Figure 3.8A-D). Idle GnRHR activity, as predicted for tonically firing neurons during P_E, is not expected to be affected by the antagonist. Yet, the cetrorelix treatment reduces the CV_{ISI} value even further. This indicates that either the low, pulsatile endogenous GnRH release may have activated GnRHR, or GnRHR, a G protein-coupled receptor (GPCR), exhibits agonist-independent activity that can be prevented by the antagonist. The cetrorelix exposure during late proestrus and estrus abolishes the burst firing pattern, basically neutralizing GnRH-induced activity. According to the calculation of CV_{ISI}, GnRHR neurons in these two stages can be reclassified as tonically firing (Figure 3.8D). In comparison with late proestrus and estrus, the data collected during metestrus and diestrus

significantly modify the action potential firing (Figure 3.8D) but do not reduce the CV_{ISI} values below the threshold for reclassifying the neurons as tonically firing. The GnRHR activity during these two stages of the reproductive cycle may not be the sole driver, inducing the burst activity. Nonetheless, during late proestrus and estrus, our results indicate that endogenous GnRH release acting on the GnRHR should be the main trigger for burst firing in these neurons.

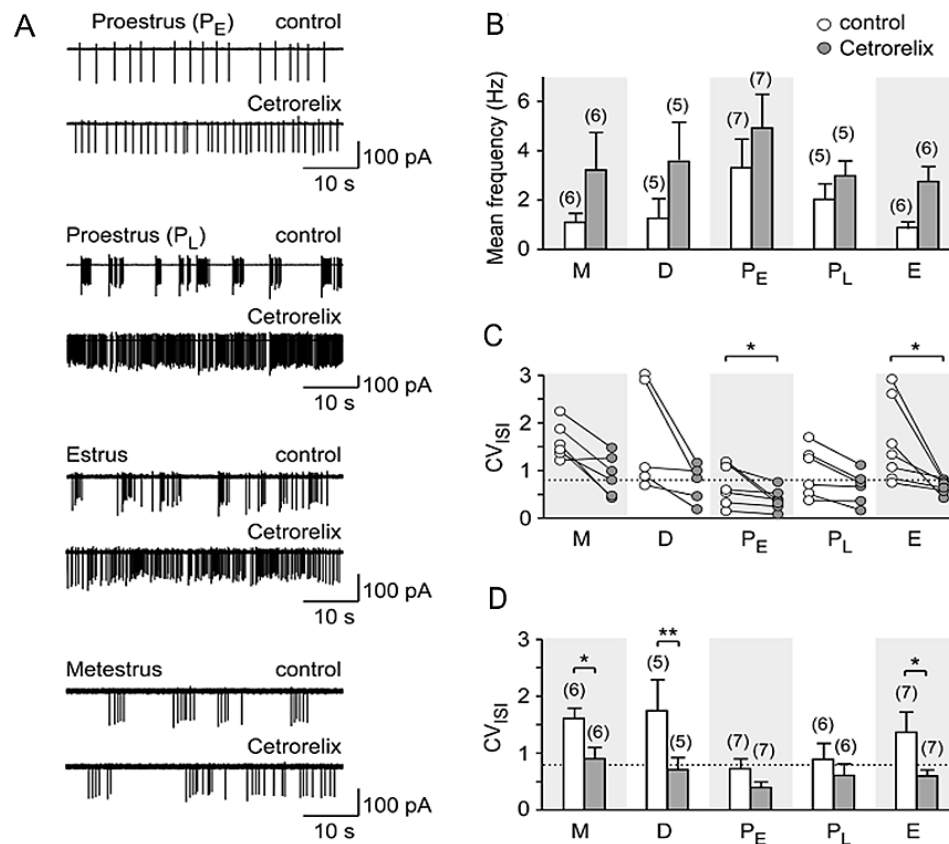


Figure 3.8 Cetrorelix abolish the endogenous GnRH effect. A - D, Cetrorelix inhibits action potential burst activity. A: Extracellularly recorded, action-potential-driven capacitive current traces of GnRHR neuron before (control) and after 10 min cetrorelix (10 μ M) in female mice at various reproductive stages. B - D, Bar histogram of the mean spike frequency (B), change in CV_{ISI} of individual neurons (C) (Wilcoxon: * $P < 0.05$) and CV_{ISI} summary as bar histogram (D) (ANOVA: $F_{9,50} = 3.958$; $P < 0.001$, least significant difference: * $P < 0.5$, ** $P < 0.01$) before (control, white bars/symbols) and after cetrorelix treatment (gray bars/symbols) for the various reproductive stages (metestrus, M; diestrus, D; early proestrus, PE; late proestrus, PL; estrus, E). The number of recordings is plotted in brackets above each bar. (Schauer, Tong et al., 2015)

3.3 Discussion

Mammalian reproduction is highly dependent upon the precise secretion of GnRH from the brain. Via HPG axis, GnRH acts on gonadotrope cells through GnRHR in the anterior pituitary gland. In addition, GnRHR has been reported to be expressed in many brain areas (Badr and Pelletier, 1987; Jennes et al., 1997; Wen et al., 2011), but it has not been understood how GnRH modulates these GnRHR neurons in the brain and thus brain function. My experiments indicate that the spontaneous firing activity of τ GFP-labelled GnRHR neurons from Pe of female mice alternate their action potential firing pattern in synchrony with the estrous cycle. These neurons switch their mode of activity from tonic to burst firing depending on the presence of GnRH. The switching of firing activity can be reversed by an antagonist of GnRH, cetrorelix. Furthermore, our results demonstrate that the endogenous GnRH during late proestrus and estrus is the main trigger for burst firing.

Cyclic transformation of GnRHR neuron activity is in synchrony with the estrous cycle. The spontaneous firing activity of GnRHR neuron in different estrous stages shows that these neurons mainly fire tonically in early proestrus and fire in the burst during the other stages. Considering that GnRH surge occurs between the early proestrus and late proestrus, the burst firing behavior in late proestrus could be induced by the increased endogenous release of GnRH (Sisk et al., 2001). Furthermore, to exclude the influence of GnRHR neuron from synaptic input, we record the spontaneous firing activity of GnRHR neurons in the presence of synaptic blockers during the estrous cycle. In the late proestrus, all of the GnRHR neurons fire in burst, but in metestrus and diestrus, the percentage of burst firing neuron is decreased (Figure 3.3D, G). The redistribution of tonic and burst neurons indicate that during the preovulatory period the network dampens the occurrence of burst firing GnRHR neurons, but in metestrus and diestrus the network enhances the presence of burst firing neurons. These suggest that GnRHR neurons in Pe are also modulated by the state- (or hormone)-dependent network pathways. It is well known that the estradiol level rises during the estrous cycle, peaking during proestrus (Butcher et al., 1974). The positive feedback effect of estrogen is the mechanism to drive the preovulatory surge in GnRH and LH secretion in the female causing ovulation (Knobil and Neill, 2006). The increase in the number of tonically firing GnRHR neurons correlates with the change

of estradiol levels during the estrous cycle. Therefore, it is reasonable to consider that estradiol may regulate GnRHR neurons firing tonically. The direct effect of estradiol-generated tonicity of GnRHR neuron firing could result from the prevention of intrinsic cascades known to induce oscillatory spike behavior (Bal et al., 1995; Chu et al., 2010). Another possible indirect effect of estradiol could be the modulation of the local network activity (Christian and Moenter, 2007; Velísková and Velísek, 2007). Estrogen receptor ER α expression is not detected in GnRHR neurons of the Pe (Kumar et al., 2015), which is against genomic estrogen effects in these cells. Estradiol is well known as an initiator of burst activity. Therefore, it might act on adjacent cells that do express ER α to modulate GnRHR neurons. In addition, progesterone is another steroid hormone associated with modulating GnRH secretion (Bashour and Wray, 2012) which could also be involved in regulating GnRHR neuron firing activity. Both estrogen and progesterone might be needed to switch GnRHR neuron firing tonically during proestrus, thus preparing them to respond the heightened activity of the GnRH/LH pulse generator. Future experiments are required to identify the change in firing activity of GnRHR neuron during the female reproductive cycle using stimulation of estradiol or progesterone with or without synaptic blocker presence.

GnRH stimulation triggers the burst firing activity of GnRHR neurons in Pe.

By blocking the network with synaptic blocker cocktail, puffing application of GnRH induces the increase of the firing frequency of GnRHR neuron, which demonstrates that GnRHR neurons express functional GnRHR. The whole-cell patch recordings by my collaborator Thomas Blum confirms the finding that GnRHR neurons show a rise in spike frequency and an extended elevation of the membrane potential after GnRH stimulation, indicating that GnRH activates a depolarizing conductance (Schauer et al., 2015). The first spike latency is a time delay that a neuron takes to respond a particular stimulus. Thus it consists of the temporal information of the response (Chase and Young, 2007; Pawlas et al., 2010). The first-spike latency of GnRH-induced responses significantly decrease from 340 to 60 ms with increasing GnRH concentration. Some other metabotropic receptor-coupled signal transduction cascades show latencies ranging from 7 ms in phototransduction (Cobbs and Pugh, 1987; Hestrin and Korenbrot, 1990) up to 150-300 ms in olfaction (Firestein et al., 1990; Leinders-Zufall et al., 1998). The difference in response

latency reflects the speed of the signaling cascade linking the GPCR to its effector proteins and ion channels that ultimately modify the membrane potential. However, the mechanism by which GnRH modulates and triggers the action potential pattern in a concentration-dependent manner is not known. It is well known that GnRHR is a G-protein coupled receptor (Tsutsumi et al., 1992) and studies showed that GnRH acts via $G_{q/11}$ -coupled GnRHR to activate phospholipase C (PLC) resulting in the mobilization of Ca^{2+} , but the involvement of other G-proteins, like $G\alpha_i$, $G\alpha_s$, have also been proposed (Cohen-Tannoudji et al., 2012; Naor and Huhtaniemi, 2013). Interestingly, using Ca^{2+} imaging, Wen et al., 2011 also observed two types of somatic Ca^{2+} transients in Pe GnRHR neurons having a 25s delay between the responses at saturating GnRH. In my study, puffing application of GnRH directly on GnRHR neuron not only induce a relative faster first response, but also induce a delay secondary response, triggering the transformation of firing activity from tonic to burst. The latency of the GnRH-induced long-lasting secondary response is in a similar range (Figure 3.5), indicating a role for Ca^{2+} in adjusting the action potential activity pattern in these neurons. Future experiments are needed to clarify the involvement of the intracellular pathways in regulating Pe GnRHR neuron activity.

Endogenous GnRH regulating GnRHR neurons act as the main trigger for burst firing during female reproductive cycle. Burst firing neurons during the preovulatory period that have been prestimulated with GnRH can be reversed to tonically firing again in the presence of the antagonist. This suggests that the activity of GnRHR itself triggers the transformation in action potential firing in Pe neurons. Moreover, cetrorelix significantly inhibits the activity in GnRHR neurons during metestrus and diestrus but could not cause the complete shift to tonic firing, which could be due to the involvement of other hormones or synaptic input from adjacent neuron. Studies have reported that GnRH has a half-life about 2-6 min (Pimstone et al., 1977); therefore, endogenous GnRH might not be sufficient to induce the different action potential pattern as observed in the recording obtained in acute slice preparation. However, if GnRH-secreting fiber is still active even after cutting from their cell body, they may continuously release GnRH into the vascular system or 3V. On the other hand, the GnRH half-time could depend on the degradation and clearance of GnRH. Human patients with liver or renal dysfunction have GnRH half-life times up to 20 min (Pimstone et al., 1977).

Currently, my data support a modulation of GnRHR neurons in Pe by the hormone-dependent network during metestrus, diestrus, and early proestrus, followed by a switch in action potential activity from tonic to burst firing initiated by endogenous GnRH release during the late phase of proestrus and estrus. However, GnRHR neurons located in other brain areas may not necessarily depend on GnRH linked to the reproductive cycle and could be influenced by variations in gonadal steroids or other hormones. Future experiments need to clarify which of the intrinsic membrane properties, ion channels and second messenger pathways, as well as hormonal signals, like estrogen and progesterone, are involved in determining the action potential output mode, which may help understand the information processing that takes place in this circuit.

Reference

1. Badr, M., and Pelletier, G. (1987). Characterization and autoradiographic localization of LHRH receptors in the rat brain. *Synap. N. Y. N* 1, 567–571.
2. Bal, T., von Krosigk, M., and McCormick, D.A. (1995). Role of the ferret perigeniculate nucleus in the generation of synchronized oscillations in vitro. *J. Physiol.* 483 (Pt 3), 665–685.
3. Barran, P.E., Roeske, R.W., Pawson, A.J., Sellar, R., Bowers, M.T., Morgan, K., Lu, Z.-L., Tsuda, M., Kusakabe, T., and Millar, R.P. (2005). Evolution of constrained gonadotropin-releasing hormone ligand conformation and receptor selectivity. *J. Biol. Chem.* 280, 38569–38575.
4. Bashour, N.M., and Wray, S. (2012). Progesterone directly and rapidly inhibits GnRH neuronal activity via progesterone receptor membrane component 1. *Endocrinology* 153, 4457–4469.
5. Butcher, R.L., Collins, W.E., and Fugo, N.W. (1974). Plasma concentration of LH, FSH, prolactin, progesterone and estradiol-17beta throughout the 4-day estrous cycle of the rat. *Endocrinology* 94, 1704–1708.
6. Chase, S.M., and Young, E.D. (2007). First-spike latency information in single neurons increases when referenced to population onset. *Proc. Natl. Acad. Sci.* 104, 5175–5180.

7. Christian, C.A., and Moenter, S.M. (2007). Estradiol induces diurnal shifts in GABA transmission to gonadotropin-releasing hormone neurons to provide a neural signal for ovulation. *J. Neurosci. Off. J. Soc. Neurosci.* 27, 1913–1921.
8. Chu, Z., Takagi, H., and Moenter, S.M. (2010). Hyperpolarization-activated currents in gonadotropin-releasing hormone (GnRH) neurons contribute to intrinsic excitability and are regulated by gonadal steroid feedback. *J. Neurosci. Off. J. Soc. Neurosci.* 30, 13373–13383.
9. Cobbs, W.H., and Pugh, E.N. (1987). Kinetics and components of the flash photocurrent of isolated retinal rods of the larval salamander, *Ambystoma tigrinum*. *J. Physiol.* 394, 529–572.
10. Cohen-Tannoudji, J., Avet, C., Garrel, G., Counis, R., and Simon, V. (2012). Decoding high Gonadotropin-releasing hormone pulsatility: a role for GnRH receptor coupling to the cAMP pathway? *Front. Endocrinol.* 3.
11. Dyer, R.G., and Dyball, R.E.J. (1974). Evidence for a direct effect of LRF and TRF on single unit activity in the rostral hypothalamus. *Nature* 252, 486–488.
12. Firestein, S., Shepherd, G.M., and Werblin, F.S. (1990). Time course of the membrane current underlying sensory transduction in salamander olfactory receptor neurones. *J. Physiol.* 430, 135–158.
13. Gore, A.C. (2002). *GnRH: The Master Molecule of Reproduction* (Kluwer Academic Publishers).
14. Hazum, E., and Conn, P.M. (1981). Luteinizing Hormone Release and Gonadotropin-Releasing Hormone (GnRH) Receptor Internalization: Independent Actions of GnRH. *Endocrinology* 109, 2040–2045.
15. Hestrin, S., and Korenbrot, J.I. (1990). Activation kinetics of retinal cones and rods: response to intense flashes of light. *J. Neurosci. Off. J. Soc. Neurosci.* 10, 1967–1973.
16. Jennes, L., Eyigor, O., Janovick, J.A., and Conn, P.M. (1997). Brain gonadotropin releasing hormone receptors: localization and regulation. *Recent Prog. Horm. Res.* 52, 475–490.
17. Knobil, E., and Neill, J.D. (2006). *Knobil and Neill’s Physiology of Reproduction* (Gulf Professional Publishing).
18. Kumar, D., Candlish, M., Periasamy, V., Avcu, N., Mayer, C., and Boehm, U. (2015). Specialized subpopulations of kisspeptin neurons communicate with GnRH neurons in female mice. *Endocrinology* 156, 32–38.

19. Leinders-Zufall, T., Greer, C.A., Shepherd, G.M., and Zufall, F. (1998). Imaging Odor-Induced Calcium Transients in Single Olfactory Cilia: Specificity of Activation and Role in Transduction. *J. Neurosci.* *18*, 5630–5639.
20. Leinders-Zufall, T., Cockerham, R.E., Michalakis, S., Biel, M., Garbers, D.L., Reed, R.R., Zufall, F., and Munger, S.D. (2007). Contribution of the receptor guanylyl cyclase GC-D to chemosensory function in the olfactory epithelium. *Proc. Natl. Acad. Sci. U. S. A.* *104*, 14507–14512.
21. Lu, Z.-L., Gallagher, R., Sellar, R., Coetsee, M., and Millar, R.P. (2005). Mutations remote from the human gonadotropin-releasing hormone (GnRH) receptor-binding sites specifically increase binding affinity for GnRH II but not GnRH I: evidence for ligand-selective, receptor-active conformations. *J. Biol. Chem.* *280*, 29796–29803.
22. Moss, R.L., and McCann, S.M. (1973). Induction of mating behavior in rats by luteinizing hormone-releasing factor. *Science* *181*, 177–179.
23. Moss, R.L., and Foreman, M.M. (1976). Potentiation of lordosis behavior by intrahypothalamic infusion of synthetic luteinizing hormone-releasing hormone. *Neuroendocrinology* *20*, 176–181.
24. Moss, R.L. (1977). Role of hypophysiotropic neurohormones in mediating neural and behavioral events. *Fed. Proc.* *36*, 1978–1983.
25. Naor, Z., and Huhtaniemi, I. (2013). Interactions of the GnRH receptor with heterotrimeric G proteins. *Front. Neuroendocrinol.* *34*, 88–94.
26. Pawlas, Z., Klebanov, L.B., Benes, V., Prokesová, M., Popelár, J., and Lánský, P. (2010). First-spike latency in the presence of spontaneous activity. *Neural Comput.* *22*, 1675–1697.
27. Pfaff, D.W. (1973). Luteinizing hormone-releasing factor potentiates lordosis behavior in hypophysectomized ovariectomized female rats. *Science* *182*, 1148–1149.
28. Pimstone, B., Epstein, S., Hamilton, S.M., LeRoith, D., and Hendricks, S. (1977). Metabolic clearance and plasma half disappearance time of exogenous gonadotropin releasing hormone in normal subjects and in patients with liver disease and chronic renal failure. *J. Clin. Endocrinol. Metab.* *44*, 356–360.
29. Reissmann, T., Schally, A.V., Bouchard, P., Riethmiiller, H., and Engel, J. (2000). The LHRH antagonist cetrorelix: a review. *Hum. Reprod. Update* *6*, 322–331.
30. Schauer, C., Tong, T., Petitjean, H., Blum, T., Peron, S., Mai, O., Schmitz, F., Boehm, U., and Leinders-Zufall, T. (2015). Hypothalamic gonadotropin releasing hormone (GnRH) receptor neurons fire in synchrony with the female reproductive cycle. *J. Neurophysiol.* *114*(2), 1008–1020.

31. Selinger, J.V., Kulagina, N.V., O'Shaughnessy, T.J., Ma, W., and Pancrazio, J.J. (2007). Methods for characterizing interspike intervals and identifying bursts in neuronal activity. *J. Neurosci. Methods* 162, 64–71.
32. Sisk, C.L., Richardson, H.N., Chappell, P.E., and Levine, J.E. (2001). In vivo gonadotropin-releasing hormone secretion in female rats during peripubertal development and on proestrus. *Endocrinology* 142, 2929–2936.
33. Tsutsumi, M., Zhou, W., Millar, R.P., Mellon, P.L., Roberts, J.L., Flanagan, C.A., Dong, K., Gillo, B., and Sealfon, S.C. (1992). Cloning and functional expression of a mouse gonadotropin-releasing hormone receptor. *Mol. Endocrinol.* 6, 1163–1169.
34. Velísková, J., and Velíšek, L. (2007). Beta-estradiol increases dentate gyrus inhibition in female rats via augmentation of hilar neuropeptide Y. *J. Neurosci. Off. J. Soc. Neurosci.* 27, 6054–6063.
35. Wen, S., Schwarz, J.R., Niculescu, D., Dinu, C., Bauer, C.K., Hirdes, W., and Boehm, U. (2008). Functional characterization of genetically labeled gonadotropes. *Endocrinology* 149, 2701–2711.
36. Wen, S., Götze, I.N., Mai, O., Schauer, C., Leinders-Zufall, T., and Boehm, U. (2011). Genetic identification of GnRH receptor neurons: a new model for studying neural circuits underlying reproductive physiology in the mouse brain. *Endocrinology* 152, 1515–1526.

Chapter 4

Modulation of GnRHR neuron activity in the periventricular hypothalamus after systemic cetorelix treatment

Abstract

The GnRH/GnRHR signaling pathway plays an important role in the hypothalamic-pituitary-gonadal (HPG) axis regulating the physiological reproductive function in mammals; however, many of its functions in the brain are not yet clarified. In the previous chapter, we found that GnRHR neurons in Pe alternate their action potential firing pattern in synchrony with the estrous cycle and show pronounced burst firing during the preovulatory period when various reproductive hormone levels including GnRH are increased. GnRH stimulation is sufficient to trigger GnRHR neurons to convert their mode of activity from tonic to burst firing. These data suggest that endogenous GnRH could act on GnRHR neurons and triggers burst firing. Due to GnRH could profoundly affect spike firing activity of GnRHR neurons, I propose that endogenous GnRH during the female reproductive cycle modulates the neuronal activity of Pe GnRHR neurons. To strengthen this idea, I first examined what type of input could provide GnRH to the GnRHR neurons. Using immunohistochemistry, I observed that GnRHR neurons possess close appositions to Pe capillaries, but GnRH-secreting fibers are never found in close proximity to any GFP-tagged Pe neurons. The results from electron microscope observation show that the endothelial cells of capillaries in Pe contain many caveolae-like structures, suggesting a less constrained blood-brain barrier (BBB). Considering a less constrained BBB in Pe, GnRHR neuronal activity in the brain may be susceptible to systemic treatment with GnRHR antagonist. I find that subcutaneous injection of the GnRHR antagonist cetorelix can effectively block the HPG axis as shown by an increase in the number of tertiary follicles concomitant with a significant inhibition of follicle rupture and corpora lutea

formation. Furthermore, GnRHR neuron firing activity is also susceptible to systemic treatment with 10 μg and 50 μg cetrorelix. Preeminently 50 μg cetrorelix treatment can modulate GnRHR neuron activity and cause Pe neurons to fire more tonically and to mimic spike firing similar as early proestrus. In this part of my study, I demonstrate that GnRHR agonists and antagonists can act on GnRHR neurons that are not part of the classical HPG axis; therefore my data may have important clinical implications since agonists and antagonists of GnRH are widely used in clinical treatments.

4.1 Introduction

Mammalian reproduction relies on an appropriate secretion of GnRH via the hypothalamic-pituitary-gonadal (HPG) axis. GnRH-secreting neurons located in the ventral preoptic area project to the median eminence and release pulses of GnRH into the hypophyseal portal system (Clarke et al., 1978; Fink and Jamieson, 1976; Gore, 2002). The pulsatile release of GnRH increases in magnitude and frequency during the preovulatory period. Secreted GnRH travels down in the hypophyseal portal system and binds to the receptors in the anterior pituitary to stimulate the release of luteinizing hormone (LH) and follicle-stimulating hormone (FSH). In female mice, both of these two gonadotropins circulate in the blood and stimulate the secretion of estrogen and progesterone in the ovaries, subsequently regulating the oocyte maturation and ovulation during the female estrus cycle (Knobil and Neill, 2006; Sisk et al., 2001).

Based on the advances in understanding of this classical HPG axis, agonists and antagonists of GnRH receptor are widely used in clinical treatments, for example in assisted reproductive technologies (ART), like *in vitro* fertilization (IVF) and intracytoplasmic sperm injection (ICSI). Cetrorelix, one antagonist of GnRHR, is a decapeptide with a modified GnRH sequence. It is well known for leading to an immediate inhibition of gonadotropins by blocking GnRHR in the pituitary. In ART, cetrorelix is used for the prevention of the premature luteinizing hormone surge in controlling ovarian stimulation cycles to make sure enough oocytes can be collected for IVF (Reissmann et al., 2000; Duijkers et al., 1998; Shrestha et al., 2015). In addition, several reproductive-related

cancers are identified expressing GnRHR, and studies find that the activation of GnRHR shows inhibitory effects on these cancer cells (e.g. prostate, breast, ovarian and endometrial cancers) (Limonta et al., 2012). As is now more established (Badr and Pelletier, 1987a; Jennes et al., 1997a; Wen et al., 2011) GnRHR is not only expressed in the pituitary or cancer cells but also expressed in multiple brain areas. Thus, GnRH agonist/antagonist actions may not be restricted to the pituitary (Badr and Pelletier, 1987; Jennes et al., 1997) and could potentially have undesirable side effects by acting on GnRHR-expressing neurons in the brain.

In this chapter, we investigate the potential source of GnRH, such as GnRH-secreting neuronal fibers, third ventricular cerebrospinal fluid or the cerebrovascular system (Caraty and Skinner, 2008; Cottrell and Ferguson, 2004; Skinner et al., 1997). By immunostaining, we demonstrate that GnRHR neurons possess close appositions to Pe capillaries. In addition, in the electromicroscopy study, we find that the endothelial cells in Pe blood vessels contain many caveolae-like structures. These suggest a less constrained blood-brain barrier (BBB) in Pe. The previous chapter shows that GnRHR neurons in Pe alternate their action potential firing pattern in synchrony with the estrus cycle and display predominant burst firing during the preovulatory period. *In vitro* bath application of cetorelix is sufficient to reverse GnRHR neuron firing activity from bursting firing to tonic. Together with the anatomical information, I hypothesize that cetorelix may cross the BBB and regulate the firing activity of GnRHR neurons in Pe by systemic injection. Interestingly, we find that systemic injection of cetorelix can effectively block the HPG axis and GnRHR neuronal activity. Thus, my results could point to a potential side effect of cetorelix treatment in clinical patients.

4.2 Results

4.2.1 GnRHR neurons possess close appositions to Pe capillaries

GnRH modulates the firing activity of GnRH neurons in Pe during the reproductive cycle (see Chapter 3). To investigate the source of GnRH, I first examined the direct contact points between GnRH-secreting fibers and GnRHR neuron. The relationship between GFP-tagged GnRHR neurons and GnRH-secreting fibers are analyzed by the immune-

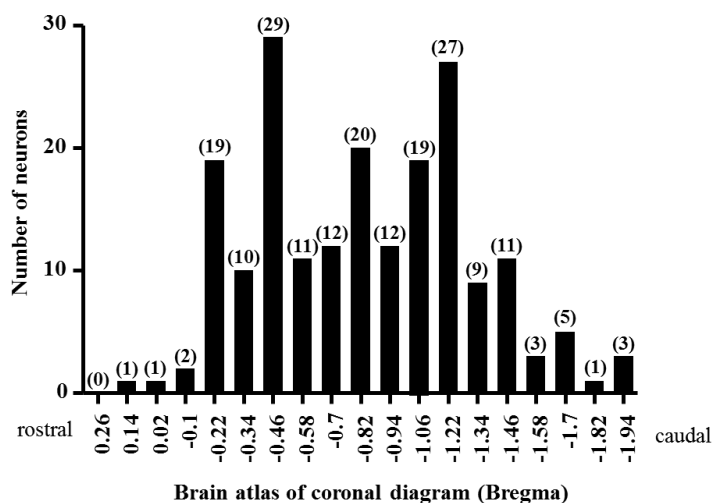


Figure 4.1 The distribution of GnRHR neurons in Pe from rostral to caudal. Periventricular hypothalamus Pe is located between bregma +0.26 and -1.94 mm based on the brain atlas from Paxinos and Franklin, 2004. Most GnRHR neurons in Pe are found in the medial region between -0.22 to -1.46 mm (~16 somata/slice). The most rostral area (four sections between bregma +0.26 and -0.1 mm), as well as the more caudal region (four sections between bregma -1.58 and -1.94 mm), contain between zero and five GnRHR neurons somata per brain slice (~two somata/slice).

histochemistry (Figure 4.2). As described in Methods chapter 2.2.3, I analyzed in the beginning brain slices between bregma +0.26 and -1.94 mm which are approximately the boundaries of the periventricular nucleus (Paxinos and Franklin, 2004). The distribution of the GFP-tagged GnRHR neurons in Pe shows that the more rostral area (four sections between bregma 0.26 and -0.1 mm), as well as the more caudal region (four sections between bregma -1.58 and -1.94 mm), contain between zero and five somata per brain slices (~ two somata/slice). Most GnRHR neurons are found in the medial region between bregma -0.22 and -0.46 mm (~16 somata/slice) (Figure 4.1). Therefore, I evaluated 26 GnRHR neurons in 6 coronal brain slices of the medial region of Pe (Bregma -0.22 to -1.26 mm) from 3 early proestrous female mice. No potential contact points (appositions, < 0.3 μ m) are detected between GnRH-secreting fibers and GnRHR neurons (Figure 4.2A). In contrast, appositions between GnRH fibers and GnRHR neurons are easily identified in the arcuate nucleus (Arc) (Figure 4.2B). Still, even if I could not detect any contact between GnRH-secreting fibers and GnRHR neurons, communication between these neurons cannot be entirely excluded, since both neurons possess fibers with extensive length as has been shown previously for GnRH-secreting neurons (Boehm et al., 2005) and now also for GnRHR neurons (Figure 4.2)(Schauer, Tong et al., 2015).

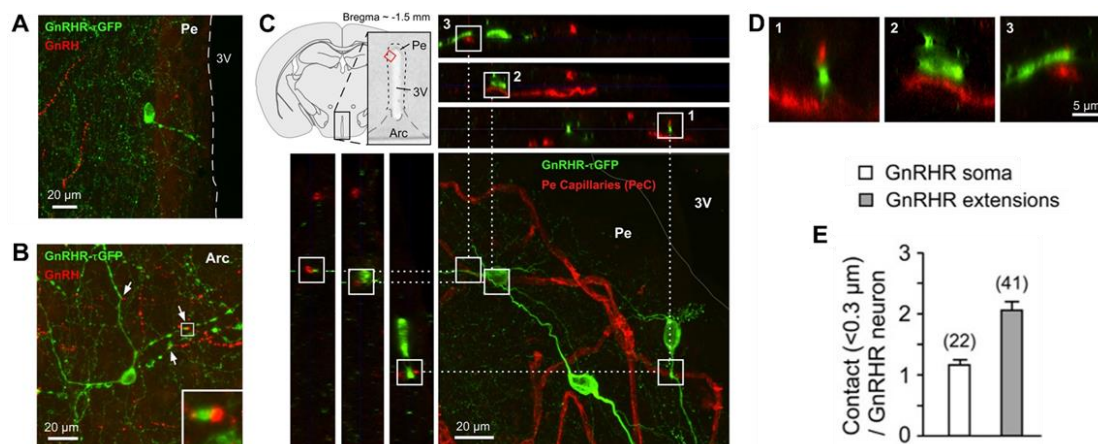


Figure 4.2 Multiple close appositions between GnRHR neurons and capillaries. *A:* Confocal image of a coronal brain slice (Bregma -0.82) showing a green fluorescent (GFP)-positive GnRHR-expressing neurons (*green*) and GnRH-expressing fibers (*red*) in the periventricular hypothalamic nucleus (Pe). No potential contact points (appositions) between these structures were observed ($n = 26$, 3 female mice). The dashed line indicates the border between the Pe and the third ventricle (3V). *B:* GnRHR neurons of the arcuate nucleus (Bregma -1.58) possess various appositions ($< 0.3 \mu\text{m}$) per identified GnRHR neuron ($n = 5$, 3 female mice). *Inset:* higher magnification of the apposition indicated by the white box. Arrows: appositions identified using transverse confocal sectioning. *C:* Confocal images of a coronal brain slice showing GFP-positive GnRHR expressing neurons (*green*) and Pe capillaries (*red*). *Top left:* Overview and higher magnification of a coronal brain slice showing the location of the periventricular (Pe) and arcuate nucleus (Arc) of the hypothalamus next to the 3V. Optical *xyz*-sections (*right lower corner of C*) were merged to obtain a high-resolution *xy*-image with a thickness of $20 \mu\text{m}$. The location and perimeter of the 3V are indicated in gray. Transverse confocal sections (*top: xz* or *left: yz*) allowed the examination of appositions (*white boxes*) between GnRHR neurons and Pe capillaries. *D:* Regions indicated by the numbered white boxes in *C* at higher magnification (*xz*-plane) show the close apposition of GnRHR fibers (1, 3) and a soma (2) to the Pe capillaries. *E:* Number of appositions between capillaries and GFP-marked soma or extensions per GnRHR neuron. Appositions of the GFP-tagged extension were counted only when the soma of the GnRHR neuron could be identified and was located within the Pe. (Schauer, Tong et al., 2015)

In HPG axis, GnRH is released at the median eminence and travels down in the blood stream to the anterior pituitary, where the venous drainage carries the hormones into general circulation (Wislocki, 1937, 1938). Capillary connections between the median eminence and the Pe have been proposed to serve as the basis for a short-loop feedback of hormones (Page, 1982; Page et al., 1978). Our data also show that GnRHR neuron activity in Pe follows the occurrence of a plasma GnRH surge. Since blood vessels could serve as a GnRH source, we examine the potential contact points between GFP-tagged GnRHR neurons and CD31-marked capillaries up to a depth of approximately $25 \mu\text{m}$ in 10 coronal slices from 4 female mice (Figure 4.2C-E). We find a total of 49 GnRHR neurons within

$52 \times 10^6 \mu\text{m}^3$ Pe area, revealing the existence of 1 GnRHR neuron per $10^6 \mu\text{m}^3$ Pe. Surprisingly, the majority of GnRHR neurons (43 out of 49) show that somata and/or extensions have multiple appositions to the capillaries (110 counted contact sites, Figure 4.2C). The magnifications illustrate that GnRHR neurons are positioned next to blood capillaries ($< 0.3 \mu\text{m}$) with either their somata (26 out of 110 sites; 24%) or their extensions (84 out of 110 sites; 76%) (Figure 4.2D). On average, we observed one soma and two GnRHR extensions per GnRHR neuron in $< 0.3 \mu\text{m}$ distance from a capillary (Figure 4.2E). Appositions of GFP-tagged extension were only counted if they could be traced back to an existing soma.

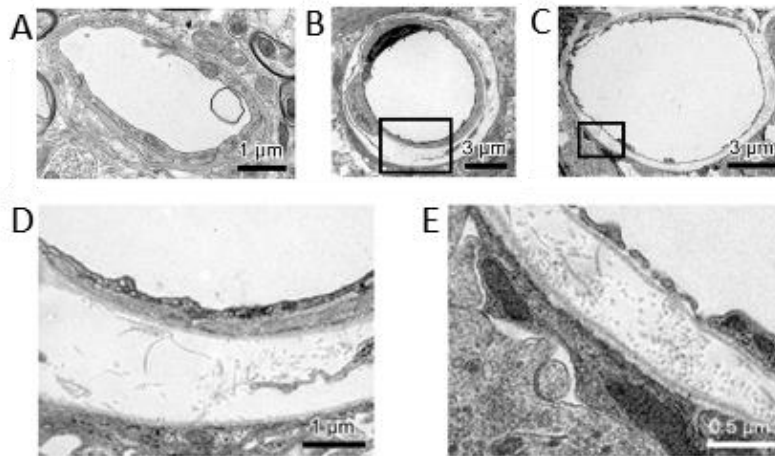


Figure 4.3 Electron micrographs of different capillary types in the hypothalamus. Both the classical continuous non-fenestrated brain capillary (A) and capillaries in which endothelial cells contain numerous vesicular structures that look like caveolae (B, D) were detected in the periventricular area. Similar to those seen in the median eminence (C, E), these capillaries have a widened, translucent perivascular space. Fenestrated capillaries (C, E) were found only in the area of the median eminence. The black boxes in B and C are magnified in D and E, respectively. (Schauer, Tong et al., 2015)

Since GnRHR neurons possess close appositions to Pe capillaries, it will be interesting to investigate the anatomic structures that could mediate the communication between GnRHR neurons and blood stream. Prof. Frank Schmitz (Department of Anatomy, School of Medicine, Saarland University) observed different types of capillaries in Pe using the electron microscope (Figure 4.3). The majority of capillary walls in the brain are classical continuous non-fenestrated brain capillary with the continuous endothelial cells

connected by tight junctions and a continuous basement membrane (Figure 4.3A). It forms a physical barrier against the passage of various substances. Interestingly, in addition to classical capillaries, capillaries with endothelial cells containing many caveolae-like structures are found in the periventricular area (Stan, 2005) (Figure 4.3B, D). These findings strengthen my proposal of a less constraint BBB in this region of the CNS. The classical fenestrated capillaries with discontinuous BBB as present in the median eminence are not observed in Pe (Figure 4.3C, E). Communication between neurons and capillaries does not necessarily indicate open access from the blood to the brain but suggest that some components could travel more easily across this barrier. Besides the source from the capillaries and GnRH-secreting fibers, the third ventricle is possible another source from which the GnRH can diffuse to the GnRHR neuron in Pe (Rodríguez et al., 2010).

4.2.2 Subcutaneous injection of cetrorelix affects reproductive cycle of female mice

Considering a less constrained BBB in Pe, GnRHR neuronal activity in the brain may be susceptible to systemic treatment with GnRHR antagonists, like cetrorelix. The latter is known to block GnRH/GnRHR signaling at the level of the gonadotropes in the anterior pituitary and is frequently used in reproductive techniques and hormone-dependent diseases. Systemic injection of cetrorelix can directly block the GnRHR in the anterior pituitary and thus no FSH and LH are released into the circulation. Consequently, no estrogen is produced to initiate the positive feedback necessary to stimulate GnRH and thus LH release to induce ovulation. Therefore, I predict that the reproductive cycle will linger in a phase before ovulation and have ovaries showing a lot of tertiary follicles. To test whether systemic subcutaneous cetrorelix treatment (Figure 4.4A) is capable of influencing GnRH/GnRHR signaling of Pe neurons, we daily inject 0.9% sodium chloride (SHAM, n = 7), 10 µg (n = 5) or 50 µg (n = 5) of cetrorelix per mouse for continuous 9 days and start all groups at either metestrus or diestrus (t = 0) (Figure 4.4B). Before and during the treatment, the estrous cycle stages are determined using vaginal cytology (Caligioni, 2009). All SHAM mice show continuous normal estrous cycle and reach metestrus on day 9 in all but one case. Interestingly, both 10 µg and 50 µg cetrorelix-treated females display impaired reproductive cycles, remaining longer in proestrus (Figure 4.4B). This suggests

that systemic cetrorelix subcutaneous injection can effectively influence the reproductive cycle of the female mouse.

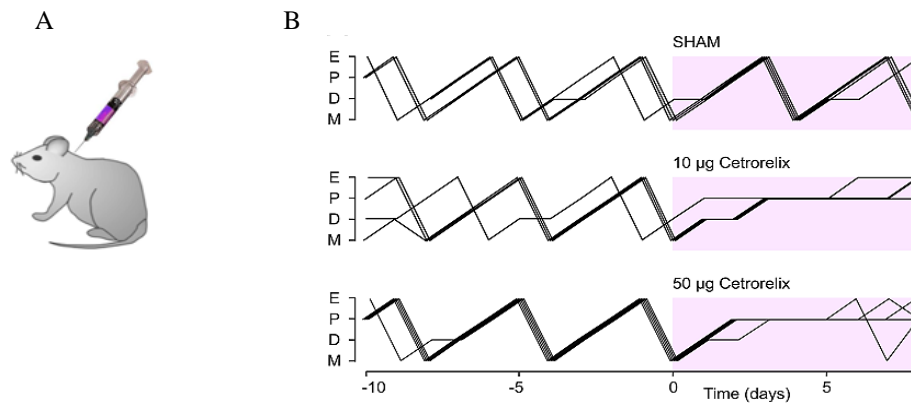


Figure 4.4 Influence of subcutaneous injection of cetrorelix on the vaginal cytology of the female mice. *A*: Schematic picture showing subcutaneous injection. *B*: Plot of the estrous cycle of GRIC/eR26- τ GFP mice (at least 5 females per treatment) demonstrating a normal 4 - 5 day cycle length prior to the start of the subcutaneous application ($t = 0$) of either 10 μ g or 50 μ g cetrorelix for 9 days. SHAM-treated females continued their normal reproductive cycles, in contrast to cetrorelix-treatment groups that stayed mostly in preovulation stage. (Schauer, Tong et al., 2015)

4.2.3 Cetrorelix inhibits the HPG axis

To demonstrate that cetrorelix can induce an effective arrest of the HPG axis function, we determine the ratio of uterus to body mass (Evans et al., 1941) in SHAM ($n=7$), 10 μ g ($n=5$) or 50 μ g cetrorelix-treated ($n=5$) and proestrous females ($n=8$) because it is known that the weight of uterus changes in synchrony with the female reproductive cycle reflecting the preparation for an eventual pregnancy (Croy et al., 2013). Most mice in the SHAM group end in metestrus having relative small uteri. With cetrorelix-treatment, the relative uterus weight is significantly increased to the SHAM females in metestrus, but is indistinguishable from untreated proestrous females (Figure 4.5). Cetrorelix-treated females stay mainly in proestrus as has been previously reported by inhibiting GnRHR in the pituitary (Duijkers et al., 1998; Reissmann et al., 2000). Cetrorelix treatment keeps females in a reproductive stage that prepares for ovulation followed by embryo implantation (nidation). All ova need to be developed before the LH surge occurs, and the uterine lining needs to prepare for nidation. This latter phenomenon increases the uterine weight (Figure 4.5).

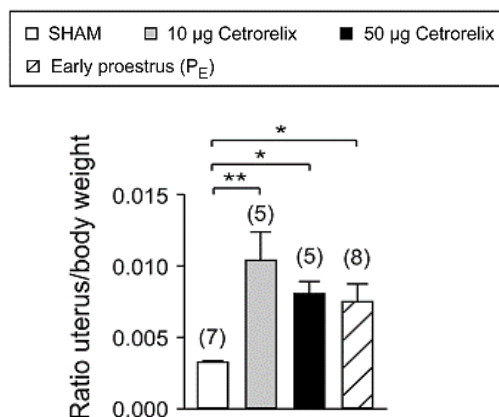


Figure 4.5 Uterus to body mass ratio in SHAM, 10µg, 50µg cetorelix-treated and proestrous females. Uterus weight increased following cetorelix treatment compared to the SHAM group but was indistinguishable from females in early proestrus (SHAM: 0.0033 ± 0.00001 g; 10µg cetorelix 0.0103 ± 0.0020 g; 50 µg cetorelix 0.0081 ± 0.0013 g; proestrus females 0.0075 ± 0.0008 g. ANOVA: $F_{3,16} = 4.754$; $p < 0.01$, Tukey: * $p < 0.5$, ** $p < 0.01$. The number of mice is plotted in brackets above each bar. (Schauer, Tong et al., 2015)

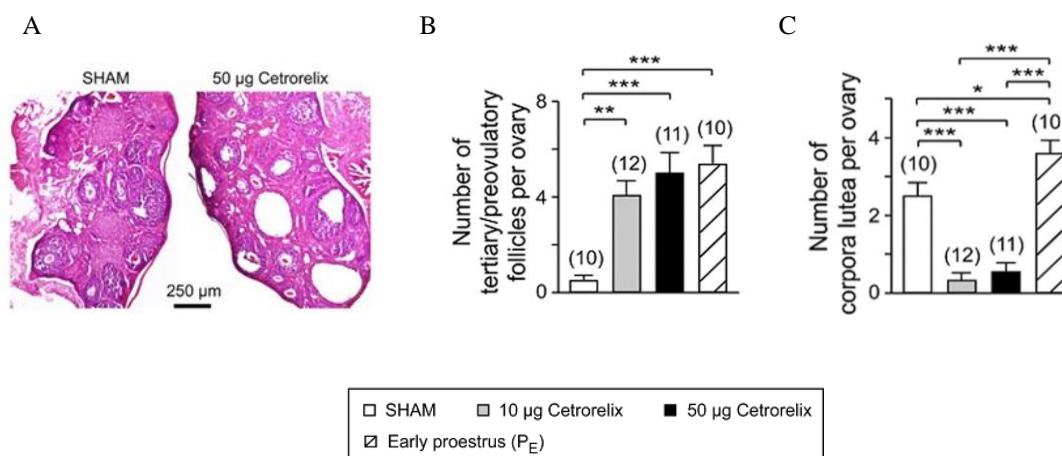


Figure 4.6 Quantification of tertiary/preovulatory follicles and corpora lutea in SHAM, 10µg or 50µg cetorelix-treated and proestrous females. A: Effect of cetorelix on morphological appearance of mouse ovary. Sections taken from SHAM- and 50 µg cetorelix-treated mice. B: Cetorelix-treatment group (10 µg cetorelix group: 4.08 ± 0.58 /ovary; 50 µg cetorelix group: 5.00 ± 0.86 /ovary) and proestrus group (5.4 ± 0.76 /ovary) have more tertiary/preovulatory follicles than the SHAM group (0.5 ± 0.22 /ovary). ANOVA: $F_{3,39} = 10.70$; $p < 0.0001$, Tukey: ** $p < 0.01$, *** $p < 0.001$. C: The number of corpora lutea in SHAM group (2.5 ± 0.34 /ovary) is significant higher than that in cetorelix-treatment group (10 µg cetorelix group: 0.33 ± 0.19 /ovary; 50 µg cetorelix group: 0.55 ± 0.25 /ovary). ANOVA: $F_{3,39} = 31.99$; $p < 0.0001$, Tukey: * $p < 0.05$, ** $p < 0.01$, *** $p < 0.001$. The number of ovaries is plotted in brackets above each bar. (Schauer, Tong et al., 2015)

To establish that cetrorelix females do not ovulate which is another indication for an effective blockage of the HPG axis, I examined the amount of tertiary/preovulatory follicles and corpora lutea in ovaries. In SHAM group the ovaries have relatively more corpora lutea and fewer tertiary/preovulatory follicles, which is consistent with the typical ovaries in metestrus (Figure 4.6A) (Croy et al., 2013). However, ovaries of cetrorelix-treated mice as well as females in early proestrus reveal high numbers of tertiary and preovulatory follicles compared to the SHAM-treated group (Figure 4.6B). Simultaneously, cetrorelix treatment also reduces the presence of corpora lutea when compared to SHAM-treated and early proestrus females (Figure 4.6C). Confirming previous results in mice and humans (Bittner et al., 2011; Duijkers et al., 1998; Reissmann et al., 2000), thus treatment with 10 μg and 50 μg cetrorelix can effectively block the HPG axis as indicated by the increase in the number of tertiary/preovulatory follicles and reduction in the presence of corpora lutea (LSD: $p=0.73$ and 0.94 , respectively).

4.2.4 Systemic cetrorelix treatment prevents the switch in burst firing of GnRHR neurons during preovulatory period

Studies have shown that systemic injection of cetrorelix can penetrate the BBB marginally at doses of approximately 1-10 μg (Schwahn et al., 2000, Telegdy et al., 2009). However, it is unclear whether higher dose, like 50 μg cetrorelix, can cross BBB and have a stronger influence on GnRHR neurons in the brain. Therefore, using loose-patch recording and checking the same parameters to characterize the firing activity as described in Methods chapter 2.2.5.1, the spontaneous activity of GnRHR neurons in Pe are measured and analyzed from SHAM- and cetrorelix-treated females. Interestingly, we find that the mean spike firing frequency of GnRH neurons is increased in the cetrorelix-treatment groups compared to the SHAM females (Figure 4.7A). In addition, 50 μg cetrorelix application cause a significant change in spike firing having a $CV_{ISI} < 0.8$, and these neurons can be classified as tonically firing (Figure 4.7B; LSD: $p < 0.001$). The distribution of tonic and bursting GnRHR neurons in the SHAM and the two cetrorelix-treated groups indicate that the amount of tonically firing neurons rise with increasing cetrorelix concentration. In 50 μg cetrorelix-treated group, the distribution is as similar as in early proestrus (Figure 4.7C). 10 μg cetrorelix treatment seems to be below the threshold for appreciable modulation of

Pe neuron activity (Figure 4.7B; LSD: $p = 0.18$), although a significant effect of cetrorelix could be detected at the level of the ovaries (Figure 4.6). From these observations, we can conclude that systemic application of 50 μg cetrorelix influences the GnRHR neuron activity and thus brain function.

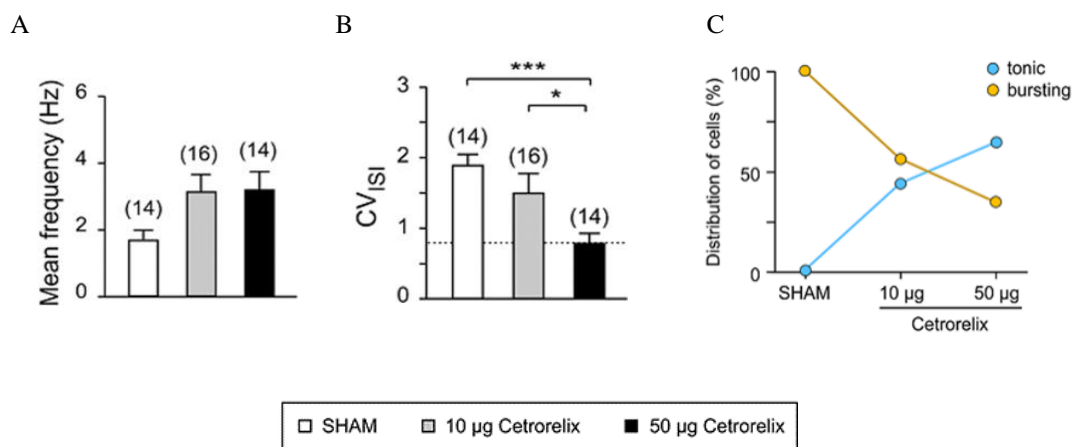


Figure 4.7 Influence of systemic cetrorelix injection on GnRHR neuron firing activity. A-B: Bar histogram of the mean spike frequency and the CV_{ISI} of GnRHR neurons during SHAM, 10 μg and 50 μg cetrorelix applications. A: The mean spike firing frequency of GnRH neurons increased in the cetrorelix-treatment groups (10 μg cetrorelix group: 3.12 Hz, $n = 16$; 50 μg cetrorelix group: 3.18 Hz, $n = 14$) compared to the SHAM females (1.69 Hz \pm 0.29, $n = 14$) (ANOVA: $F_{2,41} = 3.037$; $p = 0.06$). B: CV_{ISI} in 50 μg cetrorelix-treatment group (0.82 \pm 0.13) is smaller than in SHAM-and 10 μg cetrorelix-treatment group (SHAM group: 1.89 \pm 0.15; 10 μg cetrorelix group: 1.5 \pm 0.28; ANOVA: $F_{2,41} = 6.556$; $p < 0.01$, Tukey: * $p < 0.05$, *** $p < 0.001$). The number of neurons is plotted in brackets above each bar. C: Plot of the distribution of all GnRHR neurons firing either tonically (blue symbols) or in bursts (yellow symbols) (SHAM: $n = 14$; 10 μg cetrorelix: $n = 16$; 50 μg cetrorelix: $n = 14$). (Schauer, Tong et al., 2015)

4.3 Discussion

Systemic injection of cetrorelix can effectively block the HPG axis and influence the firing activity of GnRHR neurons in Pe, likely through a less constrained BBB, especially with higher concentration 50 μg . The fact that agonists and antagonists of GnRH are widely used in clinical treatments, my findings may have important clinical implications.

GnRHR neurons in Pe may sense the change of GnRH level through a less constrained BBB. In the previous chapter, we find that with the change of endogenous GnRH level, GnRHR neuron firing synchronizes with the female estrous cycle; therefore, we investigate the source of GnRH focusing on three structures: GnRH-secreting fibers,

blood vessels, and third ventricle. Immunohistochemistry studies show that GnRH-secreting fibers are never observed in close proximity to any GFP-tagged Pe neurons in contrast to the arcuate hypothalamic nucleus (Arc) (Figure 4.2A, B), suggesting GnRHR neuron may not sense the GnRH from the GnRH-secreting fibers. However, both GnRH-secreting and GnRHR neuron fibers possess branches of extensive length. Therefore, synaptic input from GnRH-secreting neurons onto Pe GnRHR neurons cannot be excluded. It is known that GnRH is secreted near the pituitary portal vasculature and travels in the blood stream from the median eminence to the pars anterior, where the venous drainage will carry the hormones into the general circulation (Wislocki, 1937, 1938). The existence of capillary connections between the median eminence and the Pe has been proposed to serve as the basis for a short-loop feedback of hormones (Page, 1982; Page et al., 1978). By immunostaining of CD-31 marked blood vessel and τ GFP-labeled GnRHR neuron, we observed that GnRHR neurons possess close appositions to Pe capillaries. Results from electron microscope show that endothelial cells in Pe capillaries contain many caveolae-like structures. It has been reported that the endothelial caveolae are involved in capillary permeability by its participation in the process of transcytosis (Stan, 2002). The caveolae-like structure on Pe capillaries may offer an anatomical structure to make the GnRHR neuron sense the GnRH level change in the blood stream. In addition to the capillaries, the third ventricle could be another source of GnRH (Rodríguez et al., 2010; Barrera et al., 1992). Many studies have shown that GnRH is present in mammalian cerebrospinal fluid (CSF) (Gazal et al., 1998; Skinner and Caraty, 2002; Skinner et al., 1997; Yoshioka et al., 2001). Like hypophyseal portal-GnRH, this CSF-GnRH displays both a pulsatile and a surge profile (Yoshioka et al., 2001); therefore, GnRH in CSF may affect the Pe GnRHR neurons during the female estrous cycle.

Systemic injection of cetrorelix can effectively block the HPG axis. Cetrorelix treatment, a well-established GnRHR antagonist, efficiently inhibits gonadotropin release by blocking GnRHR in the pituitary, thereby also reducing the rate of ovulation (Duijkers et al., 1998; Reissmann et al., 2000; Bittner et al., 2011). As introduced in Chapter 1.1.1 and 1.1.2, HPG axis regulates the reproductive changes during estrous cycle. GnRH from the hypothalamus reaches the anterior pituitary and stimulates the release of LH and FSH. Under the influence of FSH the follicles in ovaries mature and will develop into

tertiary/preovulatory follicles during proestrus. In the estrus period, the preovulatory follicles are ruptured and transform into corpora lutea. The increase of LH is caused by a preovulatory surge of GnRH during the late proestrus (Croy et al., 2013; Knobil and Neill, 2006). In cetrorelix-treated female mice, as the GnRHR in anterior pituitary is blocked by continuous injection of cetrorelix, the GnRH surge is absent during the late proestrus. Thus, there is no increase of LH to induce the ovulation. This is in agreement with my observation that subcutaneous cetrorelix injection leads to an increase in the number of tertiary/preovulatory follicles concomitant with a significant inhibition of follicle rupture and corpora lutea formation. These indicate that HPG axis is effectively blocked and thus lead to a suppression of LH secretion and inhibition of ovulation.

Systemic injection of cetrorelix can modulate the firing activity of GnRHR neurons in Pe, especially with a higher dose of 50 μ g. The current understanding of GnRH agonist/antagonist actions is mainly restricted to the pituitary; however, the potentially undesirable side effects by acting on GnRHR-expressing neurons in multiple brain areas are still not clear. Many peptides, including GnRH, have been reported to cross the blood-brain barrier (BBB) (Banks, 2009; Barrera et al., 1991), but this is still controversial. Cetrorelix is reported to penetrate the BBB only marginally at previously tested doses of approximately 1-10 μ g (Schwahn et al., 2000; Telegdy et al., 2009). Theoretically, higher cetrorelix concentrations might be able to pass the BBB. My data demonstrate that subcutaneous 50 μ g cetrorelix treatment can affect GnRHR neuron activity in the brain. These findings support the proposal that therapeutic drugs similar to cetrorelix may gain access to the brain to modulate GnRHR neuron activity there and thus brain function. Investigations on Alzheimer's disease (AD) have shown that the dysregulation of the HPG axis at menopause and andropause are implicated in the neuropathological processes underlying AD (Meethal et al., 2005; Nuruddin et al., 2014). Furthermore, it was shown that GnRHR agonist therapy decelerated aging animals (Zhang et al., 2013) and reduced the risk of developing AD in prostate cancer patients (D'Amico et al., 2010). In an animal behavior study, Telegdy et al. (2009) observed that cetrorelix can elicit anxiolytic and anti-depressive behavior in mice by administration of cetrorelix into the lateral brain ventricle, suggesting that systemic injection of cetrorelix can influence the animal behavior. However, how GnRH antagonist and agonist are involved in neuronal

degenerative disease and how they modulate animal behavior are not clear. Detailed analysis of the functional activity of GnRHR neurons in various brain regions will be essential for a complete understanding of the central control of animal behavior by the mammalian brain. In my studies, I show that the neuron firing activity in Pe is modulated by *in vivo* cetrorelix treatment. This establishes the methods and a basis for investigating the function of GnRHR neurons in different brain areas and their involvement in animal behavior regulation.

Reference

1. Badr, M., and Pelletier, G. (1987). Characterization and autoradiographic localization of LHRH receptors in the rat brain. *Synap. N. Y. N* 1, 567–571.
2. Banks, W.A. (2009). Characteristics of compounds that cross the blood-brain barrier. *BMC Neurol.* 9, S3.
3. Barrera, C.M., Kastin, A.J., Fasold, M.B., and Banks, W.A. (1991). Bidirectional saturable transport of LHRH across the blood-brain barrier. *Am. J. Physiol.* 261, E312–E318.
4. Bittner, A.-K., Horsthemke, B., Winterhager, E., and Grümmer, R. (2011). Hormone-induced delayed ovulation affects early embryonic development. *Fertil. Steril.* 95, 2390–2394.
5. Boehm, U., Zou, Z., and Buck, L.B. (2005). Feedback loops link odor and pheromone signaling with reproduction. *Cell* 123, 683–695.
6. Caligioni, C. (2009). Assessing Reproductive Status/Stages in Mice. *Curr. Protoc. Neurosci.* APPENDIX 4, Appendix – 4I.
7. Caraty, A., and Skinner, D.C. (2008). Gonadotropin-releasing hormone in third ventricular cerebrospinal fluid: endogenous distribution and exogenous uptake. *Endocrinology* 149, 5227–5234.
8. Clarke, I.J., Fraser, H.M., and McNeilly, A.S. (1978). Active immunization of ewes against luteinizing hormone releasing hormone, and its effects on ovulation and gonadotrophin, prolactin and ovarian steroid secretion. *J. Endocrinol.* 78, 39–47.
9. Cottrell, G.T., and Ferguson, A.V. (2004). Sensory circumventricular organs: central roles in integrated autonomic regulation. *Regul. Pept.* 117, 11–23.

10. Croy, B.A., Yamada, A.T., DeMayo, F.J., and Adamson, S.L. (2013). *The Guide to Investigation of Mouse Pregnancy* (Academic Press).
11. D'Amico, A.V., Braccioforte, M.H., Moran, B.J., and Chen, M.-H. (2010). Luteinizing-hormone releasing hormone therapy and the risk of death from Alzheimer disease. *Alzheimer Dis. Assoc. Disord.* *24*, 85–89.
12. Duijkers, I.J., Klipping, C., Willemsen, W.N., Krone, D., Schneider, E., Niebch, G., and Hermann, R. (1998). Single and multiple dose pharmacokinetics and pharmacodynamics of the gonadotrophin-releasing hormone antagonist Cetrorelix in healthy female volunteers. *Hum. Reprod. Oxf. Engl.* *13*, 2392–2398.
13. Evans, J.S., Varney, R.F., and Koch, F.C. (1941). The mouse uterine weight method for the assay of estrogens. *Endocrinology* *28*, 747–752.
14. Fink, G., and Jamieson, M.G. (1976). Immunoreactive luteinizing hormone releasing factor in rat pituitary stalk blood: effects of electrical stimulation of the medial preoptic area. *J. Endocrinol.* *68*, 71–87.
15. Gazal, O.S., Leshin, L.S., Stanko, R.L., Thomas, M.G., Keisler, D.H., Anderson, L.L., and Williams, G.L. (1998). Gonadotropin-releasing hormone secretion into third-ventricle cerebrospinal fluid of cattle: correspondence with the tonic and surge release of luteinizing hormone and its tonic inhibition by suckling and neuropeptide Y. *Biol. Reprod.* *59*, 676–683.
16. Gore, A.C. (2002). *GnRH: The Master Molecule of Reproduction* (Kluwer Academic Publishers).
17. Jennes, L., Eyigor, O., Janovick, J.A., and Conn, P.M. (1997). Brain gonadotropin releasing hormone receptors: localization and regulation. *Recent Prog. Horm. Res.* *52*, 475–490.
18. Knobil, E., and Neill, J.D. (2006). *Knobil and Neill's Physiology of Reproduction* (Gulf Professional Publishing).
19. Limonta, P., Marelli, M.M., Mai, S., Motta, M., Martini, L., and Moretti, R.M. (2012). GnRH Receptors in Cancer: From Cell Biology to Novel Targeted Therapeutic Strategies. *Endocr. Rev.* *33*, 784–811.
20. Meethal, S.V., Smith, M.A., Bowen, R.L., and Atwood, C.S. (2005). The gonadotropin connection in Alzheimer's disease. *Endocrine* *26*, 317–326.
21. Nuruddin, S., Syverstad, G.H.E., Lillehaug, S., Leergaard, T.B., Nilsson, L.N.G., Ropstad, E., Krogenæs, A., Haraldsen, I.R.H., and Torp, R. (2014). Elevated mRNA-Levels of Gonadotropin-Releasing Hormone and Its Receptor in Plaque-Bearing Alzheimer's Disease Transgenic Mice. *PLOS ONE* *9*, e103607.

22. Page, R.B. (1982). Pituitary blood flow. *Am. J. Physiol. - Endocrinol. Metab.* *243*, E427–E442.
23. Page, R.B., Leure-duPree, A.E., and Bergland, R.M. (1978). The neurohypophyseal capillary bed. II. Specializations within median eminence. *Am. J. Anat.* *153*, 33–65.
24. Paxinos, G., and Franklin, K.B.J. (2004). *The Mouse Brain in Stereotaxic Coordinates* (Gulf Professional Publishing).
25. Reissmann, T., Schally, A.V., Bouchard, P., Riethmiiller, H., and Engel, J. (2000). The LHRH antagonist cetrorelix: a review. *Hum. Reprod. Update* *6*, 322–331.
26. Rodríguez, E.M., Blázquez, J.L., and Guerra, M. (2010). The design of barriers in the hypothalamus allows the median eminence and the arcuate nucleus to enjoy private milieus: The former opens to the portal blood and the latter to the cerebrospinal fluid. *Peptides* *31*, 757–776.
27. Schauer, C., Tong, T., Petitjean, H., Blum, T., Peron, S., Mai, O., Schmitz, F., Boehm, U., and Leinders-Zufall, T. (2015). Hypothalamic gonadotropin releasing hormone (GnRH) receptor neurons fire in synchrony with the female reproductive cycle. *J. Neurophysiol.* *114*(2), 1008–1021.
28. Schwahn, M., Schupke, H., Gasparic, A., Krone, D., Peter, G., Hempel, R., Kronbach, T., Locher, M., Jahn, W., and Engel, J. (2000). Disposition and metabolism of cetrorelix, a potent luteinizing hormone-releasing hormone antagonist, in rats and dogs. *Drug Metab. Dispos. Biol. Fate Chem.* *28*, 10–20.
29. Shrestha, D., La, X., and Feng, H.L. (2015). Comparison of different stimulation protocols used in in vitro fertilization: a review. *Ann. Transl. Med.* *3*, 137.
30. Sisk, C.L., Richardson, H.N., Chappell, P.E., and Levine, J.E. (2001). In vivo gonadotropin-releasing hormone secretion in female rats during peripubertal development and on proestrus. *Endocrinology* *142*, 2929–2936.
31. Skinner, D.C., and Caraty, A. (2002). Measurement and possible function of GnRH in cerebrospinal fluid in ewes. *Reprod. Camb. Engl. Suppl.* *59*, 25–39.
32. Skinner, D.C., Caraty, A., Malpoux, B., and Evans, N.P. (1997). Simultaneous Measurement of Gonadotropin-Releasing Hormone in the Third Ventricular Cerebrospinal Fluid and Hypophyseal Portal Blood of the Ewe. *Endocrinology* *138*, 4699–4704.
33. Stan, R.-V. (2002). Structure and function of endothelial caveolae. *Microsc. Res. Tech.* *57*, 350–364.
34. Stan, R.V. (2005). Structure of caveolae. *Biochim. Biophys. Acta BBA - Mol. Cell Res.* *1746*, 334–348.

35. Telegdy, G., Tanaka, M., and Schally, A.V. (2009). Effects of the LHRH antagonist Cetrorelix on the brain function in mice. *Neuropeptides* 43, 229–234.
36. Telegdy, G., Adamik, A., Tanaka, M., and Schally, A.V. (2010). Effects of the LHRH antagonist Cetrorelix on affective and cognitive functions in rats. *Regul. Pept.* 159, 142–147.
37. Wen, S., Schwarz, J.R., Niculescu, D., Dinu, C., Bauer, C.K., Hirdes, W., and Boehm, U. (2008). Functional characterization of genetically labeled gonadotropes. *Endocrinology* 149, 2701–2711.
38. Wen, S., Götze, I.N., Mai, O., Schauer, C., Leinders-Zufall, T., and Boehm, U. (2011). Genetic identification of GnRH receptor neurons: a new model for studying neural circuits underlying reproductive physiology in the mouse brain. *Endocrinology* 152, 1515–1526.
39. Wislocki, G.B. (1937). The vascular supply of the hypophysis cerebri of the cat. *Anat. Rec.* 69, 361–387.
40. Wislocki, G.B. (1938). The vascular supply of the hypophysis cerebri of the rhesus monkey and man. *Res Publ Assoc Res Nerv Ment Dis* 17, 48–68.
41. Yoshioka, K., Suzuki, C., Arai, S., Iwamura, S., and Hirose, H. (2001). Gonadotropin-releasing hormone in third ventricular cerebrospinal fluid of the heifer during the estrous cycle. *Biol. Reprod.* 64, 563–570.
42. Zhang, G., Li, J., Purkayastha, S., Tang, Y., Zhang, H., Yin, Y., Li, B., Liu, G., and Cai, D. (2013). Hypothalamic programming of systemic ageing involving IKK- β , NF- κ B and GnRH. *Nature* 497, 211–216.

Chapter 5

GnRH modulates firing activity of GnRHR neurons in arcuate nucleus through calcium-dependent pathway

Abstract

The arcuate nucleus (Arc) is a cluster of neurons in the hypothalamus, which plays an important role in appetite regulation and reproduction. In mice, this hypothalamic region can be influenced by olfactory cues affecting pregnancy (Bruce effect). Studies have shown that gonadotropin-releasing hormone receptor (GnRHR) neurons are found in Arc, but the physiological function of these neurons are not clear. In this chapter, the spontaneous firing activity of Arc GnRHR neurons is first determined using loose-patch recording during the female reproductive cycle. I find that GnRHR neurons show a higher firing frequency in late proestrus, however the spike firing in Arc neurons can be abolished in the presence of synaptic blocker. This suggests that the action potential firing activity of Arc GnRHR neurons does not depend on the reproductive cycle but on network properties. Under the synaptic blocker, GnRH stimulation can increase the firing activity of GnRHR neuron, indicating that GnRHR neurons contain functional GnRHR and receive modulation from both GnRH and network. By developing a new protocol to simultaneously measure the firing activity and intracellular calcium fluctuation, I observed that the action potential burst activity of GnRHR neuron is correlated with the increase in calcium signal. GnRH can simultaneously induce the increase of firing activity and intracellular calcium of GnRHR neuron in Arc, suggesting that the change of intracellular calcium is involved in GnRH-GnRHR signaling pathway. In the presence of tetrodotoxin (TTX) and synaptic blockers, GnRH does not induce the increase of cytoplasmic calcium, indicating that the GnRH-induced response may depend on the action-potential-driven influx of calcium. These studies establish a series of methods and provide indications for the future studies of the intracellular signaling pathway in Arc GnRHR neurons.

5.1 Introduction

In rodents, socially relevant chemosensory signals exert profound effects on reproductive physiology and sexual behavior. It is known that odor and pheromone ligands are detected respectively by the main olfactory epithelium (MOE) and the vomeronasal organ (VNO) in the nasal cavity of rodents. Both organs project fibers to the main olfactory bulb (MOB) and accessory olfactory bulb (AOB), respectively, which subsequently send the information to various brain areas to ultimately influence the social behavior and the endocrine status of the individual (Tirindelli et al., 2009). For example, when female mice are exposed to the scent of an unfamiliar male, their pregnancy is interrupted and the female returns to estrous cycle. This phenomenon is named the Bruce effect since it was discovered by biologist Hilda Margaret Bruce in 1959 (Bruce, 1959). Yet, how the olfactory system impinges onto different output neurons in the brain that are mediating these effects remains largely unknown. Evidence showed that olfactory cues can modulate the pregnancy by influencing the prolactin level (Bellringer et al., 1980). This special kind of behavior in mice depends on the lactotroph axis (Brennan and Zufall, 2006; Leinders-Zufall et al., 2004). In this axis, tuberoinfundibular dopamine (TIDA) neurons in arcuate nucleus (Arc) project to the median eminence, in which they secrete dopamine into the pituitary portal system to inhibit pituitary prolactin (PRL) release. Significant lower activation of dopaminergic neurons in the Arc of the hypothalamus was observed in female mice exposed to familiar versus unfamiliar male bedding using immediate early gene expression combined with immunocytochemistry (Matthews et al., 2013). The familiar male's odor keeps dopamine levels low and thus prolactin levels high, which stimulates progesterone and thus the build-up of the uterine lining to enable nidation. In contrast, the unfamiliar male's odor raises the dopamine levels and therefore reduces prolactin levels. This explains why the corpus luteum is not stimulated. The latter causes a drop in progesterone and thus a disruption in the uterine lining and pregnancy failure. However, the link between odor detection and dopaminergic neurons in Arc influencing the prolactin level is still unclear. Boehm et al. used a genetic transneuronal tracer and suggested that both the accessory and the main olfactory system relay information to GnRH neurons (Boehm et al., 2005). GnRH-target neurons referred as GnRHR neurons, have been reported to be broadly distributed in many brain areas, including the Arc (Wen et al., 2011).

In addition, studies showed that GnRH neurons communicate directly with TIDA neurons in the adult female by immunohistochemical staining coupled with confocal microscopy (Mitchell et al., 2003). Therefore, I speculate that GnRHR neurons in the Arc may be the missing link between odor detection and dopaminergic neurons affecting the prolactin levels. If the GnRHR neurons in Arc are TIDA neurons, their activity should be similar to the firing pattern described for these neurons that can influence prolactin. Furthermore, the increase in burst activity of GnRHR neuron might play a role in modulating dopamine release from these cells.

As the first step, the spontaneous spike activity patterns of GnRHR neurons are measured using the loose-patch recording. The result reveals that GnRHR neurons exhibit higher firing frequency in late proestrus, which can be abolished in the presence of synaptic blocker. This implies that the intrinsic firing activity of these neurons in Arc does not depend on the reproductive cycle. Puff application of 0.5nM GnRH can increase the firing activity of GnRHR neuron. Thus, these neurons in Arc contain functional GnRHR and receive both modulations from both GnRH and network. By developing a new protocol to simultaneously measure intracellular Ca^{2+} signal and firing activity, the relationship between intracellular Ca^{2+} fluctuation and firing activity is investigated. The results show that the action potential burst activity of GnRHR neuron is correlated with an increase in Ca^{2+} signal. GnRH stimulation can induce the simultaneous increase of intracellular Ca^{2+} and firing activity in GnRHR neurons in Arc. The increase of cytoplasmic Ca^{2+} cannot be observed in the presence of tetrodotoxin (TTX) that blocks the action-potential-driven external Ca^{2+} influx, indicating that the GnRH-induced increase of Ca^{2+} results from an influx of Ca^{2+} . All of these results build up a series of methods and provide indications for the future studies of the intracellular signaling pathway in Arc GnRHR neurons.

5.2 Results

5.2.1 The intrinsic spike activity of GnRHR neurons in the Arc does not depend on the reproductive cycle.

Using GRIC/eR26- τ GFP female mice, GnRHR neurons in Arc can be visualized by a combination of fluorescence and IR-DIC illumination (Wen et al., 2011) (Figure 5.1A, B).

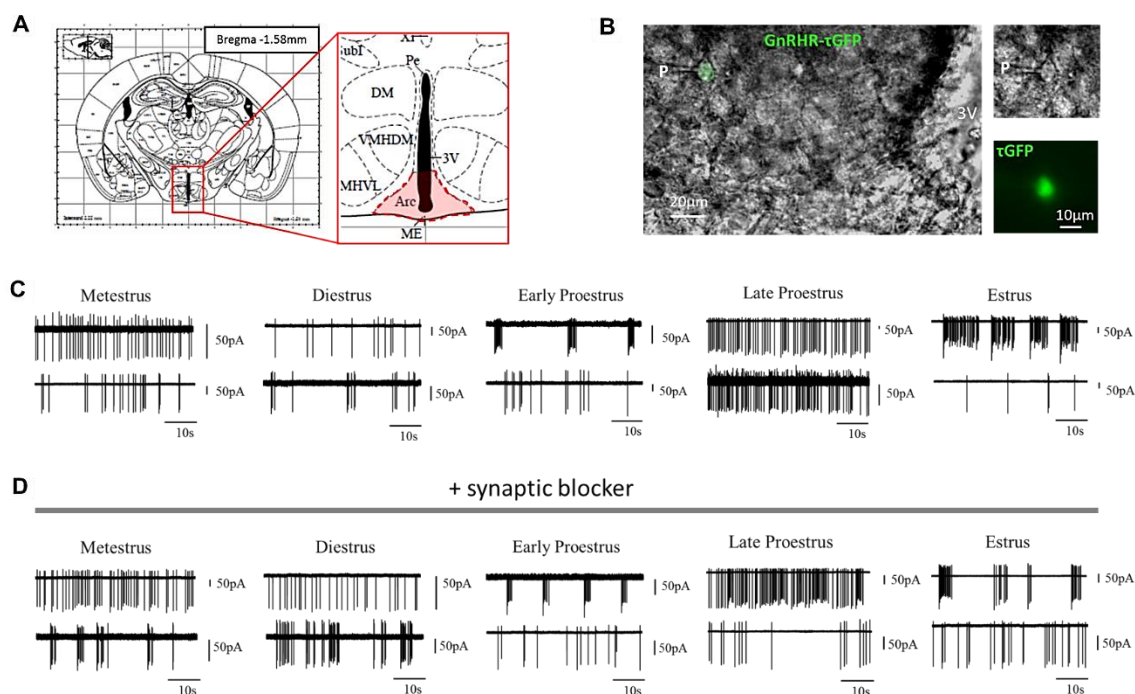


Figure 5.1 The spontaneous spike activity of GnRHR neurons in Arc during the female reproductive cycle with and without the synaptic blocker. **A:** Arcuate nucleus (red) is mediobasal hypothalamus located at the bottom of the third ventricle (3V) next to Pe. **B:** Overlay of a fluorescence image on the top of an infrared-differential interference contrast (IR-DIC) micrograph of a brain tissue slice identifying a GnRHR neuron in the Arc. The soma of the GnRHR neuron is clearly visible in the IR-DIC image (*upper right*) and expresses tau green fluorescent protein (τ GFP) (*lower right*) after *cre*-mediated excision of a transcriptional stop sequence, depending on the activation of the *GnRHR* promoter. P, patch electrode. **C:** Example recordings of trains of extracellularly recorded in the absence of synaptic blocker, action-potential-driven capacitive currents of 10 different GnRHR neurons (two different neurons per reproductive stage). **D:** Example recordings of trains of extracellularly recorded in the presence of synaptic blocker, action-potential-driven capacitive currents of 10 different GnRHR neurons (two different neurons per reproductive stage). The pipette potential was 0 mV. Neuronal activity during proestrus was recorded in brain slices obtained either in the morning [early proestrus, P_E (800 – 1200 hours)] or afternoon [late proestrus, P_L: (1500 – 1800 hours)]

The spontaneous firing activity of GnRHR neurons ($n=53$) in Arc is investigated during female mouse cyclicity and recorded as action-potential-driven capacitive currents using loose-patch from 19 gonadally intact female mice. The activity of GnRHR neurons in Arc are recorded either in the morning (early proestrus, P_E: 800 – 1200 hours) or afternoon (late proestrus, P_L: 1500 – 1800 hours) due to the preovulation GnRH surge (Sisk et al., 2001). All of these GnRHR neurons in Arc show a relatively lower spontaneous firing activity in metestrus, diestrus, early proestrus, and estrus, but a higher firing frequency in late proestrus (Figure 5.1C). However, a question rises as to whether the increase of firing frequency in the late proestrus is directly caused by GnRH surge or by the fast-acting

neurotransmitters from the network. To answer this question, female mice brain slices ($n = 36$) from 26 gonadally intact female mice are incubated in synaptic blockers cocktail at least 15 min before experiments. Using loose-patch recording, the firing activity of GnRHR neurons ($n = 48$) in Arc from these brain slices are measured. In the presence of synaptic blocker, GnRHR neurons during late proestrus exhibit a lower firing activity, which is similar to the other estrous stage (Figure 5.1D). To represent the change in the firing frequency during the female reproductive cycle, the mean spike frequency is calculated in each estrous stage (Figure 5.2). The results show that in the absence of synaptic blocker the firing frequency of GnRHR neurons significantly increases up to 3.5 Hz during P_L compared with other stages, at which the frequency is smaller than 1 Hz ($P < 0.05$; Figure 5.2A). However, in the presence of synaptic blocker, the increase of firing activity in late proestrus is abolished and displays a relative lower firing frequency (1.5 ± 0.8 Hz) similar to that in the other estrous stages (Figure 5.2B). These suggest that the fast-acting neurotransmitters are involved in regulating the firing activity of GnRHR neurons in Arc, especially during the late proestrus. The intrinsic spike activity of GnRHR neurons in the Arc does not depend on the reproductive cycle.

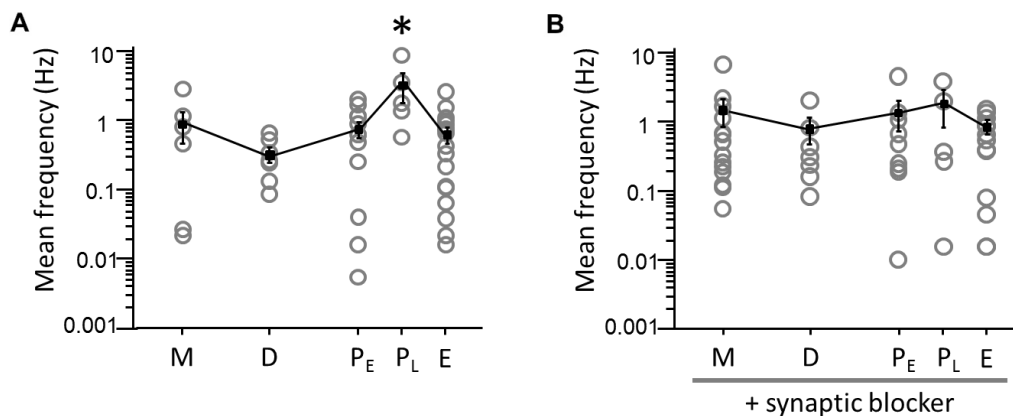


Figure 5.2 The increase of firing frequency during late proestrus is abolished in the presence of synaptic blocker. A: The mean spike frequency of GnRHR neurons in Arc changes during the estrous cycle without synaptic blocker (ANOVA: $F_{5,53} = 6.19$, $P < 0.0001$), peaking at late proestrus. M, metestrus: 0.8 ± 0.3 Hz; D, diestrus: 0.3 ± 0.08 Hz; P_E, early proestrus: 0.8 ± 0.2 Hz; P_L, late proestrus: 3.5 ± 1.6 Hz; E, estrus: 0.7 ± 0.2 Hz). Tukey: * $P < 0.05$. Each recorded neuron is shown as the grey circle. B: The mean spike frequency of GnRHR neurons in Arc changes during the estrous cycle in the presence of synaptic blocker (ANOVA: $F_{5,48} = 0.47$, $P > 0.05$). M: 1.2 ± 0.5 Hz; D: 0.6 ± 0.3 Hz; P_E: 1.1 ± 0.5 Hz; P_L: 1.5 ± 0.8 Hz; E: 0.7 ± 0.2 Hz). Each recorded neuron is shown as the grey circle.

5.2.2 GnRH is sufficient to increase the firing rate in Arc GnRHR neurons

To establish whether GnRH can regulate the firing activity of GnRHR neuron, GnRH-induced responses are recorded in the presence of synaptic blocker. I find that GnRHR neurons in Arc can respond to GnRH stimulation. All of the brain slices are incubated in synaptic blockers at least 15 min before experiments. Puff application of 0.5nM GnRH directly on GnRHR neurons ($n = 6$) in Arc can induce immediate responses (Figure 5.3A). GnRHR neurons increase the spike frequency within the first 60s following GnRH stimulation, from 0.54 ± 0.16 Hz to 1.24 ± 0.58 Hz (Figure 5.3B). Our results demonstrate that GnRH can directly affect τ GFP-labeled GnRHR neurons in Arc and increase their firing activity. This suggests that these neurons contain functional GnRHR and receive regulation from both GnRH and network.

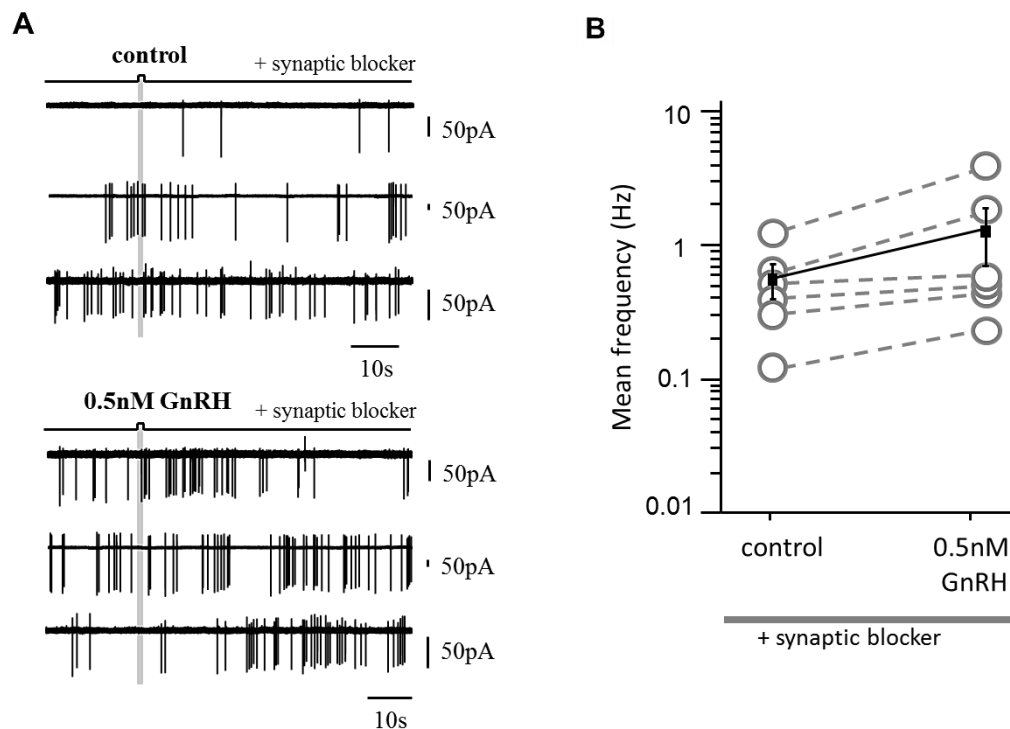


Figure 5.3 GnRH induces the increase of firing activity in Arc GnRHR neurons. A: Examples of three individual GnRHR neurons responding to 1s-pulse of 0.5nM GnRH with an increase in extracellular recorded action-potential-driven capacitive currents in the presence of a cocktail of synaptic blockers (pipette potential, 0mV). B: GnRH increases the spike frequency in the 60s after the stimulation in all tested GnRHR neurons, compared with the control stimulation (gray circles connected by dashed lines). Control, 0.54 ± 0.16 Hz ($n = 6$); GnRH, 1.24 ± 0.58 Hz ($n = 6$). Paired t -test $t(5) = 1.632$, $P = 0.16$.

5.2.3 Action potential burst activity is paired with an increase in calcium signal.

Calcium plays a major role in neurons to induce neurotransmitter release and thus regulate neuronal physiological function (Neher and Sakaba, 2008). Understanding of the basic mechanisms of Ca^{2+} oscillations and fluctuations in neurons has remained obscure. I start to examine the connection between the firing pattern and the intracellular Ca^{2+} signal, which may help further understand the physiological properties of GnRHR neuron in Arc. To correlate Ca^{2+} fluctuations with spike firing behavior, I developed a new protocol to simultaneously measure the electrical activity (loose-patch) and intracellular Ca^{2+} changes by a calcium dye fura-2 (calcium imaging) in the same Arc neuron without further interrupting its environment (Figure 5). In the presence of synaptic blockers, all the τGFP -labeled GnRHR neurons in Arc exhibit a simultaneous change in the spontaneous firing activity together with intracellular calcium signaling (Figure 5.4B). Figure 5.4C-F exhibit the relationship between burst firing activity and calcium signal. For a quantitative analysis, parameters such as the start time of burst (t_1), the end time of burst (t_2), the duration of burst (Δt), and the number of spikes in the burst (NSiB) are used to characterize the burst (Figure 5.4C). The time-to-peak of the calcium signal (t_{cp}) and the amplitude of calcium peak signal (A_{cp}) are used to quantify the calcium signal (Figure 5.4C). Figure 5.4 D shows the start time of the burst (t_1) plot against the time-to-peak of the calcium signal (t_{cp}) after each burst. The data can be well fitted by a linear function,

$$t_1 = a * t_{cp} + b,$$

where the yielded constants are $a = 1$, $b = 3.27 \pm 0.38$ s. This suggests that the burst firing activity and the increase of calcium signal are linearly correlated ($r = 1$, $P < 0.0001$). The calcium peak signal always occurs at 3.27 ± 0.38 s after each burst. This delay indicates that it should be caused by a second messenger pathway causing either the activation of ion channels, calcium stores or both. Figure 5.4E and F show the duration of the burst (Δt) and the number of spikes in the burst (NSiB) plot against the amplitude of calcium peak signal (A_{cp}), respectively. Both of the data can be fitted by an exponential function,

$$y = y_0 + A \exp\left\{\frac{-(x - x_0)}{\tau}\right\},$$

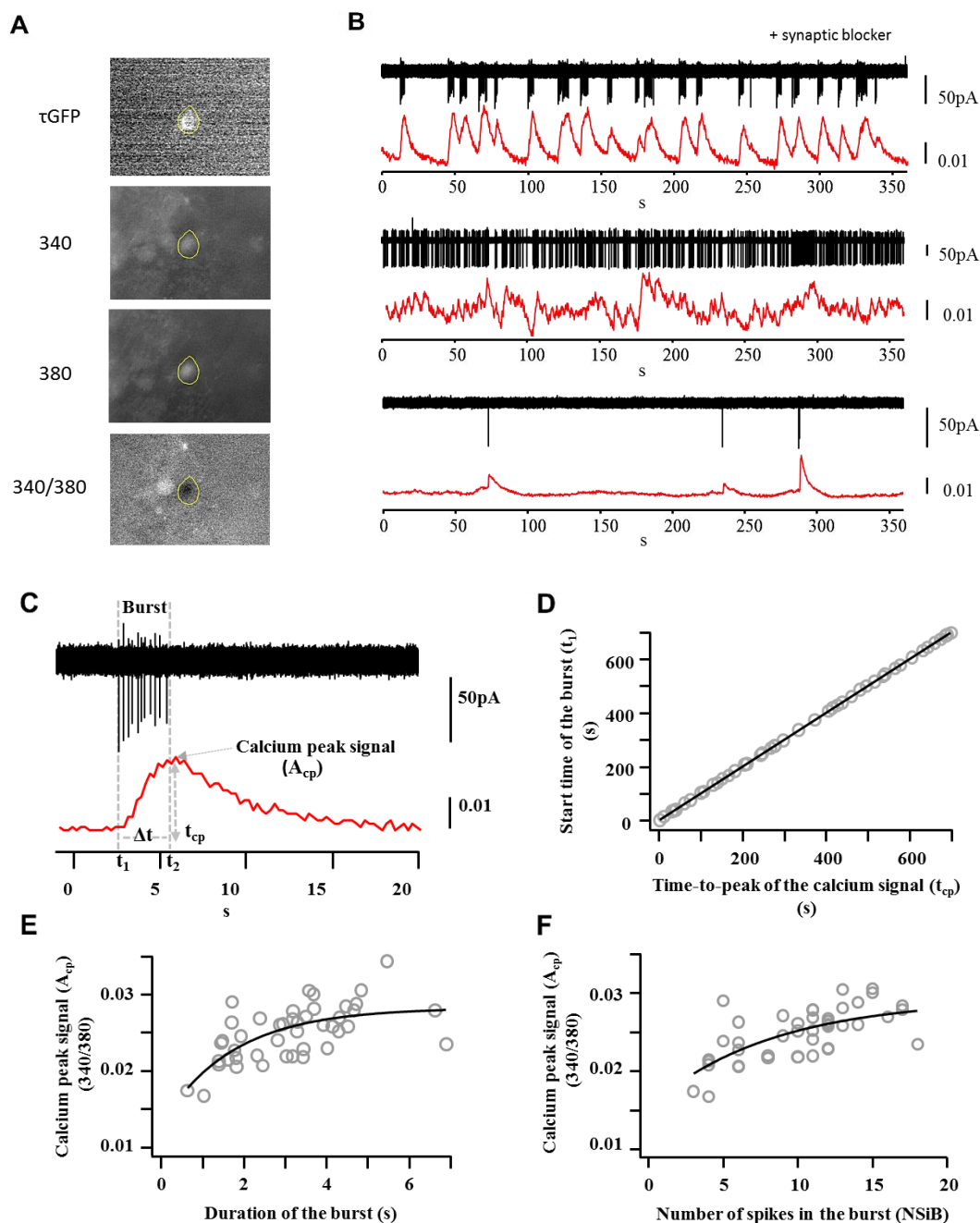


Figure 5.4 The simultaneous change in spontaneous spike activity and intracellular calcium activity of GnRHR neuron in Arc. *A*: Identification of a GnRHR- τ GFP neuron and simultaneous acquisition of the fura-2 fluorescence in the Arc on coronal mouse brain slices. *B*: Three examples of extracellular recorded action-potential-driven, capacitive currents (black) (pipette potential, 0mV) and simultaneously intracellular calcium signal (red) in the presence of the synaptic blockers. *C*: Parameters to describe the action potential burst activity and the calcium signal peak. t_1 : the start time of burst; t_2 : the end time of burst; Δt : duration of the burst; t_{cp} : time-to-peak of the calcium signal; A_{cp} : Amplitude of calcium peak signal. *D*: The start time of the burst (t_1) is plotted versus the time-to-peak of the calcium signal (t_{cp}). The plot is fitted by linear function (black line). $r = 1$, $P < 0.0001$. *E*: The duration of the burst (Δt) is plotted versus the Amplitude of calcium peak signal (A_{cp}), which is fitted by an exponential function (black line), $r = 0.66$. *F*: The number of spikes in the burst (NSiB) is plotted versus the Amplitude of calcium peak signal (A_{cp}), which is fitted by an exponential function (black line) $r = 0.67$.

where $y_0 = 0.029 \pm 0.004$, $A = -0.010 \pm 0.003$, $\tau = 8.18 \pm 6.86$, $x_0 = 0.629$ s ($r = 0.45$) are fitted constants for the duration of the burst (Δt) (Figure 5.4 E); and $y_0 = 0.028 \pm 0.002$, $A = -0.010 \pm 0.002$, $\tau = 1.74 \pm 0.89$, $x_0 = 3$ ($r = 0.44$) for the number of spikes in the burst (NSiB) (Figure 5.4 F). These data indicate that the action potential burst event in the Arc GnRHR neuron can induce Ca^{2+} fluctuation responses reaching a saturation at either long bursts (>6 s) or at >20 spikes.

5.2.4 GnRH induce the simultaneous increase of intracellular calcium and firing activity in GnRHR neurons in Arc.

The previous results suggest that GnRHR neurons in Arc contain functional GnRHR and can increase firing activity under GnRH stimulation in the presence of synaptic blockers. If the calcium involves the intracellular pathway to respond to GnRH stimulation, then the intracellular calcium should simultaneously rise with the increase of firing frequency. Therefore, using simultaneously loose-patch recording and calcium imaging technique, I repeated the previous experiment and applied 0.5nM GnRH directly on GnRHR neurons in the presence of synaptic blockers ($n = 5$) (Figure 5.5A, B). Compared to the control stimulation, the firing frequency after GnRH stimulation increases from 0.84 ± 0.33 Hz to 1.36 ± 0.53 Hz ($n = 6$, $P = 0.06$) (Figure 5.5 C). Simultaneously, the intracellular calcium signal, quantified as the area under the curve (AUC), significantly increases 2.05 ± 0.23 fold ($n = 6$, $P < 0.05$) (Figure 5.5 D) with the firing frequency. This indicates that GnRH stimulation not only increases the firing rate of the Arc neuron, but also induces a change in the intracellular calcium concentration via a GnRH-GnRHR signaling pathway.

5.2.5 Action-potential-driven Ca^{2+} influx might involve in GnRH-induced response on GnRHR neuron.

From above results, I find that the spontaneous intracellular calcium signal of GnRHR neurons changes in synchrony with firing activity, and the GnRH stimulation can induce an increase of both firing frequency and intracellular calcium signal. A question needs to be answered: what is the origin of the increase of intracellular Ca^{2+} after GnRH stimulation. It can result from either the internal calcium store release, the external calcium influx, or both. The extracellular Ca^{2+} could influx through the Ca_v family and/or TRP superfamily

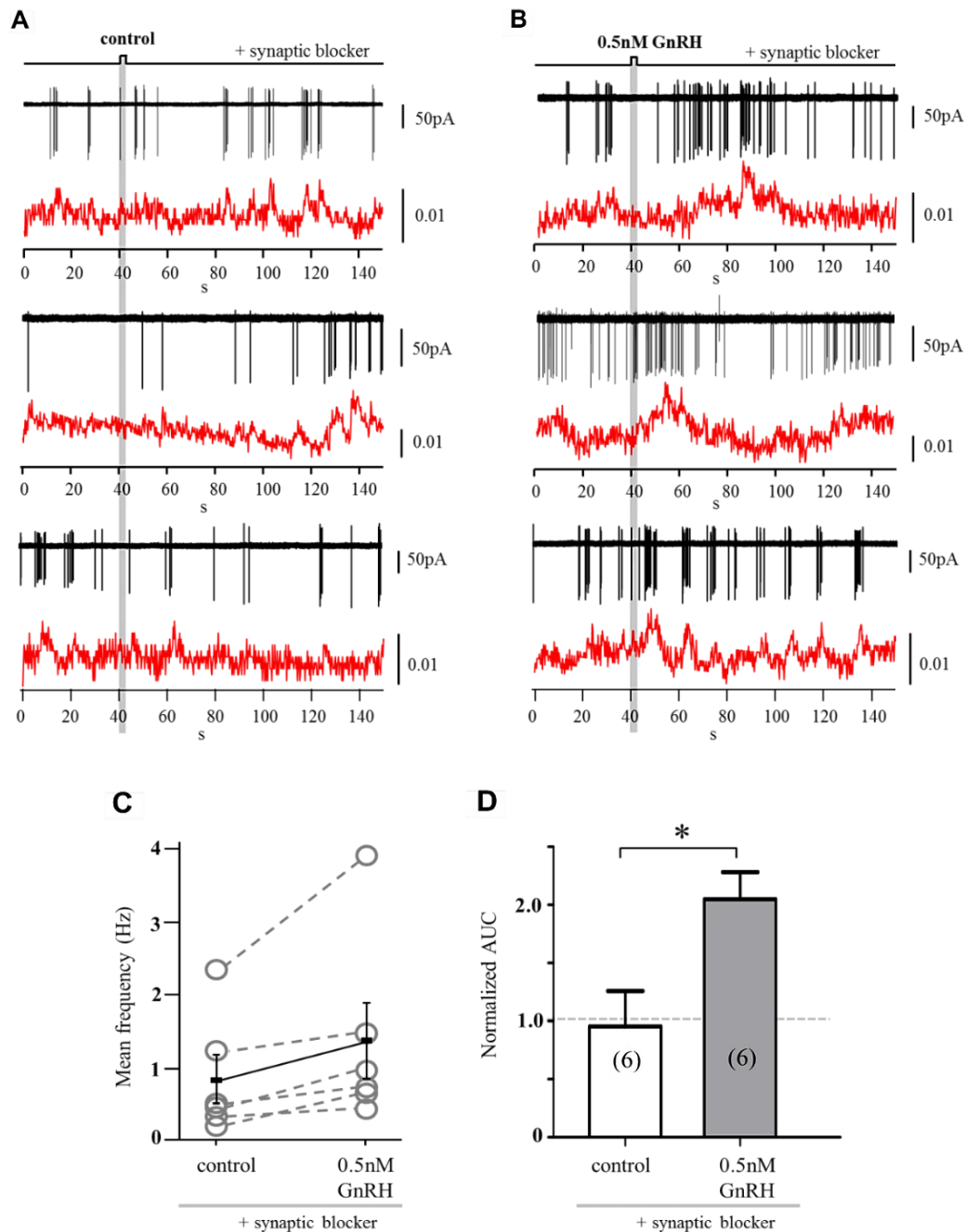


Figure 5.5 GnRH can simultaneously induce an increase of intracellular calcium and firing activity in GnRHR neuron in Arc. *A*: Examples of three individual GnRHR neurons responding to control stimulation without change of firing activity (black) and intracellular calcium (red) in the presence of a cocktail of synaptic blockers. *B*: Three GnRHR neurons as control responding to 1s-pulse of 0.5nM GnRH with a simultaneous increase in firing frequency, recorded action-potential-driven capacitive currents (pipette potential, 0mV), and intracellular calcium signal. *C*: The mean spike frequency increases following 0.5nM GnRH stimulation, compared with the mean spike frequency in control (gray circles connected by dashed lines; the mean value indicated as a black line). Control, 0.84 ± 0.33 Hz ($n = 6$); 0.5nM GnRH, 1.36 ± 0.53 Hz ($n = 6$). Paired t-test $t(5) = 2.34$, $P = 0.06$. *D*: The normalized area under the curve (AUC) of calcium imaging increases following 0.5nM GnRH stimulation, compared with the normalized AUC in control. Control, 0.95 ± 0.3 ($n = 6$); 0.5nM GnRH, 2.05 ± 0.23 ($n = 6$). Paired t-test $t(5) = 3.31$, $* P < 0.05$.

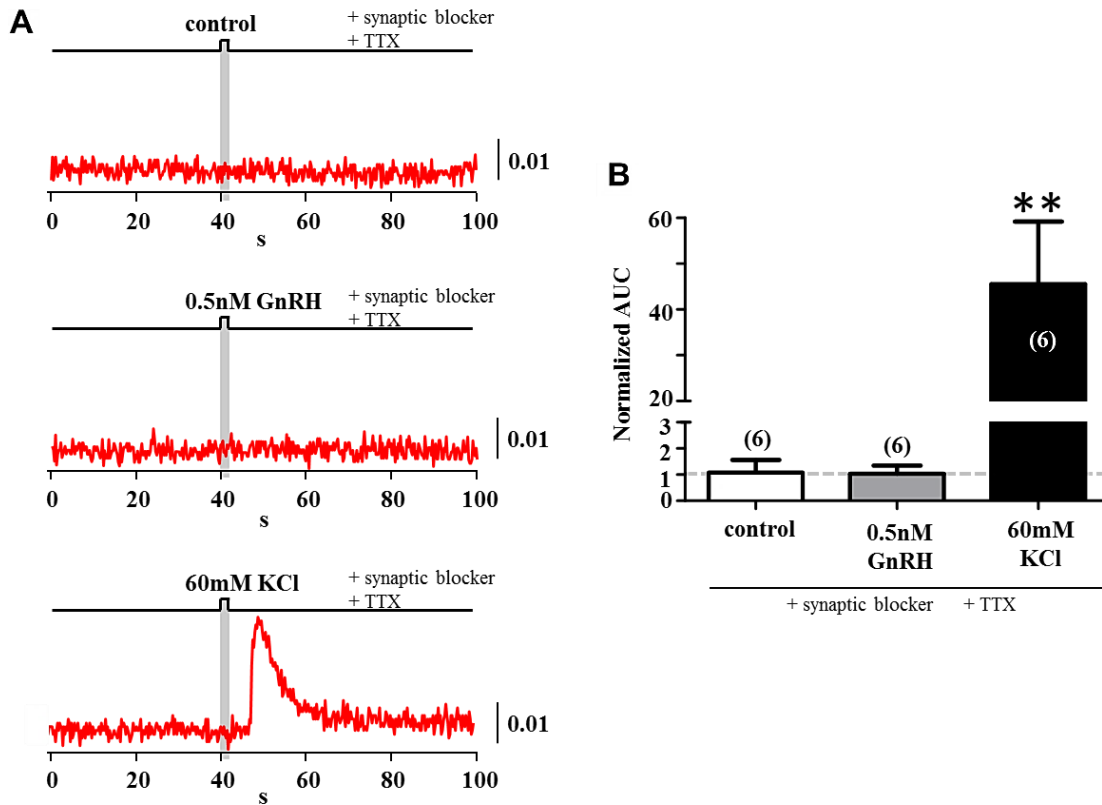


Figure 5.6 In the presence of TTX and synaptic blockers, GnRHR neurons in Arc cannot respond to GnRH stimulation. *A*: One example to show that 1s 0.5nM GnRH stimulation cannot induce the increase of intracellular calcium signal (red) in the presence of TTX and synaptic blocker. *B*: Bar histogram of the normalized area under the curve (AUC) show that 0.5nM GnRH stimulation cannot induce the increase of intracellular calcium compared with control. 60mM KCl stimulation significantly increases the intracellular calcium. Control, 1.07 ± 0.49 ($n = 6$); 0.5nM GnRH, 1.03 ± 0.34 ($n = 6$), 60mM KCl, 45.52 ± 13.61 . (LSD ** $P < 0.01$).

(Kunert-Keil et al., 2006; Van Goor et al., 2000). In a first step, the action-potential-driven external Ca^{2+} influx through Ca_v family was hampered by treating the brain slices with tetrodotoxin (TTX, 10 μM) and preventing depolarization from synaptic input using the synaptic blocker cocktail (see chapter 2.1.2). Under these circumstances, voltage-gated sodium channels were blocked and the spontaneous fluctuation of intracellular calcium signal disappeared together with the spontaneous firing activity (Figure 5.6 A). Puff application of 0.5nM GnRH could not induce the rise in intracellular calcium signal compared to the control without TTX treatment (Figure 5.6 A, B). However, the 60mM KCl stimulation induced a significant increase of intracellular calcium up to 45.52 ± 13.61 fold (Figure 5.6 B). These results imply that (1) external Ca^{2+} influx through voltage-

dependent Ca^{2+} channels are the cause for the calcium signals underlying the burst firing pattern, and (2) GnRH-induced calcium responses are mainly due to changes induced to voltage-dependent Ca^{2+} channels. At this moment it is not yet clear what type of GnRHR neuron I recorded from, since the population of GnRHR neurons appear to be heterogenous as indicated by their more tonic to burst firing pattern (Figure 5.1C, D) and the knowledge that Arc neurons could belong to the group of dopaminergic (TIDA) neurons, POMC neurons or one of the many GABAergic interneurons. The TIDA neurons are known for the burst firing pattern, but due to the use of TTX and no other markers, the identity of the neurons can only be determined using posthoc immunocytochemistry which should be done in the follow-up experiments.

5.3 Discussion

The arcuate nucleus (Arc) is an important neuroendocrine brain area next to Pe and involved in regulation of energy metabolism (Cone et al., 2001; Kim et al., 2014; Sainsbury and Zhang, 2010), cardiovascular system (Sapru, 2013), and reproductive system (Crowley, 2015; Lehman et al., 2010; Voogt et al., 2001; Yeo, 2013). It also plays an important role in the neural circuitry underlying olfactory-encoded behavior in mammals. GnRHR neurons are identified in Arc (Badr and Pelletier, 1987; Wen et al., 2011), but the function of these neurons is unclear. In this chapter the firing activity and calcium signal of GnRHR neurons in Arc are investigated. I find that the intrinsic spike activity of GnRHR neurons in the Arc is not dependent on the reproductive cycle but that these neurons can be modulated by GnRH and the network. The network seems to be able to significantly rise the mean firing frequency during late proestrus, suggesting that some neurons are modulated in the network by the reproductive cycle. By simultaneously measuring firing activity and intracellular Ca^{2+} signals, I find that the action potential burst activity of GnRHR neuron is paired with an increase in intracellular calcium concentration. GnRH stimulation can simultaneously induce the increase of firing frequency in the GnRHR neuron and their intracellular calcium, which may originate from Ca^{2+} influx through voltage-dependent calcium channels.

GnRHR neurons in the Arc are regulated by both GnRH and network. GnRHR neurons in Arc increase their spontaneous firing frequency in late proestrus, while

they show a lower firing frequency in other estrous stages. However, in the presence of synaptic blocker that blocks the most fast-acting neurotransmitters, the high firing frequency of GnRHR neuron in Arc during the late proestrus is attenuated. These neurons display the similar firing frequency as those in the other estrous stages. In this light, the intrinsic spike activity of GnRHR neurons in the Arc is independent of the reproductive cycle and the network is involved in regulating their firing behavior. One candidate of the fast-acting neurotransmitter is glutamate, an excitatory amino acid, which may increase the firing activity of GnRHR neurons in Arc during the late proestrus. There is evidence that excitatory neurotransmitter glutamate is prominently involved in puberty onset and the preovulatory gonadotropin surge in female rat (Brann and Mahesh, 1991; Eyigor and Jennes, 2000). In addition, studies showed that strong immunoreactivity for glutamate exists in Arc and immunoreactive glutamate axons are in synaptic contact with dendrites and cell bodies in this region (Brann and Mahesh, 1995; van den Pol, 1991; van den Pol et al., 1990). All of these suggest that the glutamate neurotransmitter may involve in regulating the firing activity of Arc GnRHR neurons. However, the future experiment is needed to confirm that glutamate could modulate the firing activity of GnRHR neurons in Arc. Moreover, as the discussed in Chapter 2, some other reproductive hormones could also regulate firing activity of GnRHR neurons in Arc, for example, estradiol and progesterone. Confocal microscopic studies by Michell et al. suggested that GnRH neurons send inputs to dopaminergic neurons in Arc containing estrogen receptor α (ER α) (Mitchell et al., 2003). Except the ER α , evidence have shown that most TIDA neurons express the prolactin receptor (Prlr) (Kokay and Grattan, 2005; Lerant and Freeman, 1998) and can respond to increased prolactin (Brown et al., 2012, 2016). I infer that if dopaminergic neurons in Arc express GnRHR, then the GnRHR neurons in Arc could be modulated by estradiol or prolactin or both. Direct evidence that dopaminergic neurons in Arc express GnRHR is needed. In addition, studies reported that approximately 90% kisspeptin neurons in Arc express ER α (Kumar et al., 2015). Kisspeptin neurons are believed to play an important role in regulation female reproductive system and regulate the activity of GnRH neurons (Tassigny and Colledge, 2010). However, there is no direct evidence to support that kisspeptin neuron connects with GnRHR neurons in Arc. Kisspeptin neurons in Arc, regulated by estradiol, might modulate GnRHR neurons through the adjacent network. The

future experiment is required to clarify whether GnRHR neurons in Arc are regulated by other reproductive hormones with or without synaptic blocker presence.

GnRHR neurons showing burst firing activity exhibit simultaneous a rise in intracellular calcium. To enable me to examine a link between burst firing activity and changes in intracellular calcium, a protocol combining loose-patch and calcium imaging recording on brain slices was developed. I observed that the intracellular Ca^{2+} of Arc GnRHR neuron is changing simultaneously with their firing activity. By analyzing the parameters of firing activity and calcium signals, a correlation between them is identified. At the start of the burst, the intracellular calcium signal starts rising. The peak of the calcium signal occurs at the end of the burst and decays immediately thereafter. One possible explanation is that at the beginning of the burst the neuron is depolarized, which could lead to Ca^{2+} entry through low voltage-activated calcium channels (Cain and Snutch, 2013). With the small influx of Ca^{2+} , the membrane potential is further depolarized to activate the voltage-dependent sodium channel and high voltage-activated calcium channels allowing more Ca^{2+} entry and generation of action potentials (Cain and Snutch, 2010; Xu and Clancy, 2008). The concentration of intracellular Ca^{2+} is building up. Neurons continuously firing until the low voltage-activated calcium channels are inactivated and calcium-dependent potassium channels are activated, which makes the neurons return to the initial potential (Jahnsen and Llinás, 1984). The burst terminates and the intracellular Ca^{2+} concentration begins to decay slowly (Grinnell, 1988). To start a new burst of action potentials, neurons need to overcome a set point (threshold potential). The identity of this depolarizing conductance is at this moment elusive. However, the details about which and how the ion channels regulating the burst firing activity need further investigation by whole-cell recording. Burst firing is a character of many neuroendocrine cells and is an efficient firing pattern to release neurotransmitters or hormones (Chu et al., 2012; Lyons et al., 2010; Morozova et al., 2016). Lyons et al. demonstrated that TIDA neurons in Arc discharge rhythmically in a robust oscillation (Lyons et al., 2010). Since GnRHR neurons in Arc exhibit burst firing, it is reasonable to consider that GnRHR neurons may represent TIDA neurons. This could be confirmed by immunostaining using tyrosine hydroxylase antibodies (Lyons et al., 2012).

GnRH modulates firing activity of Arc GnRHR neuron through a calcium-dependent pathway. A short application (1s pulse) of 0.5 nM GnRH can increase the firing frequency of GnRHR neuron and the intracellular Ca^{2+} , indicating that the increase of the intracellular Ca^{2+} is part of the response to the GnRH stimulation. GnRHR is a Rhodopsin related G-protein-coupled receptor (Millar and Pawson, 2004; Reinhart et al., 1992; Tsutsumi et al., 1992). Most studies of GnRH-GnRHR intracellular pathway are based on the function of type I GnRHR receptor in pituitary gonadotropes. It was proposed that GnRHR in pituitary gonadotropes interacts mainly with $\text{G}\alpha_{q/11}$, which subsequently activates phospholipase C (PLC) (Grosse et al., 2000; Hsieh and Martin, 1992; Naor et al., 1986). In our case, in the absence of TTX and presence of synaptic blocker cocktails, the increase of firing activity and intracellular calcium under GnRH stimulation is observed. This indicates that a voltage-dependent Ca^{2+} influx, most likely candidates are Cav channels, might be involved in the GnRH-induced response. However, the link between GPCRs and the activation of Cav channels is missing. In the classical PLC pathway, the activation of PLC hydrolyzes phosphatidylinositol 4,5-bisphosphate (PIP_2) into the second messenger inositol 1, 4, 5-tris-phosphate (IP_3) and diacylglycerol (DAG) (Neves et al., 2002). DAG could induce external Ca^{2+} influx, for example, via transient receptor potential (TRP) channels (Numata et al., 2011). Meanwhile, the intracellular IP_3 leads to the release of Ca^{2+} from the endoplasmic reticulum (ER) into the cytosol. Future experiments are needed to distinguish the source of the increase of intracellular calcium under GnRH stimulation, from internal or external. This can be identified using thapsigargin, a Ca^{2+} -ATPase inhibitor, to empty the ER Ca^{2+} store or the low- Ca^{2+} extracellular solution. Furthermore, in the presence of TTX and synaptic blocker cocktails, which blocks voltage-dependent sodium channels and the fast-synaptic input, often the main source of a depolarization, prevents from an increase in calcium in these Arc GnRHR neurons. How the membrane potential changes remains unclear. It needs further investigation using whole-cell clamp technique under the same experiment circumstance to test whether a slow depolarizing conductance is involved in starting the burst firing. TRP channels have lately been indicated as potential targets for GPCRs (Flockerzi and Nilius, 2007). Using different TRP channel blockers could help identify which and how the TRP channels are involved in the GnRH-induced response.

This chapter establishes a series of methods and triggers interesting questions to be investigated. Future experiments are needed to identify whether GnRHR neurons in Arc are TIDA neurons. Furthermore, it is worth investigating which channels are involved in GnRH-GnRHR signaling pathway and modulate the firing activity of GnRHR neurons, which would help better to understand the cellular mechanism linking GnRHR activation to an increase in the firing pattern and rise in the calcium signal.

References

1. Badr, M., and Pelletier, G. (1987). Characterization and autoradiographic localization of LHRH receptors in the rat brain. *Synap. N. Y. N 1*, 567–571.
2. Bellringer, J.F., Pratt, H.P.M., and Keverne, E.B. (1980). Involvement of the vomeronasal organ and prolactin in pheromonal induction of delayed implantation in mice. *J. Reprod. Fertil.* 59, 223–228.
3. Boehm, U., Zou, Z., and Buck, L.B. (2005). Feedback loops link odor and pheromone signaling with reproduction. *Cell* 123, 683–695.
4. Brann, D.W., and Mahesh, V.B. (1991). Endogenous excitatory amino acid involvement in the preovulatory and steroid-induced surge of gonadotropins in the female rat. *Endocrinology* 128, 1541–1547.
5. Brann, D.W., and Mahesh, V.B. (1995). Glutamate: a major neuroendocrine excitatory signal mediating steroid effects on gonadotropin secretion. *J. Steroid Biochem. Mol. Biol.* 53, 325–329.
6. Brennan, P.A., and Zufall, F. (2006). Pheromonal communication in vertebrates. *Nature* 444, 308–315.
7. Brown, R.S.E., Piet, R., Herbison, A.E., and Grattan, D.R. (2012). Differential Actions of Prolactin on Electrical Activity and Intracellular Signal Transduction in Hypothalamic Neurons. *Endocrinology* 153, 2375–2384.
8. Brown, R.S.E., Kokay, I.C., Phillipps, H.R., Yip, S.H., Gustafson, P., Wyatt, A., Larsen, C.M., Knowles, P., Ladyman, S.R., LeTissier, P., et al. (2016). Conditional Deletion of the Prolactin Receptor Reveals Functional Subpopulations of Dopamine Neurons in the Arcuate Nucleus of the Hypothalamus. *J. Neurosci.* 36, 9173–9185.

9. Bruce, H.M. (1959). An exteroceptive block to pregnancy in the mouse. *Nature* *184*, 105.
10. Cain, S.M., and Snutch, T.P. (2010). Contributions of T-type calcium channel isoforms to neuronal firing. *Channels Austin Tex* *4*, 475–482.
11. Cain, S.M., and Snutch, T.P. (2013). T-type calcium channels in burst-firing, network synchrony, and epilepsy. *Biochim. Biophys. Acta BBA - Biomembr.* *1828*, 1572–1578.
12. Chu, Z., Tomaiuolo, M., Bertram, R., and Moenter, S.M. (2012). Two types of burst firing in gonadotrophin-releasing hormone neurones. *J. Neuroendocrinol.* *24*, 1065–1077.
13. Cone, R.D., Cowley, M.A., Butler, A.A., Fan, W., Marks, D.L., and Low, M.J. (2001). The arcuate nucleus as a conduit for diverse signals relevant to energy homeostasis. *Int. J. Obes. Relat. Metab. Disord. J. Int. Assoc. Study Obes.* *25 Suppl* *5*, S63–S67.
14. Crowley, W.R. (2015). Neuroendocrine regulation of lactation and milk production. *Compr. Physiol.* *5*, 255–291.
15. Eyigor, O., and Jennes, L. (2000). Kainate receptor subunit-positive gonadotropin-releasing hormone neurons express c-Fos during the steroid-induced luteinizing hormone surge in the female rat. *Endocrinology* *141*, 779–786.
16. Flockerzi, V., and Nilius, B. (2007). *Transient Receptor Potential (TRP) Channels* (Springer Science & Business Media).
17. Grinnell, A.D. (1988). *Calcium and Ion Channel Modulation* (Springer Science & Business Media).
18. Grosse, R., Schmid, A., Schöneberg, T., Herrlich, A., Muhn, P., Schultz, G., and Gudermann, T. (2000). Gonadotropin-releasing hormone receptor initiates multiple signaling pathways by exclusively coupling to G_(q/11) proteins. *J. Biol. Chem.* *275*, 9193–9200.
19. Hsieh, K.P., and Martin, T.F. (1992). Thyrotropin-releasing hormone and gonadotropin-releasing hormone receptors activate phospholipase C by coupling to the guanosine triphosphate-binding proteins G_q and G₁₁. *Mol. Endocrinol. Baltim. Md* *6*, 1673–1681.
20. Jahnsen, H., and Llinás, R. (1984). Voltage-dependent burst-to-tonic switching of thalamic cell activity: an in vitro study. *Arch. Ital. Biol.* *122*, 73–82.
21. Kim, J.D., Leyva, S., and Diano, S. (2014). Hormonal regulation of the hypothalamic melanocortin system. *Front. Physiol.* *5*.

22. Kokay, I.C., and Grattan, D.R. (2005). Expression of mRNA for Prolactin Receptor (Long Form) in Dopamine and Pro-Opiomelanocortin Neurons in the Arcuate Nucleus of Non-Pregnant and Lactating Rats. *J. Neuroendocrinol.* *17*, 827–835.
23. Kumar, D., Candlish, M., Periasamy, V., Avcu, N., Mayer, C., and Boehm, U. (2015). Specialized subpopulations of kisspeptin neurons communicate with GnRH neurons in female mice. *Endocrinology* *156*, 32–38.
24. Kunert-Keil, C., Bisping, F., Krüger, J., and Brinkmeier, H. (2006). Tissue-specific expression of TRP channel genes in the mouse and its variation in three different mouse strains. *BMC Genomics* *7*, 159.
25. Lehman, M.N., Coolen, L.M., and Goodman, R.L. (2010). Minireview: Kisspeptin/Neurokinin B/Dynorphin (KNDy) Cells of the Arcuate Nucleus: A Central Node in the Control of Gonadotropin-Releasing Hormone Secretion. *Endocrinology* *151*, 3479–3489.
26. Leinders-Zufall, T., Brennan, P., Widmayer, P., S, P.C., Maul-Pavicic, A., Jäger, M., Li, X.-H., Breer, H., Zufall, F., and Boehm, T. (2004). MHC Class I Peptides as Chemosensory Signals in the Vomeronasal Organ. *Science* *306*, 1033–1037.
27. Lerant, A., and Freeman, M.E. (1998). Ovarian steroids differentially regulate the expression of PRL-R in neuroendocrine dopaminergic neuron populations: a double label confocal microscopic study. *Brain Res.* *802*, 141–154.
28. Lyons, D.J., Horjales-Araujo, E., and Broberger, C. (2010). Synchronized Network Oscillations in Rat Tuberoinfundibular Dopamine Neurons: Switch to Tonic Discharge by Thyrotropin-Releasing Hormone. *Neuron* *65*, 217–229.
29. Lyons, D.J., Hellysaz, A., and Broberger, C. (2012). Prolactin Regulates Tuberoinfundibular Dopamine Neuron Discharge Pattern: Novel Feedback Control Mechanisms in the Lactotrophic Axis. *J. Neurosci.* *32*, 8074–8083.
30. Matthews, G.A., Patel, R., Walsh, A., Davies, O., Martínez-Ricós, J., and Brennan, P.A. (2013). Mating Increases Neuronal Tyrosine Hydroxylase Expression and Selectively Gates Transmission of Male Chemosensory Information in Female Mice. *PLOS ONE* *8*, e69943.
31. Millar, R.P., and Pawson, A.J. (2004). Outside-in and inside-out signaling: the new concept that selectivity of ligand binding at the gonadotropin-releasing hormone receptor is modulated by the intracellular environment. *Endocrinology* *145*, 3590–3593.
32. Mitchell, V., Loyens, A., Spergel, D.J., Flactif, M., Poulain, P., Tramu, G., and Beauvillain, J.-C. (2003). A confocal microscopic study of gonadotropin-releasing hormone (GnRH) neuron inputs to dopaminergic neurons containing estrogen receptor alpha in the arcuate nucleus of GnRH-green fluorescent protein transgenic mice. *Neuroendocrinology* *77*, 198–207.

33. Morozova, E.O., Myroshnychenko, M., Zakharov, D., di Volo, M., Gutkin, B.S., Lapish, C.C., and Kuznetsov, A.S. (2016). Contribution of synchronized GABAergic neurons to dopaminergic neuron firing and bursting. *J. Neurophysiol.* jn.00232.2016.
34. Naor, Z., Azrad, A., Limor, R., Zakut, H., and Lotan, M. (1986). Gonadotropin-releasing hormone activates a rapid Ca²⁺-independent phosphodiester hydrolysis of polyphosphoinositides in pituitary gonadotrophs. *J. Biol. Chem.* 261, 12506–12512.
35. Neher, E., and Sakaba, T. (2008). Multiple Roles of Calcium Ions in the Regulation of Neurotransmitter Release. *Neuron* 59, 861–872.
36. Neves, S.R., Ram, P.T., and Iyengar, R. (2002). G Protein Pathways. *Science* 296, 1636–1639.
37. Numata, T., Kiyonaka, S., Kato, K., Takahashi, N., and Mori, Y. (2011). Activation of TRP Channels in Mammalian Systems. In *TRP Channels*, M.X. Zhu, ed. (Boca Raton (FL): CRC Press/Taylor & Francis),.
38. van den Pol, A.N. (1991). Glutamate and aspartate immunoreactivity in hypothalamic presynaptic axons. *J. Neurosci. Off. J. Soc. Neurosci.* 11, 2087–2101.
39. van den Pol, A.N., Wuarin, J.P., and Dudek, F.E. (1990). Glutamate, the dominant excitatory transmitter in neuroendocrine regulation. *Science* 250, 1276–1278.
40. Reinhart, J., Mertz, L.M., and Catt, K.J. (1992). Molecular cloning and expression of cDNA encoding the murine gonadotropin-releasing hormone receptor. *J. Biol. Chem.* 267, 21281–21284.
41. Sainsbury, A., and Zhang, L. (2010). Role of the arcuate nucleus of the hypothalamus in regulation of body weight during energy deficit. *Mol. Cell. Endocrinol.* 316, 109–119.
42. Sapru, H.N. (2013). Role of the hypothalamic arcuate nucleus in cardiovascular regulation. *Auton. Neurosci. Basic Clin.* 175, 38–50.
43. Tassigny, X. d'Anglemont de, and Colledge, W.H. (2010). The Role of Kisspeptin Signaling in Reproduction. *Physiology* 25, 207–217.
44. Tirindelli, R., Dibattista, M., Pifferi, S., and Menini, A. (2009). From pheromones to behavior. *Physiol. Rev.* 89, 921–956.
45. Tsutsumi, M., Zhou, W., Millar, R.P., Mellon, P.L., Roberts, J.L., Flanagan, C.A., Dong, K., Gillo, B., and Sealson, S.C. (1992). Cloning and functional expression of a mouse gonadotropin-releasing hormone receptor. *Mol. Endocrinol.* 6, 1163–1169.

46. Van Goor, F., Krsmanovic, L.Z., Catt, K.J., and Stojilkovic, S.S. (2000). Autocrine regulation of calcium influx and gonadotropin-releasing hormone secretion in hypothalamic neurons. *Biochem. Cell Biol. Biochim. Biol. Cell.* 78, 359–370.
47. Voogt, J.L., Lee, Y., Yang, S., and Arbogast, L. (2001). Regulation of prolactin secretion during pregnancy and lactation. *Prog. Brain Res.* 133, 173–185.
48. Wen, S., Götze, I.N., Mai, O., Schauer, C., Leinders-Zufall, T., and Boehm, U. (2011). Genetic identification of GnRH receptor neurons: a new model for studying neural circuits underlying reproductive physiology in the mouse brain. *Endocrinology* 152, 1515–1526.
49. Xu, J., and Clancy, C.E. (2008). Ionic mechanisms of endogenous bursting in CA3 hippocampal pyramidal neurons: a model study. *PloS One* 3, e2056.
50. Yeo, S.-H. (2013). Neuronal circuits in the hypothalamus controlling gonadotrophin-releasing hormone release: the neuroanatomical projections of kisspeptin neurons. *Exp. Physiol.* 98, 1544–1549.

Chapter 6

Summary

Gonadotropin-releasing hormone (GnRH) is a master hormone in regulating the mammalian reproductive physiology through the hypothalamus-pituitary-gonadal (HPG) axis (Gore, 2002; Knobil and Neill, 2006). GnRH-target neuron, GnRHR neurons, not only exist in anterior pituitary, but also are distributed in multiple brain areas which are associated with different functions, for example reproductive behavior, odor and pheromone processing, and various social behaviors (Badr and Pelletier, 1987; Jennes et al., 1997; Wen et al., 2008, 2011). The physiological function of GnRHR neurons in the brain is still unclear. Due to the development of a new mouse model by the Boehm laboratory, GnRHR neurons can be visualized in live brain slices by the co-expression of τ GFP, a green fluorescent protein (Wen et al., 2011). In this latter study, they found that GnRHR neurons respond in a nucleus specific manner to the GnRH stimulation using calcium imaging. In the present work, I investigate more specifically GnRHR neuron during the female reproductive cycle in the periventricular hypothalamus (Pe) and arcuate nucleus (Arc).

6.1 GnRHR neurons exhibit different firing activity in different brain area

GnRHR neurons in Pe alternate their action potential firing patterns in concert with the female reproductive cycle and change firing activity from tonic to burst during the preovulatory period, which is even more pronounced in the presence of synaptic blockers. GnRHR neurons in the Arc show also a change in firing frequency in late proestrus, which does not include a change from tonic to burst firing pattern, but a total increase in the mean firing frequency. This change in firing frequency is however abolished in the presence of synaptic blockers. These results suggest that the intrinsic firing activity of GnRHR neurons are different in the two brain areas. Both GnRHR neurons seem to be modulated by a state- (or hormone)-dependent network pathways as apparent by the increase of burst firing GnRHR neuron under synaptic blocker during the preovulatory period in Pe (Figure 3.3 D, G) and the synaptic blockers that abolish the high firing frequency during late proestrus in

Arc (Figure 5.2). Several reproductive hormones fluctuate during the female reproductive cycle, for example: estradiol and progesterone, which might be involved in regulating GnRHR neuron firing activity, (Butcher et al., 1974; Bashour and Wray, 2012; Knobil and Neill, 2006). These hormones could regulate GnRHR neuron through directly interaction with their receptors on GnRHR neurons or through regulation of local network. In Pe, the number of tonically firing GnRHR neurons increase during early proestrus, which correlates with the change of estradiol levels during the estrous cycle. Therefore, it is reasonable to consider that estradiol may regulate GnRHR neurons firing tonically. Nevertheless, estrogen receptor ER α expression is not detected in GnRHR neurons of the Pe (Kumar et al., 2015). Estradiol might act on adjacent cells that do express ER α to modulate GnRHR neurons, which needs further experiment to clarify. By contrast to Pe, it was shown that GnRH neurons send inputs to dopaminergic neurons in Arc containing estrogen receptor α (ER α) (Mitchell et al., 2003). If these dopaminergic neurons in Arc also express GnRHR, then the GnRHR neurons in Arc could be directly modulated by estradiol. This conjecture need to be tested by further studies to clarify whether GnRHR neuron in Arc expresses tyrosine-hydroxylase using immunostaining and how estradiol modulates the firing activity of GnRHR neurons in Arc.

6.2 Endogenous GnRH modulates the spike code activity of GnRHR neurons in both Pe and Arc

The action potential pattern of both Pe and Arc GnRHR neurons are affected by GnRH stimulation, but in a different manner. GnRHR neurons in Pe alternate their action potential firing patterns from tonic to burst during the preovulatory period, and it is known that pulsatile GnRH release increases in frequency and amplitude in the preovulatory period (Sisk et al., 2001). Consequently, I proposed that the changing firing activity of GnRHR neuron in Pe from tonic to burst is due to the GnRH stimulation. Puff application of GnRH produces a biphasic short-lived response followed by longer-latency and long-lasting changes in action potential activity. This is consistent with Wen et al. (2011) study where two types of somatic Ca²⁺ transients in Pe GnRHR neurons were observed having a 25s delay between the responses at saturating GnRH. Bath application of GnRH directly on brain slices triggers the conversion of the mode of activity of GnRHR neurons from tonic

to burst firing, which can be reversed by an antagonist of GnRHR, cetrorelix. Furthermore, bath application of cetrorelix on GnRHR neurons in different estrous stages reiterates that the endogenous GnRH stimulation is likely to be the main source for converting the mode of action potential firing during the preovulatory period. These properties enable GnRHR neurons to switch their firing modes depending on fluctuations in GnRH level during the estrous cycle, thus suggesting important functional roles in female reproductive performance. In contrast to the Pe, GnRHR neurons in Arc are very heterogenous in their spiking pattern on any day of the reproductive cycle. These neurons vary between irregular, tonic, and burst firing. Yet, stimulation with GnRH still changes the firing pattern, mainly increasing the mean spike firing rate. The underlying change of the increase in spike frequency is an increase in calcium. The diverse calcium signals between Pe and Arc that I found are in agreement with the previous finding of Wen et al. (2011).

6.3 GnRHR neurons in different brain area receive different source of GnRH

The sources of GnRH focusing on three structures are investigated using immunohistochemistry: GnRH-secreting fibers, blood vessels, and third ventricle. I observed that GnRHR neurons possess close appositions to Pe capillaries (appositions, < 0.3 μm), but GnRH-secreting fibers are never found in the proximity to any GFP-tagged Pe neurons. Due to the extensive length of the fibers of both GnRH-secreting and GnRHR neurons in the Pe, synaptic input from GnRH-secreting neurons onto Pe GnRHR neurons cannot be excluded. Electron microscope observations, performed in collaboration with Prof. Frank Schmitz' laboratory, show that the endothelial cells of capillaries in Pe contain many caveolae-like structures, suggesting a less constrained blood-brain barrier (BBB). In addition, the dependence of the action potential activity on the estrous cycle suggests that GnRH released into the blood might be the main source to modify the firing activity of these Pe neurons. In contrast to Pe, Arc exhibits different anatomical structure. The appositions between GnRH fibers and GnRHR neurons are easily identified (Figure 4.2B), suggesting GnRHR neurons in Arc might directly sense the GnRH from the GnRH-secreting fibers. GnRH-secreting fibers can also release glutamate (Kiss et al., 2003) suggesting that the previously mentioned glutamate influence is likely modulated by the

GnRH release on the GnRHR neurons in the Arc. My results indicate that GnRHR neurons in different brain areas are regulated by the different sources of GnRH.

6.4 Systemic injection of cetrorelix, an antagonist of GnRHR, can influence the firing activity of GnRHR neurons in the brain

Cetrorelix, a well-established GnRHR antagonist, is widely used to treat clinical patients in a wide range of hormone-dependent diseases such as precocious puberty, cancer, as well as *in vitro* fertilization protocols (Delemarre et al., 2008; Layman, 2007; Shrestha et al., 2015). It can efficiently inhibit gonadotropin release by blocking GnRHR in the pituitary, thereby reducing the rate of ovulation (Duijkers et al., 1998; Reissmann et al., 2000; Bittner et al., 2011). However, potential adverse effects of cetrorelix on GnRHR neurons in the brain is still a matter of debate. Considering a less constrained BBB in Pe, GnRHR neuronal activity in the brain may be susceptible to the systemic treatment with cetrorelix. As expected, subcutaneous injection of the GnRHR antagonist cetrorelix can effectively block the HPG axis, as manifested by an increase in the number of tertiary follicles concomitant with a significant inhibition of follicle rupture and more corpora lutea formation (chapter 4.2.3). Furthermore, GnRHR neuron firing activity is susceptible to the systemic treatment with 10 µg and 50 µg cetrorelix. Especially a 50 µg cetrorelix treatment can modulate the GnRHR neuron activity and induce Pe neurons to fire more tonically and to mimic spike firing activity in early proestrus. From all these data I demonstrate that the antagonist of GnRHR can act on GnRHR neurons in the brain which are not a part of the classical HPG axis; therefore, supporting the scenario that previously dismissed therapeutic drugs may gain access to the brain and modulate neuronal activity as observed with the GnRHR neurons in the Pe.

6.5 GnRH-induced action potential burst activity induces a calcium increase via voltage-dependent ion channels in Arc GnRHR neurons

To investigate the GnRH-GnRHR intracellular signaling pathway, an increase of the intracellular Ca^{2+} and firing frequency is observed using puff application of GnRH on Arc GnRHR neuron in the presence of the synaptic blocker cocktail. This indicates that the increase of the intracellular Ca^{2+} is part of the response to the GnRH stimulation. Studies

have shown that GnRHR is a Rhodopsin related G-protein-coupled receptor (Millar and Pawson, 2004; Reinhart et al., 1992; Tsutsumi et al., 1992). It was proposed that GnRHR might interact with $G\alpha_{q/11}$, which subsequently activates phospholipase C (PLC) pathway (Grosse et al., 2000; Hsieh and Martin, 1992; Naor et al., 1986). The activation of PLC hydrolyzes phosphatidylinositol 4,5-bisphosphate (PIP_2) into the second messenger inositol 1, 4, 5-tris-phosphate (IP_3) and diacylglycerol (DAG). The IP_3 can lead to the release of Ca^{2+} from endoplasmic reticulum (ER) into the cytosol while the DAG could induce external Ca^{2+} influx (Neves et al., 2002), for example, via transient receptor potential (TRP) channels (Numata et al., 2011). Therefore, in our case, the GnRH-induced increase of cytoplasmic Ca^{2+} might come from the ER Ca^{2+} store release or from the external Ca^{2+} influx, for example, from voltage-dependent Ca^{2+} channel or TRP channel. Thapsigargin is a Ca^{2+} -ATPase inhibitor. Future experiment may test the GnRH-induced response after thapsigargin emptying the internal ER Ca^{2+} store or after bath application of the low- Ca^{2+} extracellular solution to distinguish the source of increased intracellular Ca^{2+} . Furthermore, in the presence of TTX and synaptic blocker cocktails, which blocks voltage-dependent sodium channels and the fast-synaptic input, often the main source of a depolarization, prevents from an increase in calcium in these Arc GnRHR neurons. This indicates the action-potential-driven Ca^{2+} influx might be involved in the GnRH-GnRHR intracellular signaling pathway. In further experiments, how the change of the membrane potential under GnRH stimulation needs to be investigated using whole-cell clamp technique and to test which channel is taking part in the GnRH-induced change of the membrane potential. It was suggested that TRP channels is a potential target for GPCRs (Flockerzi and Nilius, 2007). Using different TRP channel blockers will help understand the role of TRP channels in the GnRH-induced response.

Reference

1. Badr, M., and Pelletier, G. (1987). Characterization and autoradiographic localization of LHRH receptors in the rat brain. *Synap. N. Y. N 1*, 567–571.

2. Bashour, N.M., and Wray, S. (2012). Progesterone directly and rapidly inhibits GnRH neuronal activity via progesterone receptor membrane component 1. *Endocrinology* *153*, 4457–4469.
3. Bittner, A.-K., Horsthemke, B., Winterhager, E., and Grümmer, R. (2011). Hormone-induced delayed ovulation affects early embryonic development. *Fertil. Steril.* *95*, 2390–2394.
4. Butcher, R.L., Collins, W.E., and Fugo, N.W. (1974). Plasma concentration of LH, FSH, prolactin, progesterone and estradiol-17beta throughout the 4-day estrous cycle of the rat. *Endocrinology* *94*, 1704–1708.
5. Delemarre, E.M., Feliuss, B., and Delemarre-van de Waal, H.A. (2008). Inducing puberty. *Eur. J. Endocrinol. Eur. Fed. Endocr. Soc.* *159 Suppl 1*, S9–S15.
6. Duijkers, I.J., Klipping, C., Willemsen, W.N., Krone, D., Schneider, E., Niebch, G., and Hermann, R. (1998). Single and multiple dose pharmacokinetics and pharmacodynamics of the gonadotrophin-releasing hormone antagonist Cetrorelix in healthy female volunteers. *Hum. Reprod. Oxf. Engl.* *13*, 2392–2398.
7. Flockerzi, V., and Nilius, B. (2007). *Transient Receptor Potential (TRP) Channels* (Springer Science & Business Media).
8. Gore, A.C. (2002). *GnRH: The Master Molecule of Reproduction* (Kluwer Academic Publishers).
9. Grosse, R., Schmid, A., Schöneberg, T., Herrlich, A., Muhn, P., Schultz, G., and Gudermann, T. (2000). Gonadotropin-releasing hormone receptor initiates multiple signaling pathways by exclusively coupling to G_(q/11) proteins. *J. Biol. Chem.* *275*, 9193–9200.
10. Hsieh, K.P., and Martin, T.F. (1992). Thyrotropin-releasing hormone and gonadotropin-releasing hormone receptors activate phospholipase C by coupling to the guanosine triphosphate-binding proteins G_q and G₁₁. *Mol. Endocrinol. Baltim. Md* *6*, 1673–1681.
11. Jennes, L., Eyigor, O., Janovick, J.A., and Conn, P.M. (1997). Brain gonadotropin releasing hormone receptors: localization and regulation. *Recent Prog. Horm. Res.* *52*, 475–490.
12. Kiss, J., Kocsis, K., Csáki, A., and Halász, B. (2003). Evidence for vesicular glutamate transporter synapses onto gonadotropin-releasing hormone and other neurons in the rat medial preoptic area. *Eur. J. Neurosci.* *18*, 3267–3278.
13. Knobil, E., and Neill, J.D. (2006). *Knobil and Neill's Physiology of Reproduction* (Gulf Professional Publishing).

14. Kumar, D., Candlish, M., Periasamy, V., Avcu, N., Mayer, C., and Boehm, U. (2015). Specialized subpopulations of kisspeptin neurons communicate with GnRH neurons in female mice. *Endocrinology* *156*, 32–38.
15. Layman, L.C. (2007). Hypogonadotropic hypogonadism. *Endocrinol. Metab. Clin. North Am.* *36*, 283–296.
16. Millar, R.P., and Pawson, A.J. (2004). Outside-in and inside-out signaling: the new concept that selectivity of ligand binding at the gonadotropin-releasing hormone receptor is modulated by the intracellular environment. *Endocrinology* *145*, 3590–3593.
17. Mitchell, V., Loyens, A., Spergel, D.J., Flactif, M., Poulain, P., Tramu, G., and Beauvillain, J.-C. (2003). A confocal microscopic study of gonadotropin-releasing hormone (GnRH) neuron inputs to dopaminergic neurons containing estrogen receptor alpha in the arcuate nucleus of GnRH-green fluorescent protein transgenic mice. *Neuroendocrinology* *77*, 198–207.
18. Naor, Z., Azrad, A., Limor, R., Zakut, H., and Lotan, M. (1986). Gonadotropin-releasing hormone activates a rapid Ca^{2+} -independent phosphodiester hydrolysis of polyphosphoinositides in pituitary gonadotrophs. *J. Biol. Chem.* *261*, 12506–12512.
19. Neves, S.R., Ram, P.T., and Iyengar, R. (2002). G Protein Pathways. *Science* *296*, 1636–1639.
20. Numata, T., Kiyonaka, S., Kato, K., Takahashi, N., and Mori, Y. (2011). Activation of TRP Channels in Mammalian Systems. In *TRP Channels*, M.X. Zhu, ed. (Boca Raton (FL): CRC Press/Taylor & Francis).
21. Reinhart, J., Mertz, L.M., and Catt, K.J. (1992). Molecular cloning and expression of cDNA encoding the murine gonadotropin-releasing hormone receptor. *J. Biol. Chem.* *267*, 21281–21284.
22. Reissmann, T., Schally, A.V., Bouchard, P., Riethmüller, H., and Engel, J. (2000). The LHRH antagonist cetrorelix: a review. *Hum. Reprod. Update* *6*, 322–331.
23. Shrestha, D., La, X., and Feng, H.L. (2015). Comparison of different stimulation protocols used in in vitro fertilization: a review. *Ann. Transl. Med.* *3*, 137.
24. Sisk, C.L., Richardson, H.N., Chappell, P.E., and Levine, J.E. (2001). In Vivo Gonadotropin-Releasing Hormone Secretion in Female Rats during Peripubertal Development and on Proestrus. *Endocrinology* *142*, 2929–2936.
25. Tsutsumi, M., Zhou, W., Millar, R.P., Mellon, P.L., Roberts, J.L., Flanagan, C.A., Dong, K., Gillo, B., and Sealfon, S.C. (1992). Cloning and functional expression of a mouse gonadotropin-releasing hormone receptor. *Mol. Endocrinol.* *6*, 1163–1169.

26. Wen, S., Schwarz, J.R., Niculescu, D., Dinu, C., Bauer, C.K., Hirdes, W., and Boehm, U. (2008). Functional characterization of genetically labeled gonadotropes. *Endocrinology* *149*, 2701–2711.
27. Wen, S., Götze, I.N., Mai, O., Schauer, C., Leinders-Zufall, T., and Boehm, U. (2011). Genetic identification of GnRH receptor neurons: a new model for studying neural circuits underlying reproductive physiology in the mouse brain. *Endocrinology* *152*, 1515–1526.

Publications

Scientific journals:

- Schauer, C. *, **Tong, T***, Petitjean, H., Blum, T., Peron, S., Mai, O., Schmitz, F., Boehm, U., and Leinders-Zufall, T. (2015). Hypothalamic gonadotropin releasing hormone (GnRH) receptor neurons fire in synchrony with the female reproductive cycle. *J. Neurophysiol.* *114*(2), 1008-1020. * **co-first-author**.

Conference abstracts:

- Schauer C, Petitjean H, **Tong T**, Mai O, Götze IN, Kumar D, Boehm U, Leinders-Zufall T. (2011) Functional characterization of genetically labeled gonadotropin-releasing hormone receptor (GnRH-R) neurons in mouse brain slices. Joint Meeting SFB894/MCBO/GK1326 “Calcium Signaling: Molecular Mechanisms and Integrative Functions”. Homburg, Germany
- Schauer C, **Tong T**, Petitjean H, Mai O, Boehm U, Leinders-Zufall T. (2012) Neural circuits underlying olfactory-encoded behaviors in the mouse brain. The 16th International Symposium on Olfactory and Taste, Stockholm, Sweden
- Petitjean H, **Tong T**, Schauer C, Mai O, Boehm U, Leinders-Zufall T. (2012) Spike code modulation of GnRH-R neurons in hypothalamic brain tissue slices. SFB894 Annual Meeting 2012. Homburg, Germany

Conference talks:

- **Tong T**, Schauer C, Blum T, Boehm U, Leinders-Zufall T. (2014) Primed for reproduction: Gonadotropin releasing hormone generates burst firing behavior in the central nervous system prior to ovulation. (2014) SPP fifth annual meeting, HWK Delmenhorst, Germany

Permission for using published material:

Journal of Neurophysiology: permission is not required for reusing text and graphs in a thesis/dissertation.

Acknowledgments

I would like to express my special appreciation to my advisor Prof. Dr. Trese Leinders-Zufall for her invaluable guidance and encouragement in my research. She is a great advisor who helps me to grow as a research scientist from a student. Her advice on both research as well as on my life have been invaluable. She inspires me and makes an example to me of how a great female scientist should be.

I would also like to express my sincere thanks to Prof. Dr. Dr. Frank Zufall for his valuable perspectives and discussions. He always gives us a lot of brilliant comments and suggestions. I would like to thank Dr. Martina Pyrski, Dr. Pablo Chamero, Dr. Andreas Schmid, Dr. Jan Weiss, Dr. Anabel Perez Gomez, Dr. Bernd Bufe for always helpful advices and interesting discussions in group meetings.

I am grateful to Dr. Christian Schauer for bringing me into the project during the first year when I entered the lab. We had a lot of fun to discuss our project and solve problems. Also, I thank him for organizing many fun group activities. I thank Dr. Hugues Petitjean for interesting discussion and thoughtful advices about our project. I am thankful to Thomas Blum sharing his extensive knowledge and passion for research. Also, He helped me translate the abstract of the thesis into German. Katherin Bleymehl shares her expert knowledge and helps me a lot on my life in Germany. I am glad to have all my great office mates and we had many inspiring, valuable and enjoyable talks on and beyond science.

I am very grateful to my great colleagues and friends at Department of Physiology in University of Saarland, Dr. Timo Schumann, Dennis Bakker, Benjamin Stein, Eugenia Eckstein, Florian Bolz and all else who contribute to create such a great workplace. I am also thankful to Gabriele Mörschbacher, Michael Konzmann, Lisa Knieriemen, Kerstin Becker, Angelika Ströer, Petra Hammes for their support on my work.

I would like to give thanks to Prof. Ulrich Boehm and his group for their nice cooperation and discussion, and Prof. Dr. Frank Schmitz as well as his lab for their contributions and cooperation on the project.

I would like to thank all my friends (too many to list here but you know who you are) in Homburg, Saarbruecken, Arizona, and in the other cities around the world. With their support and companion, my world is full of fun.

A special thanks to my family. My deepest thanks go to my mother Wang, Wenli and my father Tong, Weihua for their invaluable love and support. I would like to express gratitude for all that my Husband Dr. Shuai Wei have done for me. He gives me a lot of support and encourage from my Master to Ph.D. study in Germany and always makes my life full of sunshine. I love to say thank you to my cute daughter Caroline Wei for not kicking and crying so much when I wrote my thesis. She is another achievement of my life.